OBSERVATIONS ON ATHABASKA GLACIER AND THEIR RELATION TO THE THEORY OF GLACIER FLOW

by

WILLIAM STANLEY BRYCE PATERSON

M.A. (Hons.) The University of Edinburgh, 1949

A THESIS SUBMITTED IN PARTIAL FULFILMENT OF THE REQUIREMENTS FOR THE DEGREE OF

DOCTOR OF PHILOSOPHY

in the Department

of

PHYSICS

We accept this thesis as conforming to the required standard

THE UNIVERSITY OF BRITISH COLUMBIA

May, 1962

In presenting this thesis in partial fulfilment of the requirements for an advanced degree at the University of British Columbia, I agree that the Library shall make it freely available for reference and study. I further agree that permission for extensive copying of this thesis for scholarly purposes may be granted by the Head of my Department or by his representatives. It is understood that copying or publication of this thesis for financial gain shall not be allowed without my written permission.

Department of Physics

The University of British Columbia,
Vancouver 8, Canada.

Date May 3rd, 1962.

GRADUATE STUDIES

Field of Study: Glaciology

Advanced Geophysics	J.A. Jacobs
Isotope Geophysics	R.D. Russell
Nuclear Physics	J.B. Warren

Related Studies:

Differential Equations	C.A. Swanson
Computational Methods	C. Froese
Geodesy	H.R. Bell

The University of British Columbia

FACULTY OF GRADUATE STUDIES

PROGRAMME OF THE

FINAL ORAL EXAMINATION

FOR THE DEGREE OF

DOCTOR OF PHILOSOPHY

of

WILLIAM STANLEY BRYCE PATERSON

M.A. Hons., University of Edinburgh, 1949

FRIDAY, MAY 4th, 1962, at 9:30 A.M.

IN ROOM 302, PHYSICS BUILDING

COMMITTEE IN CHARGE

F.H. Soward, Chairman

H.R. BELL	W.H. MATHEWS
R.W. BURLING	J.V. ROSS
J.A. JACOBS	R.D. RUSSELL

R.W. STEWART

External Examiner: J.F. NYE
University of Bristol, England

OBSERVATIONS ON ATHABASKA GLACIER AND THEIR RELATION TO THE THEORY OF GLACIER FLOW

ABSTRACT

The objects of the present study were to collect adequate data concerning the distribution of velocity in a typical valley glacier, to relate these to theories of glacier flow, and if necessary to suggest modifications to these theories. Surface movement, both horizontal and vertical, was measured, and movement at depth was determined by measurements in boreholes. Measurements of ice thickness were also available.

It is shown that, on the Athabaska Glacier, the longitudinal strain rate is not constant with depth, and that, for about 100 metres below the surface, the horizontal velocity is slightly greater than its surface value. Present theory does not cover these cases. Possible modifications are suggested.

The assumption, sometimes made in the past, that the width of a valley glacier can be regarded as infinite, is shown to be unjustified. The relation between the second invariants of the strain rate and stress deviator tensors is compared with the simple power law as determined by laboratory experiments with ice. Comparison is made both for borehole measurements and measurements of change of surface velocity across transverse lines. Agreement is satisfactory, within the limits of experimental error, for all the borehole results and some of the surface movement results. This is interpreted as evidence that the underlying theory is not seriously in error. In particular, the basic assumptions, made by Nye, seem to be reasonable approximations.

Of three laboratory flow laws, that of Glen for quasi-viscous creep gives the most satisfactory fit to the data. The fit would be improved if the mean temperature of the glacier were about -0.75°C rather than the pressure melting temperature. The results appear to show that the index in the power law is reduced at low stresses. Other interpretations of the data are possible, however, so that this result is not considered to be established.

PUBLICATIONS

1. W.S.B. Paterson. Altitudes on the inland ice in North Greenland. Meddelelser om Gronland, 137, 1, 1-12, 1955.

2. W.S.B. Paterson and C.G.M. Slesser. Trigonometric levelling across the inland ice in North Greenland. Empire Survey Review, 13, 100, 252-261, 1956.

3. W.S.B. Paterson. Atmospheric refraction above the inland ice in North Greenland. Bulletin Géodesique, 38, 42-54, 1956.

4. A.G. Bomford and W.S.B. Paterson. The survey of South Georgia. Empire Survey Review, 14, 107, 204-213 and 242-247, 1958.

5. W.S.B. Paterson. Movement of the Sefstroms Gletscher, North East Greenland. Journal of Glaciology, 3, 29, 845-849, 1960.

ABSTRACT

The objects of the present study were to collect adequate data concerning the distribution of velocity in a typical valley glacier, to relate these to current theories of glacier flow, and if necessary to suggest modifications to these theories.

Conventional field methods were used. Surface movement, both horizontal and vertical, was measured by triangulation of markers in the ice from fixed points on bedrock around the perimeter of the glacier. Movement at depth was determined by measurements in boreholes of the change of inclination with time. Seismic and gravity measurements of ice thickness were also available.

The methods of measurement and computation are described and their accuracy is assessed. It was observed that the vertical velocity of the top of the pipe in each borehole is equal to that of the ice in its vicinity. Methods of analysing borehole data are critically reviewed in the light of this fact. A correction term for the curvature of the pipe is also used in the analysis.

It is shown that, on the Athabaska Glacier, the longitudinal strain rate is not constant with depth, and that, for about 100 metres below the surface, the horizontal velocity is slightly greater than its surface value. Present

theory does not cover these cases. Possible modifications are suggested.

The assumption, sometimes made in the past, that the width of a valley glacier can be regarded as infinite, is shown to be unjustified. In the absence of a complete stress and velocity solution for the case of finite width, the stress solution is modified by the introduction of the "shape factor" in the stress solution.

The relation between the second invariants of the strain rate and stress deviator tensors is compared with the simple power law as determined by laboratory experiments with ice. Comparison is made both for borehole measurements and measurements of change of surface velocity across transverse lines. Agreement is satisfactory, within the limits of experimental error, for all the borehole results and some of the surface movement results. This is interpreted as evidence that the underlying theory is not seriously in error. In particular, the basic assumptions, made by Nye, that the components of strain rate and stress deviator tensors are proportional, that the constant depends only on the second invariant of the stress deviator, and that the shear stress is only a slowly varying function of distance down the glacier, seem to be reasonable approximations.

Of three laboratory flow laws, that of Glen for quasi-viscous creep gives the most satisfactory fit to the data.

The fit would be improved if the mean temperature of the glacier were about -0.75°C rather than the pressure melting temperature. This point has not been checked because of technical difficulties.

The results appear to show that the index in the power law is reduced at low stresses (i.e. less than about 0.5 bar). Other interpretations of the data are possible, however, so the result is not considered to be established.

TABLE OF CONTENTS

	Page
ABSTRACT	ii
LIST OF TABLES	vii
LIST OF FIGURES	ix
ACKNOWLEDGEMENTS	xi
1. INTRODUCTION	
1.1. The Flow of Ice in Glaciers	1
1.2. The Athabaska Glacier	4
2. FIELD METHODS	
2.1. General	9
2.2. Surface Movement	9
2.3. Ablation and Accumulation	17
2.4. Ice Thickness	18
2.5. Borehole Measurements	22
2.6. Other Data	27
3. COMPUTATIONS	
3.1. Position	28
3.2. Velocity	34
3.3. Slope	37
3.4. Strain Rates	39
3.5. Ice Thickness	42
3.6. Borehole Measurements	43
3.7. Miscellaneous Quantities	49
4. ACCURACY	
4.1. General	52
4.2. Position	52
4.3. Velocity	60
4.4. Slope	63
4.5. Strain Rates	63
4.6. Ice Thickness	65
4.7. Borehole Measurements	68
4.8. Ablation and Accumulation	72

Page

5. THEORY

5.1. Distribution of Stress and Velocity 74
5.2. Effect of Valley Sides 85
5.3. Reduction of Borehole Data 87

6. RESULTS

6.1. General 91
6.2. Configuration of Surface 91
6.3. Configuration of Bed. 93
6.4. Surface Velocity 93
6.5. Strain Rate 99
6.6. Borehole Results 101
6.7. Ablation and Accumulation 103

7. DISCUSSION

7.1. Analysis of Borehole Data 105
7.2. Validity of Assumptions 110
7.3. Variation of Longitudinal Strain Rate with Depth 114
7.4. Variation of Velocity with Depth 120
7.5. Numerical Check of Equation 18 122
7.6. The Flow Law of Ice 123
7.7. Effect of Valley Sides 132
7.8. Stress and Strain Rate at Boreholes 136
7.9. Comparison of Data with Different Flow Laws 139

APPENDIX 1

Alternative Derivation of Equation 16 145

APPENDIX 2

Generalizations of the Theory 148

BIBLIOGRAPHY 153

TABLES

FIGURES

TABLES

1. Positions and Elevations of Triangulation Stations.
2. Initial Positions and Elevations of Markers.
3. Longitudinal Surface Profile.
4. Transverse Surface Profiles.
5. Width of Glacier.
6. Ice Thickness.
7. Surface Slope.
8. Slope of Bed.
9. Curvature of Surface and Bed.
10. Horizontal Surface Velocity.
11. Horizontal Direction of Surface Velocity.
12. Horizontal Velocity at Edge of Glacier.
13. Mean Velocity on Transverse Lines.
14. Vertical Velocity and Normal Velocity.
15. Rate of Thinning of Glacier.
16. Longitudinal Surface Strain Rate.
17. Transverse Surface Strain Rate (measured).
18. Transverse Surface Strain Rate (calculated).
19. Surface Strain Rates at Boreholes.
20. Borehole Data.
21. Slopes, Velocities, Strain Rates at Boreholes.
22. Borehole Results.

23. Comparison of Mean and Surface Strain Rates.

24. Comparison of Measured and Calculated Strain Rates.

25. Strain Rates and Stresses on Transverse Lines.

26. Strain Rates and Stresses at Boreholes.

27. Ablation and Accumulation.

FIGURES

1. Map to show location of glacier.

2. Map of glacier (2 sheets) (in pocket at back).

3. General view of glacier.

4. Airphoto mosaic of glacier (in pocket at back).

5. Map of bedrock (in pocket at back).

6. Recession of glacier terminus.

7. Profiles of surface and bed - longitudinal line.

8. Profiles of surface and bed and horizontal surface velocity - line A

9. Profiles of surface and bed and horizontal surface velocity - line B

10. Profiles of surface and bed and horizontal surface velocity - line C

11. Profiles of surface and bed and horizontal surface velocity - line D

12. Profiles of surface and bed and horizontal surface velocity - line E

13. Profiles of surface and bed and horizontal surface velocity - line F

14. Profiles of surface and bed and horizontal surface velocity - line G

15. Horizontal surface velocity - longitudinal line.

16. Vertical velocity and velocity normal to surface - longitudinal line.

17. Longitudinal and transverse strain rates - longitudinal line.

18. Change in configuration - hole 322.

19. Change in configuration - hole 209.

20. Change in configuration - holes 116 and 314.

21. Variation of $\frac{\partial u}{\partial y}$ with depth - hole 322.

22. Variation of $\frac{\partial u}{\partial y}$ with depth - hole 209.

23. Variation of $\frac{\partial u}{\partial y}$ with depth - holes 116 and 314.

24. Comparison of velocities of pipe and markers.

25. Effect of "shape factor".

26. Strain rate and stress - hole 322.

27. Strain rate and stress - hole 209.

28. Strain rate and stress - transverse lines.

29. Correlation between surface velocity and ice thickness.

30. Comparison of data with flow laws.

31. Ablation on longitudinal line.

ACKNOWLEDGEMENTS

I am particularly indebted to Professor J.A. Jacobs for overall encouragement, to Dr. J.C. Savage for numerous helpful suggestions and discussions and for permission to make use of his seismic data and borehole data in advance of publication, and to Mr. J. Fairley for able assistance in the field. Mr. J.S. Stacey and Mr. J. Fairley were responsible for the overall organization in 1959 and 1960 respectively. The various projects on the glacier have involved some fifteen people from the Universities of British Columbia and Alberta, from practically all of whom I have received assistance at one time or another. The work could not have been carried out without the cooperation of the Superintendent of Jasper National Park. Mr. W. Ruddy of Snowmobile Tours deserves special mention for the provision of transport whenever requested and for assistance in numerous other ways. The work was financed by grants from the National Research Council. I am also grateful to the Director, Water Resources Branch, Department of Northern Affairs and National Resources, for survey data and copies of the map. I should also like to thank Mr. J. Allard for writing the computer programme for the reduction of the surface movement data.

1. INTRODUCTION

1.1. The Flow of Ice in Glaciers

The first systematic measurements of glacier flow were made in the Alps about 1830. Several detailed studies followed in the 1840's and 1850's. These showed that the flow of a glacier resembles that of a highly viscous fluid. Considerable controversy developed over the actual mechanism of ice flow however.

One of the first attempts at a theoretical interpretation of observations was due to S. Finsterwalder (1897). His "streamline theory" correlated accumulation and ablation with glacier flow, and explained glacier advances and recessions. This theory was mainly qualitative. In 1921 Somigliana put forward a quantitative theory. He assumed that ice behaved like a fluid of constant viscosity, and considered its stationary flow under gravity in an evenly inclined cylindrical channel. Lagally (1934) extended this theory and predicted the depth of the Pasterze Glacier. This was subsequently confirmed by seismic measurements.

The "extrusion flow" theory, put forward independently by Streiff-Becker (1938) and Demorest (1941, 1943), postulated a property of ice quite different from any assumed in previous theories. It was assumed that, under high hydrostatic pressure, the stress required to produce a given deformation in ice was reduced. Thus ice at depth in a glacier should be

squeezed out by the pressure of the overlying ice. The velocity near the bed should be considerably greater than the surface velocity. This theory was never expressed in mathematical form. But Streiff-Becker made some field measurements which could have been explained on this hypothesis (Seligman, 1947).

Both these theories proved unsatisfactory. Polycrystalline solids, such as ice, do not behave like Newtonian liquids. The velocity of a glacier is much more sensitive to small changes in its thickness than would be expected on the theory of constant viscosity. Laboratory experiments have shown that hydrostatic pressures higher than any encountered in a glacier, have no effect on the creep behaviour of ice (Rigsby, 1958). Extrusion flow was never observed in several field experiments where it would have been expected. (Gerrard and others, 1952; Sharp, 1953a, b; Mathews, 1959; Meier, 1960).

The flow law of ice and its application to glaciers have received extensive study during the past decade. Laboratory measurements include those of Glen (1952, 1955, 1958a), Steinemann (1954, 1958a), Griggs and Coles (1954), Hansen and Landauer (1958), Butkovich and Landauer (1958), Rigsby (1958), and Mellor (1959). These experiments indicate that the strain rate is proportional to the third or fourth power of the stress. The constant of proportionality depends on the temperature. The flow law is not affected by the hydrostatic pressure. There is no indication of a yield stress below which ice does not deform.

At the same time, theoretical calculations of stress and velocity in glaciers have been made by Nye (1951, 1952a, 1952b, 1957, 1958a, 1959c, 1960) and others (Weertman, 1958, 1961; Shoumskiy, 1961a, b). In his earliest papers Nye made the simplifying assumption that ice behaves as a perfectly plastic substance. All subsequent work has been based on the laboratory flow law however.

Many simplifying assumptions are of course necessary before results of laboratory experiments can be extended to the much more complex stress systems which exist in glaciers. In spite of this, Nye's theory has been conspicuously successful in explaining many observed features. Rates of deformation of boreholes (Gerrard and others, 1952; Nye, 1957; Mathews, 1959; Shreve, 1961), rates of closure of tunnels (Nye, 1953, 1959a; Glen, 1956), the occurrence of surges of increased flow (Weertman, 1958; Nye, 1958a, 1960), the profile of the Greenland ice cap (Nye, 1959c; Weertman, 1961) are four examples in which there has been substantial agreement between theory and observation. On the other hand, it has been shown that there are places in a glacier to which the theory does not apply, because the underlying assumptions break down (Nye, 1959a, Glen, 1961). In addition, Nye's formulation of the flow law for complex stress systems has been questioned (Glen, 1958c).

At present, theory has tended to outrun the making of detailed field measurements. The extent to which the

assumptions can be expected to hold in a real glacier appeared to need further investigation. The object of the present study was to obtain data for this purpose. It was also hoped to suggest modifications to the theory in the event of its being found inadequate.

The Athabaska Glacier was selected as a suitable location. It has a simple geometrical shape and is easy of accesss. The study was modelled on a similar one carried out on the neighbouring Saskatchewan Glacier (Meier, 1960). Particular emphasis was placed on measuring velocity at depth. Considerable importance was also attached to measurements of strain rate and vertical velocity at the surface along the centreline of the glacier. The shape of the glacier bed was to be determined in as much detail as possible.

1.2. The Athabaska Glacier

The Athabaska Glacier is one of the main outlet glaciers from the Columbia Icefield. The Icefield lies on the Continental Divide and is surrounded by some of the highest peaks in the Canadian Rocky Mountains. Figure 1 shows the general location of the glacier while Figure 2 is a detailed map. The Icefield has an area of over 200 sq.Km. and a mean elevation of about 3000 m. The accumulation area of the Athabaska Glacier comprises some 7 sq.Km. of this and attains a maximum elevation of 3456 m. The glacier flows in a north-easterly direction in a steep-sided valley of fairly constant

width. The terminus (latitude 52°12'N., longitude 117°14'W.) is within 2 Km. of the Banff-Jasper highway some 100 Km. from Jasper. A branch road runs to the edge of the glacier and snowmobiles for tourists are operated on the ice. This ease of access made the Athabaska Glacier a very convenient place for glaciological work. Figure 3 is a general view of the glacier and Figure 4 is an air photo mosaic.

The rim of the Icefield lies at an elevation of about 2700 m. From here the glacier descends in a series of three icefalls over a distance of 2 Km. The elevation of the ice surface at the foot of the lowest icefall is 2300 m. At the terminus it is 1920 m. This is about 120 m. higher than the terminus of the neighbouring Saskatchewan Glacier. The section from the foot of the icefalls to the terminus will be referred to as the lower section. Almost all the glaciological work was done here. The length of this section is 3.8 Km.; its width 1.1 Km. The width varies only slightly, and the only bend is a slight one about 1 Km. from the terminus. The slope of the lower section is generally between 3° and 5° but steepens to about 15° at the terminus. The western half of the terminus ends in a glacial lake and is somewhat steeper. The ice velocity decreases from about 80 m./yr. just below the lowest icefall to 15 m./yr. at the terminus. The time taken for ice to travel from the Icefield to the terminus is of the order of 150 years.

Little information is available about the thickness of

ice in the upper section of the glacier. Isolated seismic measurements give 220 m. in the accumulation area, 92 m. near the centreline below the head wall (marker S5 in Figure 2), and 195 m. on the centreline below the second icefall (L1). For 2 Km. down glacier from the lowest icefall, ice thicknesses on the centreline are in the range 250 m. to 320 m. Bedrock over almost 1 Km. of this section is below the level of the glacial lake at the terminus. Down glacier from this there are two rises in the bed. The ice then thins rapidly towards the terminus. Seismic measurements show that the cross-section of the valley is roughly parabolic. But there are suggestions of a shelf on the south-eastern side for a distance of about 1 Km. below the icefalls. Figure 5 is a map of the bedrock.

The firn limit lies about half-way up the highest icefall at an elevation of about 2500 m. The ablation area is about 6 sq.Km. in extent. The lower section of the glacier is clear of snow by early July in an average year. Annual ablation in this section averages about 4 m. of ice. Glaciers in this area are generally assumed to be temperate, but no measurements are available to confirm this. The fact that the ice is broken up in three icefalls should help to bring it to the melting temperature if it were originally colder. Copious amounts of meltwater flow from under the terminus throughout the summer.

Both sides of the glacier are heavily covered with

debris. The zone on the south-east side is about 100 m. wide, that on the north-west side about 200 m. There are conspicuous old lateral moraines on each side of the lowest kilometre of the glacier. They rise up to 100 m. above present ice surface. There are a series of terminal moraines between the terminus and the highway.

There are two tributary glaciers on the south-east side of the lower section. Neither is joined to the main glacier although the upper one contributes a small quantity of avalanche debris. The lowest point of the bed of the main glacier lies a very short distance down from the upper tributary. The lower tributary also seems to correspond with a hollow in the bed.

The first recorded visit to the glacier was that of Stutfield and Collie in 1897 (Stutfield and Collie, 1903, p. 103-122). Fluctuations of the glacier over the past two centuries have been deduced by study of moraines and growth rings on nearby trees (Field and Heusser, 1954, p. 135; Heusser, 1956, p. 282). Since 1945, parties from the Water Resources Branch, Department of Northern Affairs and National Resources, have made regular surveys of the terminus (Collier, 1960).

These studies indicate that the glacier advanced during the early 18th century. By 1714 the terminus was further forward than at any time for at least the previous 350 years. This position corresponds very roughly with the

line of the present highway. Retreat started about 1720, but another advance in the first half of the 19th century brought the glacier back almost to its maximum position. Recession began between 1841 and 1873 at different parts of the front, and still continues. Terminal moraines indicate temporary halts about 1900, 1908, 1925, and 1935.

Recession since 1873 has totalled 1150 m. or an average rate of 12.5 m./yr. Since 1945 the rate has averaged 27 m./yr. There is no sign of any halt. The behaviour of the Athabaska appears to be typical of glaciers in the area. Recession data are summarized in Figure 6.

2. FIELD METHODS.

2.1. General

Research on Athabaska Glacier was a joint undertaking of the University of British Columbia and the University of Alberta. The work was under the overall supervision of Professor J.A. Jacobs and Professor G.D. Garland, and was financed by grants from the National Research Council. Mr. J.S. Stacey was responsible for organization and was in charge in the field in 1959. These tasks were the responsibility of Mr. J. Fairley in 1960. Stacey was responsible for deep drilling in 1959. Dr. J.C. Savage was in charge of drilling and inclinometer measurements in subsequent seasons. The present author was responsible for surface movement studies. The observations were made by him and Fairley.

2.2. Surface Movement

2.2.1 General

The surface movement survey employed conventional methods. The positions of markers set in the ice were determined periodically by triangulation from stations on bedrock. When a large part of a glacier has to be covered, triangulation is much more rapid and convenient in the field than taping and levelling. The latter method is suitable for detailed study of a small area. Provided that stations are sited on bedrock and the observers are experienced, the

accuracy of triangulation is at least equal to that of taping and levelling.

2.2.2. Triangulation Stations

The survey was carried out from a network of 21 stations around the perimeter of the lower section of the glacier. These were set up during the summer of 1959 by a party from the Water Resources Branch, Department of Northern Affairs and National Resources. The stations served as ground control for the making of a map from air photos. This work has been described by Reid (1961). Most stations were on bedrock but a few had to be sited on moraine. Only one proved unsatisfactory due to lack of stability. A stake supported in a cairn was erected over the station mark when it was used as a reference object in the survey.

2.2.3. Observing Procedure

All observations were made with a Wild T2 theodolite. Angles were read to the nearest second. Markers were observed in rounds of six or seven, and each round was closed on the reference object. Horizontal angles were observed once on each face and further readings taken if the first two differed by more than 5 seconds. Vertical angles were observed twice on each face. The two observers generally took alternate rounds. Each marker was observed from three stations and a few remote markers from four or five. Except in a very few instances, all observations to

one marker were made on the same day. There were intervals of at most 5 or 6 hours between observations from different stations.

The survey was planned to obtain as satisfactory intersections as possible on each marker (ideally three rays intersecting each other at 120°). But the time factor made it necessary to keep the number of stations visited on any one day to a minimum (generally 4). Observations were made between 7 a.m. and 7 p.m. Height of instrument above station mark was measured to the nearest 5 mm.

2.2.4. Markers

Choice of markers followed the recommendations of Ward (1958). The markers were wooden stakes of 15 mm. square cross-section, 2.6 m. long. The wood was ramin, a S.E. Asian hardwood. A cloth flag was attached to the top of each stake. The markers were set in holes of circular cross-section drilled in the ice with a modified Ward-type auger of 32 mm. diameter (Ward, 1958). The holes were about 2.3 m. deep. This depth meant that the stakes had to be reset several times each season. But the start of the movement survey would have been considerably delayed if 5 m. holes had been drilled initially. Resetting consisted of deepening the existing hole. The horizontal position of the marker was thus unchanged. The stakes had to be trimmed to fit the holes and were hammered into position. Observations were

always made to the centre of the top of each marker.

These markers were not entirely satisfactory. Initially they fitted tightly in the holes. After a few days however the upper parts of the holes tended to enlarge and the markers became loose. The only solution was to keep drilling the holes deeper, and loose markers were always reset before the start of each survey. The tilt of any marker which was leaning during a survey was determined by measuring the length of stake above the ice surface and the vertical distance from the top to the surface. The approximate direction was determined in the few cases where it differed from the direction of maximum surface slope.

2.2.5. Siting of Markers

No prior information about velocity was available. The survey thus had the initial object of obtaining an overall idea of the surface movement. In icefalls access, maintainance of markers, and interpretation of movement measurements are all difficult. Nor can ice thickness be measured with any degree of accuracy in heavily crevassed areas. Work was therefore largely confined to the lower part of the glacier.

The general arrangement of markers is shown in Figure 2. Markers in the lower part of the glacier were arranged in one longitudinal and six transverse lines. The longitudinal line consisted of 30 markers (numbered L10 to L39) and extended from the foot of the icefall to the terminus.

Markers were either about 90 or 150 m. apart. The wider spacing was used where surface curvature was small. The aim was to place the longitudinal line along the centreline, i.e. line of greatest velocity. Its position was determined from velocity measurements over a period of one week. Subsequent measurements showed that the longitudinal line was about 50 m. towards the north-west edge of the glacier from the centreline.

The six transverse lines, labelled B to G, contained from 6 to 10 markers each, a total of 42. Spacing between the lines was of the order of 500 m. Spacing between individual markers varied between 40 and 200 m. The lines extended into the debris-covered ice at each side of the glacier.

Nine markers were placed in the relatively flat area between the lower two icefalls. They were arranged in a line extending about half-way across the glacier from the south-east side (markers A1 to A7), plus two markers (L1, L2) near the centreline. Large crevasses prevented the extension of this line right across the glacier.

Fifteen markers (J1 to J12, "B", "D", "E") were placed in the upper part of the glacier to obtain a rough idea of the movement in this area.

Boreholes, which will be described later, were also included in the movement survey.

2.2.6. Observation Periods

All markers except J1 to J12 were positioned in the first half of July 1959. Surveys were made between the following dates:

July 19	-	July 22
August 13	-	August 18
August 30	-	September 2

Markers were reset as necessary and all were reset immediately before the final survey.

About 90% of the markers were still in position the following summer. Those lost were in the A line and the G and L lines near the terminus. The markers were reset, and surveyed between July 22 and July 25. Thereafter attention was concentrated on the D and L lines and a few other markers. The D line was surveyed on July 31, August 7, and August 13. The other markers were surveyed between August 12 and 14.

The markers in the upper part of the glacier were set up during summer 1960 and surveyed twice over a period of 11 days.

The glacier was visited again on November 13-14, 1960 and a further survey of the D and L lines was made. Further visits were made in January and April 1961. Bad weather prevented any useful observations in January, but 10 of the L line markers were resurveyed on April 10. The remainder were buried by snow.

Most surveys included observations of surface movement at the boreholes.

Surface movement observations in July 1961 were confined to a single survey of the positions of the boreholes, the three J markers which survived the winter, and marker A7 which had travelled intact down the lowest icefall.

2.2.7. Strain Rate

The three independent components of the strain rate tensor at the surface in the region surrounding each borehole were measured by the method of Nye (1959b). Four stakes were arranged in a square with one diagonal along the centreline and the borehole at the centre. The length of the sides was roughly 150 m. Ideally, the length should be made equal to the ice thickness. The surface was not uniform over an area of this size however, so a smaller square was chosen. The lengths of the sides and diagonals of each square were measured with a 200 foot (61 m.) steel tape. A nail was inserted in the head of each stake to serve as an accurate mark. To form intermediate markers an ice auger was drilled into the ice and its handle then removed. Each leg was measured once in each direction, and further measurements made if the first two differed by more than 0.05 foot (1.5 cm.). It was not considered necessary to correct for temperature or sag. A spring balance was not used, so correct tension was merely estimated.

This method measures strain rate with reference to axes parallel to the ice surface. Strain rates deduced from the

triangulation refer to horizontal axes.

Strain rates around borehole 314 were measured between August 1959 and July 1960. For the other boreholes the period was July 1960 to July 1961.

2.2.8. Slip past Side Walls

The rate at which the glacier slips past its side walls was measured by a method similar to that of Glen (1958b). Two stakes, some 12 m. apart, were drilled into the ice about 1 m. from the edge of the glacier. A mark was painted on bedrock about half-way between the stakes. The three sides of the triangle were measured with a steel tape. Measurements were made twice in 1959 and once in 1960.

In Glen's method, one stake is placed in the ice and two marks on the rock. The present method has the advantage that longitudinal strain rate can be measured in addition to velocity. But the direction of movement is undetermined. The stakes must be placed in the estimated direction of flow.

Unfortunately there are very few places at the sides of the glacier where the ice-rock interface is exposed. The only suitable locations were on either side of the lowest icefall.

2.3. Ablation and Accumulation

2.3.1. Ablation

As the mass balance of the glacier was not being studied, accurate or extensive measurements of ablation and accumulation were not required.

Ablation was measured by periodic measurements of the length of each movement stake protruding above the ice surface. Any snow lying on the ice was removed. Measurements were made to the nearest 0.5 inch (1.25 cm.).

Measurements were made five times, at intervals of about 10 days, during summer 1959. These figures show the variations in ablation during the season. They do not give a total figure however, as ablation had started before all the markers had been set up. There was at least a foot of fresh snow on the glacier when the last set of measurements were made. It is unlikely that any further ablation of ice took place in 1959. Measurements were also made to the ice surface at those markers which were visible above the snow in April 1961. This represents the level of the ice surface at the end of the 1960 ablation season. Total ablation data for the 1960 season are thus available for these markers.

The length of each stake above the surface was also measured immediately before and after each redrilling, so that survey and ablation results could be corrected.

2.3.2. Accumulation

Few accumulation data were obtained. The net winter's accumulation up to April 1961 was measured by digging down to the ice surface at the fifteen markers which were visible. All other markers were completely buried by snow. This sample will therefore give a low estimate of the mean accumulation.

Three markers (J6, J8, J9), situated on the rim of the Columbia Icefield just above the highest icefall on the glacier, survived the winter. The net accumulation over the period August 1960 to July 1961 is known for them.

In August 1960, a snow pit was dug on the Icefield at the crest between the drainage basins of the Athabaska and Saskatchewan Glaciers. The previous summers' layer was distinguished by a faint dirt band. So the net accumulation for the previous year is known at this point.

2.4 Ice Thickness

2.4.1. Seismic Method

The seismic work was carried out by Savage and Chisholm using standard exploration procedures. A 12-trace high-resolution seismograph manufactured by Houston Technical Laboratories (now Texas Instruments) was used. Each of the 12 traces was recorded twice, once with mixing (50% to the outside) and once without. The records therefore showed 24 traces. Three 27 c.p.s. geophones were used on each trace. The interval between traces on the cable was 15.25 m. The

standard shot was a half stick of 60% Forcite set in a water-filled drill hole at a depth of 3.5 m. Occasionally a pattern of two or three such shots was used to overcome surface wave interference. The most satisfactory filter setting was found to consist of passing the 70 to 140 c.p.s. band.

Thirty-six reflection sites were occupied. At each, at least one spread transverse to the glacier and one longitudinal spread were shot. Usable records were obtained at all but four sites. The usable sites included 16 points (including two boreholes) on the longitudinal line, 8 markers in transverse lines, and one other borehole. The remaining 7 sites did not correspond to points in the movement survey. As a general rule high quality records could be obtained for ice thicknesses in excess of 200 m. The records became marginal at thicknesses less than 130 m. Reflections were obtained from ice thicknesses less than 100 m. only with the greatest difficulty.

A 2 Km. refraction line was also shot. The velocity of the P wave was determined to be 3660 $\pm$ 60 m./sec. with no indication of a variation of velocity with depth. The velocity in the glacier bed was determined to be 4500 m./sec. This latter velocity is typical of a competent bedrock. It should be noted however that the presence of a thin low velocity layer of morainal material is not excluded by refraction results.

The reflection records were interpreted for both depth and dip of the reflecting section by standard procedures. In general, all readings were made at the centre of the first well-developed trough in the reflection group. A study of the best reflection records indicated that this trough followed the beginning of the reflection group by 7 milliseconds. Several reflection records were shot with the geophone spread doubled back on itself so that the geophones of traces 1 and 12, 2 and 11, 3 and 10, etc. were side by side. Traces 1 to 6 were unfiltered and 7 to 12 filtered at the standard setting. In this manner the filter delay was determined to be 7 milliseconds. Thus the actual travel time was then the time read from the record, reading at the first trough of the reflection group, less 14 milliseconds.

2.4.2. Gravity Method

This work was carried out by Mr. E.R. Kanasewich and has been fully described (Kanasewich, 1960).

Observations were made with a Worden gravimeter at 127 stations. These included all the surface movement markers. A three-dimensional analysis was used, and terrain corrections were applied out to 12.4 Km. The estimated accuracy of these ice thickness measurements is -10% +15%.

2.4.3. Boreholes

As will be described in the next section, several boreholes were drilled in order to measure velocity-depth

profiles. Four of these reached bedrock and so provided accurate measurements of ice thickness. The approximate locations were as follows (the number of each borehole is its depth in metres).

Hole 314 - midway between L17 and L18

Hole 322 - 150 m. down glacier from C7

Hole 209 - at L29

Hole 194 - at L30 .

In August 1960 three boreholes were drilled to bedrock by a well-drilling crew under contract to the Alberta Research Council. The approximate locations were:

Hole 250 - midway between C3 and C4 and 20 m. down glacier

Hole 235 - 5 m. down glacier from D3

Hole 73 - 180 m. up glacier from G2.

In July 1961 a borehole (Hole 248) was drilled near the position occupied by L27 in 1959 to check the interpretation of the seismic records at this point. It was not certain whether this hole reached bedrock. The depth of the hole was therefore regarded as a minimum value of ice thickness. Further examination of the seismic records then indicated a thickness somewhat greater than the borehole depth.

The locations of all boreholes are shown in Figure 2.

2.5. Borehole Measurements

2.5.1. Drilling Technique

The holes were drilled by electrically-heated thermal boring elements called "hotpoints". The design was developed by Stacey and has been described by him (Stacey, 1960). Power was supplied by a portable "Homelite" gasoline-driven motor generator. It supplied 2.5 Kw. at 230 volts and weighed 64 Kg. The output voltage could be varied between 0 and 230 volts by a rheostat in the field circuit of the generator. Drilling speeds averaged 6 to 7 m./hour. Speeds of 20 to 25 m./hour have been reported with another type of thermal drill (Nizery, 1951), but this required 10 Kw. of power.

The hole was lined with aluminium pipe. The hotpoint was attached to the lower end of the pipe. The external diameters of pipe and hotpoint were 4.2 and 5.1 cm. respectively. The pipe served as one conductor; an insulated cable inside the pipe as the other. A weak joint at its lower end enabled the power cable to be withdrawn when drilling was completed. The hotpoint itself was lost however.

The holes were drilled vertically, rather than normal to the glacier surface. An estimate of the ice thickness at each drill site was available from the seismic data. When the hotpoint stopped drilling at a depth greater than this, it was kept running for several hours. If no further progress were made, it was concluded that bedrock had been

reached. The pipe was then lifted one or two metres off the bed.

One problem encountered was that the pipe tended to become seized by the ice about 7 m. below the surface. This corresponds to the depth of the previous winters' "cold wave" in the ice. This difficulty has also been reported by Meier (1960, p. 32). It was overcome by drilling a preliminary hole to this depth, lining it with a pipe open at the bottom, and pouring down antifreeze periodically. The hole was then drilled beside this pipe.

The first holes were lined with aluminium pipe of 3.5 cm. internal diameter. This left a clearance of only 1.5 mm. between pipe and inclinometer. Thus it proved difficult to lower the inclinometer down the pipe. Pipe of 4.1 cm. internal, 4.8 cm. external diameter was used after the first season, apart from one hole which was lined with the remaining narrow pipe. Increase in pipe diameter necessitated modifications in hotpoint design, and the external diameter was increased to 5.7 cm.

The pipe was supplied in 3.05 m. lengths. These were joined by screw couplings. The external diameter of the couplings exceeded that of the pipe by 0.8 cm. Various methods of sealing the couplings were tried. None of these proved completely satisfactory. The pipes were generally kept filled with a solution of antifreeze and water. Water in the pipe appeared to cause failure of hotpoints however,

so attempts were made to keep two of the later holes (holes 209 and 194) dry. At the end of the season several gallons of antifreeze were poured down each pipe and the pipes were capped to prevent the entry of snow.

These precautions proved sufficient to prevent the pipes from being badly frozen up by the following summer. Plugs of ice serveral metres thick were encountered, generally near the surface or near the bottom. This ice was melted out by a hotpoint designed by Savage for use inside the pipe. This hotpoint did not perform as expected and was barely adequate to clear the small amount of ice encountered.

2.5.2. Inclinometer

The inclinometer was rented from the Parsons Survey Company. It was of the single-shot type. The positions of a compass needle and a pendulum inside the instrument are recorded photographically after a preset interval of time. Inclinations to the vertical of up to 4° can be measured to an accuracy of 0.1°. By using shorter pendulums, inclinations up to 10° or 26° can be measured with the same relative accuracy. Azimuths can be read to 1°. During the first two summers water tended to leak into the instrument and cause damage. But a leather washer which proved to be watertight was finally fitted.

The inclinometer was lowered down the pipe on a stainless steel wire. Distance was determined by measuring the length

of wire paid out. This was done along a base line with marks at 25 foot (7.62 m.) intervals which was laid out along the glacier surface from the borehole.

2.5.3. Acid Bottles

After one year, one pipe had become so badly bent near the bottom that the inclinometer would not pass. Acid bottles were improvised to make the measurements. Glass bottles about 10 cm. long were half filled with hydrofluoric acid and filled up with oil. This prevented the hydrostatic pressure of water in the pipe from breaking the glass. No appreciable etching of the glass should occur during the few minutes necessary for lowering the bottle. A suitable acid concentration had therefore to be determined by experiment. The bottles were left stationary in the pipe for 20 to 30 minutes. The accuracy of this method was tested by making measurements at depths where readings could also be made with the inclinometer. Readings agreed within 1°. Acid bottles do not provide azimuth measurements.

2.5.4. Boreholes

In 1959 holes were drilled to depths of 198, 228, and 314 m. Only the last reached bedrock. The others failed because hotpoints burnt out. Six hotpoints were used during the season. The aluminium pipe was removed from the 198 and 228 m. holes. An inclinometer survey was attempted in the 314 m. hole but results were unreliable. During this survey

the pipe became permanently blocked at a depth of 50 m. by a chain which was used to add weight to the inclinometer.

In 1960 four holes were drilled to depths of 322, 209, 194 and 116 m. The first three reached bedrock. Hole 322 required four hotpoints, hole 116 two, and the other two holes, which were kept dry during drilling, one each. The locations of these holes have been given in section 2.4.3. and are shown in Figure 2. Inclinometer surveys were made in holes 322, 209, and 116, and to a depth of 50 m. in hole 314. The spacing between readings was generally 15.24 m. The spacing was 7.62 m. in the top 50 m. of hole 322 and in some sections of hole 116, however. Within five days after completion of the drilling of hole 194, ice formed within the pipe. An attempt to clear it with a hotpoint supplied by W.H. Mathews failed after 50 m. had been cleared at an average rate 0.5 m./hr. Cause of failure was the formation of ice above the hotpoint which prevented its removal.

In 1961 only one hole (hole 248) was drilled. Its sole purpose was to determine ice thickness, so the hole was not cased. Inclinometer surveys of holes 322, 209, 116 and 314 (down to 50 m.) were made at intervals of 7.62 m. Sections of pipe had to be removed to compensate for the lowering of the ice surface by ablation. But observations were made at the same points in each pipe in successive years.

It is hoped to repeat the surveys in 1962.

2.6. Other Data

2.6.1. Map

The Water Resources Branch of the Department of Northern Affairs and National Resources has produced a map from their survey and air photographs made in 1959. This is the map used for Figure 2. The map has a scale of 1:4800 and a contour interval of 10 feet (3.05 m.) below 7800 feet (2377 m.) and 40 feet (12.2 m.) above. A copy is included in the report of Reid (1961). The Branch plans to make a new map every three years. The slope of the glacier surface at the survey markers and boreholes has been determined from this map.

2.6.2. Recession Data

The Water Resources Branch made surveys of the terminus every year between 1945 and 1950, and every second year thereafter. The surveys consist of a plane table survey of the position of the terminus, a vertical profile and a horizontal velocity profile across a line some 400 m. from the present terminus. The report of the 1960 survey also contains data from all previous ones (Collier, 1960).

2.6.3. Streamflow Records

The Water Resources Branch also have flow records for the Sunwapta River at its exit from the lake at the terminus of the glacier. These records date back to 1948.

3. COMPUTATIONS

3.1. Position

3.1.1. Horizontal Position

Horizontal positions were computed in terms of a rectangular coordinate system. The origin was taken at Triangulation Station 1 of the Water Resources Branch's survey. Its position was determined from a large scale topographic map to be 52°13'12"N., 117°13'30"W.

One axis was taken along the survey base line which ran from station 1 to station 3. The azimuth of this direction was 189°25' measured clockwise from true north. The magnetic declination in 1960 was 24° E. The unit of coordinates was taken as 1 mm. The origin was given false coordinates E = 2 000 000 N = 2 000 000. The coordinates of each of the 21 stations, and all azimuths between stations which were required, were computed from the results of the Water Resources Branch's survey.

The field observations from each station were reduced as follows. For each marker, the mean of the face left reading, and the face right reading plus 180°, were taken. This angle was converted to an azimuth by the relation:

Azimuth of marker = (Azimuth of reference station) +
(observed angle to marker) -
(observed angle to reference station).

Subsequent calculations were carried out on the University of British Columbia's Alwac III C computer. The programme was written by Mr. J. Allard. Each marker was observed from three stations. The stations were taken in pairs in the three possible ways. The coordinates of the marker were determined from each pair of observations by the formulae:

$$E_P = \frac{E_A \cot A - E_B \cot B - N_A + N_B}{\cot A - \cot B}$$

$$N_P = N_A + (E_P - E_A) \cot A$$

Suffixes A, B, P refer to the two observation stations and the marker respectively. The stations must be taken in such an order that P lies to the right of the direction A to B. A, B in the formulae are the azimuths to P from stations A and B respectively. E, N are coordinates.

Alternative formulae are

$$N_P = \frac{N_A \tan A - N_B \tan B - E_A + E_B}{\tan A - \tan B}$$

$$E_P = E_A + (N_P - N_A) \tan A$$

It is generally more accurate to use the tangent formula for angles between 0° and 45° and the cotangent formula for angles between 45° and 90°. But for ease of programming only one formula, the cotangent one, was used. The accuracy of the computer calculations was still more than adequate.

The computer output consisted of three pairs of coordinates for each marker. If the spread of the three values was less than 10 cm., their mean was taken. Otherwise the three points were plotted and the centre of the inscribed circle of the triangle was taken as the position. A position was rejected if the radius of the circle represented a distance of more than 25 cm., unless there was a sound reason for rejecting the observations from one station. In this latter case the intersection of the rays from the other two stations was taken as the position.

In two or three instances, observations to a marker from one station were made a day later than the observations from the other two stations. In this case the ray from the station in question in the intersection diagram was displaced parallel to itself by an amount equal to the movement of the marker in one day. This movement was determined for another observation period.

The computer output consisted of 10 figures. Station coordinates were 7 figure numbers (mm.), but coordinates of markers were rounded to 6 figures (cm.) for subsequent calculations.

Where necessary, coordinates were corrected for the amount the marker was leaning at the time of the survey.

The computer also calculated the distance from each station to the marker, for each pair of rays. These distances were used in the height computations.

In a few instances a marker was only observed from two stations. No estimate of the accuracy can be obtained in this case. The height calculations were therefore used as a check. The heights of the marker as computed separately from the two stations were compared. If they did not agree within 10 cm. it was considered that the calculated position might be inaccurate, and it was rejected.

In November 1960, some markers were only observed from one station. It was necessary to assume a direction of movement in order to calculate the amount which the marker had moved since the previous observation period. The direction assumed was that for the period August 1959 to July 1960. The amount of movement d was calculated from

$$d = \frac{r_1 \sin(\theta_2 - \theta_1)}{\sin(A - \theta_2)}$$

where θ_1, θ_2 are the azimuths of the marker from the station as observed in August 1960 and November 1960 respectively. A is the azimuth of the assumed direction of movement. r_1 is the distance from station to marker

in August 1960. For the height calculations it was also necessary to determine r_2, the distance in November 1960. This was given by $r_2 = r_1 + \delta r$ with

$$\delta r = r_1 \sin(\theta_2 - \theta_1) \cot(\theta_2 - A)$$

Velocities determined by this method were naturally less accurate than the others.

3.1.2. Vertical Position

Calculations were carried out in millimetres and results were rounded to centimetres. To reduce the number of figures, 6000 feet (182880 cm.) was taken as datum. All heights quoted are in centimetres above datum.

The theodolite readings were converted to angles from the horizontal. The four readings (two on each face) were meaned. The computer input consisted of this mean and the height of instrument above datum. Distance from station to marker was computed as explained in the previous section. A standard correction for atmospheric refraction and earth's curvature was used. The value was $6.755 \times 10^{-11} r^2$ where r is the distance in millimetres from station to marker. This corresponds to the value of 13.6" per Km. which is generally used by surveyors.

The formula used was

$$h = h' - r \tan\theta + 6.755 \times 10^{-11} r^2$$

where

h = height in mm. of top of marker above datum

h' = height in mm. of instrument above datum

θ = observed angle of depression (positive) or elevation (negative).

The horizontal observations from the three stations were taken in pairs as explained previously. Each pair yielded two heights (one from each station). A total of six heights for each marker was thus obtained. If the spread of the six was not greater than 10 cm. the mean was taken. If the spread was greater than 10 cm. the separate heights were examined. If the observations from any station were made under conditions which might suggest anomalous refraction (observations late in the day from a station near the ice for example), these observations were rejected. This happened on a very few occasions. Otherwise all the measurements were rejected and the height was left undetermined.

Heights of markers which were leaning were corrected. Heights were also corrected for re-drilling of holes. Movement studies thus refer to the element of ice which was at the foot of each marker at the start of the 1959 season.

Observations to any one marker from three stations were regarded as simultaneous if they were made on the same day. In fact they were separated by several hours. The errors introduced by this procedure are insignificant.

3.2. Velocity

3.2.1. Horizontal Velocity

The magnitude (U) and direction (A) of the mean velocity of a marker were calculated from its coordinates at successive observation periods. This velocity is measured in a horizontal plane. Horizontal velocities are much greater than vertical ones, and the slope of the glacier seldom exceeds 10°. Thus horizontal velocities do not differ significantly from velocities measured in the plane of the glacier surface.

3.2.2. Vertical Velocity

Two velocities must be distinguished.

1. Velocity V relative to a vertical axis.
2. Velocity v relative to an axis normal to the glacier surface at the point in question.

The downward direction will always be taken as positive.

Velocities refer to a particle of ice just below the surface of the glacier (at the foot of each marker). v is not the velocity of rise or fall of the surface, because the surface level changes as a result of ablation as well as of ice flow.

The mean value of V between successive observations was calculated directly from the observed change in height above datum of the top of the marker. The mean value of v was calculated from the formula:

$$v = V \cos \alpha_s - U \cos \Delta A \sin \alpha_s$$

α_s is the angle of maximum surface slope at the marker, taken positive.

ΔA is the angle between the directions of movement of the marker and of the corresponding point on the centreline. The angle is measured in a horizontal plane.

3.2.3. Velocity of Slip past Side Walls

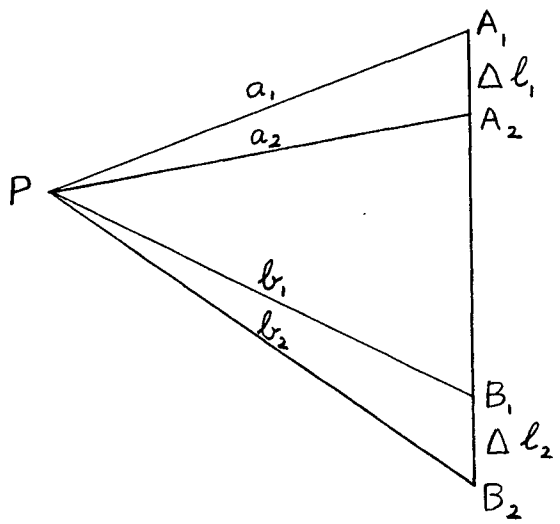

In the diagram, P is a fixed mark on rock; A_1, A_2 are the positions of one marker in the ice at successive times; B_1, B_2 are corresponding positions of the other marker.

It is assumed that A_1 A_2 B_1 B_2 is a straight line.

a_1, a_2, b_1, b_2, A_1B_1, A_2B_2 are measured.

Angles A_1 and B_2 are calculated from triangles A_1B_1P, and A_2B_2P. $A_1A_2 (= \Delta\ell_1)$, $B_1B_2 (= \Delta\ell_2)$, the distances moved by the stakes, are then calculated.

3.2.4. Velocity Averaged over Width of Glacier

It was necessary to calculate this quantity in order to use one method of estimating the transverse strain rate. The mean velocity was calculated for each transverse line of markers. Measurement of the width of the glacier is treated

in section 3.7.2. The velocity is comparatively small near the edges of the glacier. Small errors in width therefore have little effect on the mean velocity.

For each transverse line, observed velocities were plotted against distance across the glacier. Velocities at points 100 m. apart were determined by interpolation. The mean velocity was calculated by numerical integration by the repeated Simpson Rule.

For 11 points this is

$$\bar{u} = \frac{1}{30}\left(u_0 + 4u_1 + 2u_2 + 4u_3 + \cdots + 4u_9 + u_{10}\right)$$

where u_0, u_1, u_2 · · · are the velocities at the points in question.

3.2.5. Velocity Averaged over Thickness of Glacier

To make an accurate calculation of this quantity, the distribution of velocity with depth must be known. This is only known at boreholes. However, the mean velocity is not very sensitive to the velocity distribution. If it is assumed that the flow is laminar and obeys the flow law determined in laboratory experiments, it can be shown (Nye, 1952b, p. 84) that

$$u - u_s = B\, y^{n+1}$$

where u is velocity at depth y

u_s is surface velocity

B is a constant

n = 3 or 4 is the index in the flow law.

It follows that

$$\bar{u} - u_s = \frac{B}{n+2} h^{n+1}$$

where $\bar{u}$ is the velocity averaged over the total thickness h.

Also $$u_b - u_s = B h^{n+1}$$

where u_b is the velocity at the bed.

Thus

$$\frac{\bar{u} - u_b}{u_s - u_b} = \frac{n+1}{n+2}$$

For $n = 3$,

if

$u_b = 0$ $\quad \bar{u} = 0.8\ u_s$

$u_b = \frac{1}{2} u_s$ $\quad \bar{u} = 0.9\ u_s$

$u_b = u_s$ $\quad \bar{u} = u_s$

$\bar{u} = 0.9\ u_s$ was taken as a representative value.

3.3. Slope

3.3.1. Surface Slope

There were two possible methods of determining the slope of the ice surface at markers on the longitudinal line.

1. The height of the top of each marker above datum and above the ice surface, and the distances between markers were all known. The slope at a marker was taken as the mean of the slopes between it and its two adjacent markers.

2. The slope was measured from the map. With this

method, the distance over which the slope was measured could be varied. In addition, this is the only method available for markers off the centreline. For these reasons map measurement was used throughout.

For purposes of analysis the mean slope over a distance comparable with the ice thickness was required. Distances were thus about 250 m. Shorter distances were taken near the sides of the glacier and where the surface slope was changing rapidly. The map distance was always measured between an integral number of (3.05 m.) contours. Slope was always measured in the direction of maximum slope.

The map was made in 1959. Slopes at the positions of the markers in all three seasons were measured from it. This procedure can be justified because the survey showed little change in the surface configuration of the glacier, along the centreline, over the three seasons.

3.3.2. Slope of Glacier Bed

The slope of the bed in both longitudinal and transverse directions was determined from the seismic records at some 30 points. These included holes 322, 314, and 209, and 14 other points on the longitudinal line. The slope could have been calculated by numerical differentiation at other points on the longitudinal and transverse lines. These data were not required however.

3.4. Strain Rates

3.4.1. Strain Rates around Boreholes

The longitudinal strain rate $\dot{\varepsilon}_x$, the transverse strain rate $\dot{\varepsilon}_z$, and the shear strain rate $\dot{\varepsilon}_{xz}$ were determined from measurements of the squares of stakes around each borehole. These strain rates all refer to the plane of the glacier surface. The method is due to Nye (1959b).

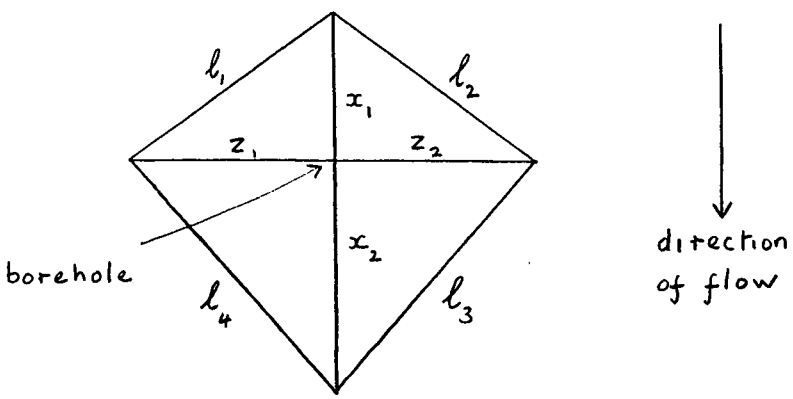

Let x_1, x_2, z_1, z_2 be the lengths of the up-glacier, down-glacier, and two transverse diagonals respectively, and ℓ_1, ℓ_2, ℓ_3, ℓ_4 the lengths of the sides of the square. Let Δ denote the change in length between two observation periods.

The quantities

$$\dot{\varepsilon}_0 = \frac{1}{2t}\left(\frac{\Delta x_1}{x_1} + \frac{\Delta x_2}{x_2}\right) \qquad \dot{\varepsilon}_{45} = \frac{1}{2t}\left(\frac{\Delta \ell_2}{\ell_2} + \frac{\Delta \ell_4}{\ell_4}\right)$$

$$\dot{\varepsilon}_{90} = \frac{1}{2t}\left(\frac{\Delta z_1}{z_1} + \frac{\Delta z_2}{z_2}\right) \qquad \dot{\varepsilon}_{135} = \frac{1}{2t}\left(\frac{\Delta \ell_1}{\ell_1} + \frac{\Delta \ell_3}{\ell_3}\right)$$

were calculated (t years is the time between observations).

The best estimates (in a least squares sense) of strain rates are then

$$\dot{\varepsilon}_x = -\tfrac{1}{4}\dot{\varepsilon}_0 + \tfrac{1}{4}\dot{\varepsilon}_{45} + \tfrac{3}{4}\dot{\varepsilon}_{90} + \tfrac{1}{4}\dot{\varepsilon}_{135}$$

$$\dot{\varepsilon}_z = \tfrac{3}{4}\dot{\varepsilon}_0 + \tfrac{1}{4}\dot{\varepsilon}_{45} - \tfrac{1}{4}\dot{\varepsilon}_{90} + \tfrac{1}{4}\dot{\varepsilon}_{135}$$

$$\dot{\varepsilon}_{xz} = \tfrac{1}{2}\dot{\varepsilon}_{45} - \tfrac{1}{2}\dot{\varepsilon}_{135}$$

The standard errors of the estimates are $\sqrt{3}\,|R|$, $\sqrt{3}\,|R|$, $\sqrt{2}\,|R|$ respectively, where $R = \frac{1}{4}(\dot{\varepsilon}_0 + \dot{\varepsilon}_{90} - \dot{\varepsilon}_{45} - \dot{\varepsilon}_{135})$. Measurements were made over a period of approximately one year. The sides of the squares were between 120 and 180 m. long. The measurements were not quite complete as some stakes were lost by ablation.

3.4.2. Longitudinal Strain Rate

The longitudinal strain rate at the surface between each pair of markers on the centreline was calculated from

$$\dot{\varepsilon}_x = \frac{2.3026}{t} \log_{10} \frac{\ell_2}{\ell_1}$$

$\dot{\varepsilon}_x$ is the strain rate averaged over the time t years between successive observations. ℓ_1, ℓ_2 are distances between the markers at the beginning and end of the period. This strain rate refers to a horizontal axis.

When $|\dot{\varepsilon}_x|$ was less than 0.02 per year the following

formula was sufficiently accurate:

$$\dot{\varepsilon}_x = \frac{+}{t} \cdot \frac{\ell_2 - \ell_1}{\ell_1}$$

3.4.3. Transverse Strain Rate

Transverse strain rates $\dot{\varepsilon}_z$ between adjacent markers were calculated for each transverse line by the formula of section 3.4.2.

The transverse strain rate, averaged over the width of the glacier, was determined at each marker in the longitudinal line by Nye's formula (Nye, 1959c, p. 506),

$$\dot{\varepsilon}_z = \frac{\bar{U}}{w} \cdot \frac{dw}{dx}$$

w is the width of the glacier

x is distance measured along the centreline

$\bar{U}$ is velocity averaged over depth and width .

A value of $\bar{U} = 0.75\ U_s$ was taken, with U_s the surface velocity at the centreline. This combines a velocity of $0.85\ U_s$ averaged over the width (the average value for the six transverse lines), and $0.9\ U_s$ averaged over the thickness. This last value was derived in section 3.2.5.

To calculate $\frac{dw}{dx}$, w was tabulated at intervals of 100 m. of x . $\frac{dw}{dx}$ at each of these points was calculated by the formula

$$100 \left(\frac{dw}{dx}\right)_0 = \mu\delta w_0 - \frac{1}{6}\mu\delta^3 w_0$$

where $\mu\delta$, $\mu\delta^3$ denote first and third mean central differences respectively. This formula is obtained by differentiating the Newton-Stirling interpolation formula. Values of $\frac{dw}{dx}$ at 100 m. intervals were then plotted, and values at each of the longitudinal markers found by interpolation.

3.4.4. Rate of Change of Normal Velocity

Values of $\frac{\partial v}{\partial x}$ (rate of change with distance down the glacier of the velocity normal to the surface) were calculated by the same method of numerical differentiation as was used to calculate $\frac{dw}{dx}$ in section 3.4.3.

3.5. Ice Thickness

The error of seismic measurements of ice thickness was considered to be smaller than that of gravity measurements. Seismic data have therefore been preferred to gravity. At boreholes, the depth of the borehole has been used in preference to the seismic value. The discrepancy between seismic and borehole measurements was very small however. Seismic measurements were made along the longitudinal line and transverse lines C and D. Gravity measurements have been used for the other transverse lines. Consistency of

results of the two methods was obtained as follows. Each gravity value on a transverse line was multiplied by the constant factor necessary to make seismic and gravity values agree at the point where the transverse line intersects the longitudinal one. For this reason, ice thicknesses quoted here sometimes differ from those given by Kanasewich (1960). It should be noted that gravity measures the vertical thickness whereas seismic measurements are normal to the bed. The difference between the two is within the standard error of the seismic data for all points on the longitudinal line.

3.6. Borehole Measurements

Inclination to the vertical, γ, of the axis of the pipe, and its azimuth, A, projected on to a horizontal plane, at various depths, were measured in two successive years. The spacing between observations was generally 15.24 m. in 1960 and half this figure in 1961. The quantity to be determined is $\frac{\partial u}{\partial y}$, the gradient of velocity parallel to the surface in the direction normal to the surface. Various methods of analysis were used to see whether they led to appreciably different results. The formulae are summarized in this section. Symbols have the same meaning throughout and are only defined once. The various methods are discussed in section 5.3.

1. Nye's formula (equation 22 of section 5.3.).

For each point at which inclinations were measured,

$$\frac{\partial u}{\partial y} = \frac{1}{t}\left(\tan\theta' - \tan\theta\right) - \frac{\partial u}{\partial x}\left(\tan\theta' + \tan\theta\right)$$

$$\theta = \arctan\left(\tan\gamma\cos\Delta A\right) - \alpha_s$$

Dashes refer to second set of observations.

γ = measured inclination

ΔA = difference between measured azimuth and azimuth of flow direction as measured at the surface.

α_s = surface slope (positive)

t = time in years between observations.

Three cases were taken.

(a) $\frac{\partial u}{\partial x} = 0$ "laminar flow".

(b) $\frac{\partial u}{\partial x} = \left(\frac{\partial u}{\partial x}\right)_s$ the surface value.

(In Nye's theory of glacier flow it is assumed that $\frac{\partial u}{\partial x}$ does not change with depth y.)

(c) Variable $\frac{\partial u}{\partial x}$

$$\frac{\partial u}{\partial x} = \left(\frac{\partial u}{\partial x}\right)_s + Ky$$

K is given by

$$\frac{1}{2}Kh = \frac{v_s - u_b \tan(\alpha_b - \alpha_s)}{h} - \left(\frac{\partial u}{\partial x}\right)_s$$

α = slope, subscripts s, b refer to surface and bed.

h = ice thickness.

This formula is derived in section 5.1. (equation 15).

2. Formula for curved pipe (section 5.3., equation 23).

$$\frac{\partial u}{\partial y} = \frac{\theta' - \theta}{t}\sec^2\bar{\theta} - 2\frac{\partial u}{\partial x}\tan\bar{\theta} + \frac{\partial v}{\partial x}\tan^2\bar{\theta} + (u\tan\bar{\theta} + v)(\sec\bar{\theta})\left(\overline{\frac{\Delta\theta}{\Delta s}}\right)$$

$$\bar{\theta} = \frac{1}{2}(\theta' + \theta)$$

The last three terms on the right hand side are relatively small correction terms. Accurate values of the separate quantities are not needed.

If inclination is measured at distances (measured along the pipe) Δs, $2\Delta s$, $\cdots$ from the top, at the n^{th} point

$$\left(\frac{\Delta\theta}{\Delta s}\right)_n = \frac{\theta_{n+1} - \theta_{n-1}}{2\Delta s}$$

$\left(\overline{\frac{\Delta\theta}{\Delta s}}\right)_n$ is the mean for the two years.

The value of u was obtained from a preliminary laminar flow analysis.

v was determined by equation 13 of section 5.1.

This gives a quadratic variation of v with depth and satisfied the boundary condition at the bed

$$v_b = u_b \tan(\alpha_b - \alpha_s)$$

The term $\frac{\partial v}{\partial x} \tan^2 \bar{\theta}$ is negligible.

Two cases were taken: (a) $\frac{\partial u}{\partial x}$ zero, (b) $\frac{\partial u}{\partial x}$ variable with depth as in the last section.

3. Integrated Method

This method is due to Savage.

Inclinations were measured at points Δs, $2\Delta s$, $\cdots$ from the top of the pipe. (The zero point for measurements was the top in the first year. Sections of pipe had to be removed later to compensate for ablation. However, readings were taken at the same points in the pipe each year, except for the reading at the top.)

The configuration of the borehole in each year was computed in terms of right-handed rectangular coordinate systems X, Y, Z and x, y, z. The X axis was horizontal, the x axis in the surface. The down-glacier direction was taken as positive.

The Y axis was vertical, the y axis normal to the surface. Both were taken positive downwards. The origin was the ice surface at the time of the first year's observations. The surface slope did not change significantly from year to year. Measurements of surface velocity gave X_o and Y_o in the second year. Z_o was again taken to be zero.

Coordinates were calculated by the formulae:

$$X_{n+1} - X_n = \frac{1}{2}\left(\sin \gamma_n \cos \Delta A_n + \sin \gamma_{n+1} \cos \Delta A_{n+1}\right) \Delta s$$

$$Y_{n+1} - Y_n = \frac{1}{2}\left(\cos \gamma_n + \cos \gamma_{n+1}\right) \Delta s$$

$$Z_{n+1} - Z_n = \frac{1}{2}\left(\sin \gamma_n \sin \Delta A_n + \sin \gamma_{n+1} \sin \Delta A_{n+1}\right) \Delta s$$

$$x_n = \left(X_n + Y_n \tan \alpha_s\right) \cos \alpha_s$$

$$y_n = \left(-X_n \tan \alpha_s + Y_n\right) \cos \alpha_s$$

$$z_n = Z_n$$

$$\textcircled{H}_n = \text{arc tan}\left(\tan \gamma_n \cos \Delta A_n\right)$$

$$\theta_n = \textcircled{H}_n + \alpha_s$$

The configuration of the pipe in the xy plane in each year was plotted. Displacement parallel to the x axis was measured from the graph, at equal intervals of y. When

converted to velocity, this quantity equals $\vartheta \sec \theta$ where ϑ is velocity normal to the pipe and θ is defined above.

$$\vartheta = u \cos \theta + v \sin \theta$$

where u, v are velocities in the x, y directions respectively. The value of u at point n was determined from

$$u_n = \vartheta_n \sec \bar{\theta}_n - v_n \tan \bar{\theta}_n$$

$\bar{\theta}_n$ is the mean value of θ at point n for the two observation periods. v_n was found by linear interpolation between its measured value at the surface and its value $u_b \tan (\alpha_b - \alpha_s)$ at the bed.

Values of $\frac{\partial u}{\partial y}$ were found by numerical differentiation.

Reduction of the data by this method was carried out by Savage. Calculation of coordinates and values of ⊛ and θ was performed on a Bendix computer at the Institute of Geophysics and Planetary Science, University of California at Los Angeles. The interpretation of this data in terms of current theories of glacier flow, given in subsequent sections of this thesis, is however the responsibility of the present author.

3.7. Miscellaneous Quantities

3.7.1. Curvature of Surface and Bed

The rate of change of slope α with distance X down the glacier was determined, for markers in the longitudinal line, by numerical differentiation. Slopes relative to the horizontal were used.

The curvature k was then calculated from

$$k = \frac{\frac{d}{dX}(\tan \alpha)}{(1 + \tan^2 \alpha)^{3/2}}$$

In most cases the denominator could be taken as unity.

3.7.2. Width of Glacier

This quantity is required both for the drawing of transverse profiles and the calculation of transverse strain rate (section 3.4.3.). The large amount of debris on each side of the glacier made location of the edge difficult. It was however determined with fair accuracy by Kanasewich (1960) for his gravity survey. The width of the glacier at different points as measured between the zero ice thickness contours on Kanasewich's Figure 4 has been used in the present study.

3.7.3. Long-period Change in Ice Thickness

A rough estimate was obtained of the rate at which the lower reaches of the glacier have been thinning during

the past century. Two triangulation stations were located on the crest of the prominent south-east lateral moraine. The heights of these points above the present ice surface were known. Evidence discussed in section 1.2. indicates that the glacier was at a maximum about 130 years ago. The level of the moraine was taken to correspond to the level of the ice at this maximum. The average rate of thinning over the past 130 years was thus calculated.

The rate of thinning over the past 15 years is known from the surveys of the Water Resources Branch. Every second year the height of the ice surface was measured across a transverse line about 350 m. from the present terminus.

Agreement between rates given by these two methods was surprisingly good.

3.7.4. Travel Time for Ice

A rough estimate was obtained of the time which ice takes to travel from the accumulation area on the Columbia Icefield to the terminus of the glacier. The integral $\int \frac{1}{u} dx$, where u is the surface velocity along the centreline, was evaluated numerically by the Euler-Maclaurin formula. Ordinates were taken at 100 m. intervals in the lower part of the glacier. Above the lowest icefall, ordinates were taken at the 10 points near the centreline where surface velocity was measured.

It was assumed in this calculation that a particle of

ice travels parallel to the surface. This is not of course the case. Thus the distance and the time were underestimated. On the other hand, the glacier appears to be thinner now than at any time during the past 100 years. (The travel time is of this order.) Hence the present velocity is likely to be considerably less than the mean velocity over this period. This will to some extent offset the other source of error.

4. ACCURACY

4.1 General

The accuracy of the various measurements will be discussed in this section. The analysis does not apply to markers J1 to J12. Measurements on these markers were of a lower standard of accuracy than measurements to the others. Throughout this discussion "error" means standard error. In the analysis, any doubtful or substandard observations were invariably rejected. The standard of accuracy of the data used should thus be fairly uniform.

Apart from inaccuracies in measurement, there is also the possibility of errors in computation. A number of extra figures sufficient to make rounding errors negligible was always carried. All computations, except those carried out on the electronic computer, were done twice, independently. It is hoped that this procedure eliminated any gross errors. Calculations on the computer were only done once, but the data input was double checked.

4.2. Position

4.2.1. Horizontal Position

The basis for determination of position is the survey of the Water Resources Branch which established triangulation stations around the perimeter of the glacier. The accuracy of the survey is not discussed in the report (Reid, 1961).

Distances are quoted to 0.01 foot (3 mm.) however. Results should therefore be accurate to 1 cm. at least. This is about ten times the degree of accuracy expected in the glacier movement survey. Any errors in positions of triangulation stations have therefore been ignored.

Accurate location of stations presented no difficulty, as each was marked by a brass plug set in rock. Their stability must be considered however, as a few were situated on moraines. Positions and elevations of markers as determined from station 9 showed a consistent difference from their positions and elevations as determined from other stations. Moreover, the discrepancy increased with time. Slumping of the station was the most plausible explanation. This was quite likely as the station was located on the crest of the south-east lateral moraine at a point where the crest is extremely narrow. All observations from station 9 were therefore rejected. None of the observations from any other station gave any indication of instability.

Each marker was observed from three stations. Observations from each station provide a line on which the position of the marker must lie. The mean of the three intersections of the three lines was taken as the position. The fact that the three intersections do not coincide can be attributed to inaccuracies in the following: alignment of theodolite and reference mark over their station marks; sighting on the marker; lateral refraction;

and the fact that observations from the three stations were not simultaneous. The effects of these inaccuracies are reduced by taking the mean of the three intersections. There are, however, other sources of error which produce a consistent effect on observations from all three stations. These are slight differences between the horizontal positions of a marker before and after the hole had been redrilled, and inaccuracies in measuring the amount by which a marker was leaning.

Over all the data, the spread (greatest distance between any two of the three intersections) had a mean value of approximately 10 cm. About 65% of the spreads did not exceed this value. This spread might be interpreted as three or four times the standard error of the mean position of the three intersections. However, it has been taken as the standard error to allow for the consistent errors as well.

During summer 1960 short term variations in velocity were studied by weekly observations of the positions of certain markers. An attempt was made to attain a higher standard of accuracy in these measurements and this was reflected in smaller spreads of the intersections. The standard error of these positions is estimated to be 5 cm.

No direct estimate of error can be obtained when markers were only observed from two stations. As was explained in section 3.1.1. however, such observations were

rejected if the heights from the two stations did not agree closely. The normal standard error of 10 cm. has therefore been taken.

As explained in section 3.1.1., some markers were only observed from one station in November 1960. The formula used was

$$d = \frac{r_1 \sin(\theta_2 - \theta_1)}{\sin(A - \theta_2)}$$

Thus $$\frac{\delta d}{d} = \frac{\delta r_1}{r_1} + \frac{\delta(\theta_2 - \theta_1)}{\theta_2 - \theta_1} + \frac{\delta(A - \theta_2)}{\tan(A - \theta_2)}$$

where δ denotes the error in a quantity. Typical values were

$\delta r = 10$ cm. $\quad \delta(\theta_2 - \theta_1) = 5'' \quad \delta(A - \theta_2) \approx \delta A = 1^\circ$

$r = 0{\cdot}8$ Km. $\quad \theta_2 - \theta_1 = 30' \quad A - \theta_2 \geq 35^\circ$

$d = 7$ m. $\quad \tan(A - \theta_2) \geq 0{\cdot}7$

Hence $\delta d \approx 20$ cm. This is the standard error of position in this case.

The standard error of positions of markers J1 to J12 is estimated from the spreads in the intersections to be 50 cm.

To sum up, the standard error of horizontal position of a marker is 5 cm. for the weekly observations in 1960, 20 cm. for some markers at the November 1960 observation period, 50 cm. for markers J1 to J12, and 10 cm. in all

other cases.

The standard error of the distance between two markers or between the positions of one marker at two different times is $\sqrt{2}$ times the standard error of position, i.e. 15 cm. in most cases.

An independent check on this accuracy is available. Distances between markers were measured by steel tape, for strain rate measurements, in a few instances. In four cases the same distances were determined by triangulation at about the same time. Taped distances were measured along the slope and so have been reduced to the horizontal. Distances have also been corrected for the time difference (up to 3 days) between the measurements, using measured values of longitudinal strain rate. Sources of error are different in the two methods. Errors in measurements by tape are due to incorrect tension, neglect of corrections for sag and temperature, and the fact that the tape was probably resting on the ice in places.

Results are given in the following table:

Markers	Date	Distance (cm.) Triangulation	Tape
L30 - L31	12/7/60	17802	17801
Hole 322 - Hole 116	23/7/60	16847	16847
Hole 322 - Hole 116	19/7/61	16473	16478
Hole 209 - Hole 186	19/7/61	15027	15021

The differences between the distances as measured by the two methods are all well within the estimated standard error of 15 cm. This is a satisfactory check on the accuracy of both methods.

4.2.2. Vertical Position

The report on the survey of the Water Resources Branch states that the closure error in the vertical plane is of the order of 1 in 77,000 (Reid, 1961, p. 7). Station elevations are quoted to 0.01 foot (3 mm.). It has been assumed that, to the standard of accuracy of the glacier movement survey, errors in station elevation are negligible.

The mean of the measurements from three stations was taken as the elevation of each marker above datum. This process reduces the effect of errors in individual measurements produced by inaccuracies in sighting on the marker and in measuring the height of the instrument, and because observations from the three stations were not simultaneous. Diurnal variation in refraction makes this time difference important.

The standard refraction correction which was used is equivalent to a height difference of 7 cm. between points 1 Km. apart. (The average distance from station to marker was 0.8 Km.; the maximum was 1.8 Km.). The difference between making no correction for refraction and refraction of double the standard value is thus

equivalent to a height difference of 11 cm. over the average path length. It is unlikely that variations of this magnitude were encountered. Most stations were 50 to 100 m. above the ice and the average vertical angle was a depression of 5°. Thus very few of the rays were close to the ice for appreciable distances.

To test variations of refraction, vertical angles were measured to two markers at intervals of half an hour throughout one day. The spreads of angles were 8" and 11" for path lengths of 1 and 2.4 Km. respectively. The greater of these corresponds to a spread of height of 12 cm. To be of much value this test should have been carried out on several days under widely different weather conditions. However, it may give some indication of the extent of diurnal variations of refraction. Moreover, anomalous conditions would have to persist throughout the day for the mean elevation to be affected by the same amount as the measurement from an individual station.

These considerations suggest that refraction conditions would have to be very exceptional to produce an error of more than 10 cm. in the mean value of the elevation of a marker.

There are factors which will produce a consistent error in elevation measurements from all three stations. There are inaccuracies in measuring the change in elevation when the hole was redrilled and the amount by which a

marker was leaning. Errors may also be introduced if the marker was not gripped firmly by the ice at all times.

The mean spread (difference between greatest and least values) of the elevation of each marker as calculated separately from the three stations was 5 cm. Readings were rejected if the spread was greater than 10 cm.

The mean spread should be greater than the standard error of the mean elevation. However, to allow for the effects of refraction and the other factors listed above, the standard error of the elevation of each marker above datum was taken to be 10 cm. For reasons explained in the preceding section, the same standard error has been taken when the markers were only observed from two stations.

In November 1960 certain markers were observed from only one station. The standard error of these elevations has been taken to be 20 cm.

For the purpose of his gravity survey, Kanasewich made an independent determination of the elevations of all markers by stadia traverses. This provided a gross check on the accuracy. Kanasewich (1960, p. 16) quotes his results to the nearest foot (30.48 cm.). All elevations determined by the two methods agreed to this order of accuracy.

Markers J1 to J12 were further away from the triangulation stations than were other markers. Distances were

up to 3 Km., so the effect of variations in refraction was greater. The standard error of the elevations of these markers may be as great as 50 cm.

4.3. Velocity

4.3.1. Horizontal Velocity

When the period between observations exceeded a week, errors in time measurement (not more than 1/4 day) can be neglected in comparison with those in distance. The error in distance measurement was estimated in section 4.2.1. to be 7 cm. for weekly observations and 15 cm. for the others (except for a few cases). Measured velocities ranged from 7 m./yr. to 270 m./yr.; 30 m./yr. was a typical value. The errors in this last velocity for measurements made over four time periods were as follows:

Time interval	1 week	3 weeks	3 months	1 year
Error in velocity (m./yr.)	4	2.5	0.6	0.15

Direction of velocity A is given by $\tan A = \frac{\Delta E}{\Delta N}$

It follows that $$\frac{2\,\delta A}{\sin 2A} = \frac{\delta(\Delta E)}{\Delta E} + \frac{\delta(\Delta N)}{\Delta N}$$

If sin 2A is given its maximum value, this reduces to

$$\delta A = \frac{\delta(\Delta E)}{\Delta E}$$

since proportional errors in E and N coordinates are roughly equal. $\delta(\Delta E)$ is not more than 15 cm.; 30 m./yr. is a typical velocity. So ΔE is about 15 m. for observations

over a period of a year. In this case $\delta A \approx 1\%$ or $1°$ say. For periods of 3 weeks and 3 months the errors are $15°$ and $4°$ respectively.

4.3.2. Vertical Velocity

Velocity V (vertical).

Values of V were generally between 0 and 4 m./yr. The standard error of the difference between two height measurements was 0.15 m. The standard error of V when measured over a period of one year was thus 0.15 m./yr. For measurements made over a period of 3 months the standard error was 0.6 m./yr. Measurements made over periods of less than 3 months were too inaccurate to be of any value.

Velocity v (normal to surface).

As in section 3.2.2.

$$v = V \cos \alpha - U \cos \Delta A \sin \alpha$$

Hence

$$\delta v = \delta V \cdot \cos \alpha + \delta \alpha \cdot V \sin \alpha + \delta U \cdot \cos \Delta A \cdot \sin \alpha$$
$$+ \delta(\Delta \alpha) \cdot U \sin \Delta A \cdot \sin \alpha + \delta \alpha \cdot U \cdot \cos \Delta A \cdot \cos \alpha$$

The following were typical values:

$\delta \alpha = 0 \cdot 3°$ $\quad \delta(\Delta A) = 1°$ $\quad \delta U = 0 \cdot 15$ m./yr.

$\cos \alpha = 1$ $\quad \cos \Delta A = 1$ $\quad U = 30$ m./yr.

$\sin \alpha = 0 \cdot 1$ $\quad \sin \Delta A = 0 \cdot 02$ $\quad \delta V = 0 \cdot 15$ m./yr.

$V = 2$ m./yr.

Hence $\delta v \approx 0.35$ m./yr. for measurements made over a period of a year.

Most values of v were between 3 and 4 m./yr.

4.3.3. Velocity of Slip Past Side Walls

In the notation of section 3.2.3.,

$$(\Delta \ell)^2 = a_1^2 + a_2^2 - 2 a_1 a_2 \cos A_1 \hat{P} A_2$$

The error in estimating the direction of flow, and hence the error in $A\hat{P}A$, greatly exceeded errors in measuring the distances a_1, a_2. Hence

$$\Delta \ell \cdot \delta(\Delta \ell) = a_1 a_2 \cdot \sin A\hat{P}A \cdot \delta(A\hat{P}A)$$

Typical values were

$$\begin{aligned} a_1, a_2 &= 8 \text{ m.} \\ \Delta \ell &= 12 \text{ m.} \\ \sin A\hat{P}A &= 0.5 \\ \delta(A\hat{P}A) &= 20^\circ \\ \delta(\Delta \ell) &\approx 1 \text{ m.} \end{aligned}$$

So the error in velocity was about 1 m./yr. or about 10%.

4.4. Slope

4.4.1. Surface Slope

This was obtained by measuring the distance between an integral number of contours on the map. A distance comparable with the ice thickness at the point was chosen.

$$\alpha = \frac{\Delta h}{\Delta L}$$

$$\frac{\delta \alpha}{\alpha} = \frac{\delta(\Delta h)}{\Delta h} + \frac{\delta(\Delta L)}{\Delta L}$$

The distance was generally of the order of 200 m. This represented a map distance ΔL of 40 mm. The error $\delta(\Delta L)$ should not have exceeded 1 mm. For an average slope, Δh was of the order of 20 m. The contour interval was 10 ft. (3.048 m.). The error has been estimated at 2 ft. (0.6 m.). An average slope was 5°. Hence $\delta\alpha$, by the above formula, was 0.3°.

4.4.2. Slope of Bed

The standard error of the slope of the bed as determined from the seismic records was estimated to be 1° for the best records and 20% for others.

4.5. Strain Rates

4.5.1. Strain Rates Measured by Taping

The least squares analysis of Nye (1959b), described in section 3.4.1., provides estimates of the standard

errors of the strain rates.

If $R = \frac{1}{4}\left(\dot{\varepsilon}_0 + \dot{\varepsilon}_{90} - \dot{\varepsilon}_{45} - \dot{\varepsilon}_{135}\right)$ the standard errors of $\dot{\varepsilon}_x$, $\dot{\varepsilon}_z$ are $\sqrt{3}|R|$ and of $\dot{\varepsilon}_{xz}$ is $\sqrt{2}|R|$.

4.5.2. Strain Rate from Triangulation

The following analysis applies equally well to longitudinal and transverse strain rates.

$$\dot{\varepsilon} = \frac{1}{t} \cdot \frac{\Delta \ell}{\ell}$$

Percentage errors in measurement of t, the time interval, and ℓ, the distance between the markers, are small compared with the error in $\Delta \ell$, the change in distance.

Thus

$$\frac{\delta \dot{\varepsilon}}{\dot{\varepsilon}} \approx \frac{\delta(\Delta \ell)}{\Delta \ell}$$

$$\delta \dot{\varepsilon} \approx \frac{\delta(\Delta \ell)}{\ell t}$$

The standard error of position is 10 cm., that of distance $\sqrt{2}$ x 10 cm., and that of change of distance $\sqrt{2} \times \sqrt{2} \times 10 = 20$ cm. A typical value of ℓ was 100 m. It follows from the formula that the standard error of strain rate measured over a year was .002 per year, and .008 per year if the period were 3 months. Over a period of less than 3 months results are too inaccurate to have much value.

Smaller errors could have been obtained by using more widely spaced markers. However, it must be assumed that strain

rate does not vary significantly over the distance over which it is measured. This would seldom be the case for marker spacings of more than 300 or 400 metres. Calculations based on the change of width of the glacier provide at best a rough estimate of transverse strain rate. It is hard to quote a standard error. Strain rates calculated in this way are compared with direct measurements in section 6.5.

4.6. Ice Thickness

4.6.1. Seismic Method

Seismic measurements made at borehole sites enabled the accuracy of the method to be tested. The comparison is as follows:

	Depths in metres	
Hole Number	Seismic	Borehole
322	316	321
314	312	317
250	247	250
209	202	209
194	177	194

For holes 209 and 194 the seismic points were displaced from the boreholes by a horizontal distance of 60 m. The seismic value which appears in the above table has been extrapolated to the borehole location by using the indicated dip at the reflection site.

The above table indicates that the seismic measurements of ice thickness are too low by about 5 m. This could be accounted for by assuming that the filter correction and the estimates of the time lapse between the beginning of the reflection and the first well developed trough were each in error by about one millisecond. In as much as the smallest time division on the seismic record is 5 milliseconds this assumption seems justified. It is to be emphasized that the differences in ice thickness between various reflection sites are probably accurate to within 1 m.

The information required, however, is not ice thickness and dip at isolated points but rather a continuous profile of the bed along several sections transverse to the glacier and a profile along a longitudinal section containing the centreline of the glacier. In the latter section important errors of representation arise for the following reason. The seismic reflection comes from the section of the bed closest to the shot point. Because of the high transverse curvature of the bed the section closest to the shot point is often displaced to one side. An extreme case of this type occurred for the reflection at L16 (see sketch).

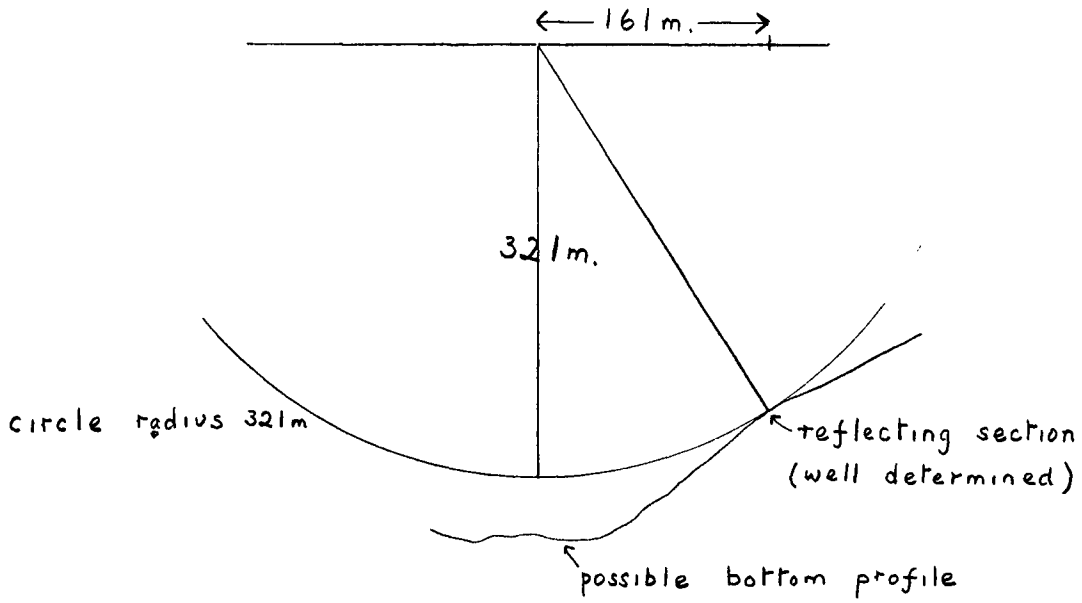

The high quality record obtained at L16 indicated that the reflecting surface was 321 m. from the shot point and that it dipped (relative to the ice surface) 30° $\pm$ 1.5° towards the right edge (looking down glacier) of the glacier. This information suffices to plot the reflecting surface on the transverse profile. It does not determine the depth beneath the shot point. In the absence of other information the depth has been taken as 321 m., although all that is certain is that it is not less than this value. This case is extreme, but reflecting surfaces of transverse dips of 10° were not uncommon for shot points on the centreline, (See Table 8). The down glacier dips were quite moderate so the transverse profiles are relatively free of this error.

4.6.2. Gravity Method

The error of ice thickness as determined by gravity measurements was estimated by Kanasewich (1960, p. 57) to be -10%, +15%.

4.7. Borehole Measurements

The first two methods of analysing the borehole data employ the formulae:

$$(1) \qquad \frac{\partial u}{\partial y} = \frac{1}{t}\left(\tan\theta' - \tan\theta\right) - \frac{\partial u}{\partial x}\left(\tan\theta' + \tan\theta\right)$$

$$(2) \qquad \frac{\partial u}{\partial y} = \frac{\theta' - \theta}{t}\sec^2\bar{\theta} - 2\frac{\partial u}{\partial x}\tan\bar{\theta} + \frac{\partial v}{\partial x}\tan^2\bar{\theta} + \left(u\tan\bar{\theta} + v\right)\left(\sec\bar{\theta}\right)\overline{\left(\frac{\Delta\theta}{\Delta S}\right)}$$

These formulae consist essentially of a first term plus small correction terms. Large errors in the correction terms will not affect the result appreciably. For the purpose of an error analysis only the first term will be considered. To a sufficient approximation, both formulae can be written as:

$$\frac{\partial u}{\partial y} = \frac{\theta' - \theta}{t}$$

Errors in measurement of t, the time interval, are negligible compared with errors in θ.

$$\theta = \arctan(\tan\gamma \cos\Delta A) - \alpha_s$$

$$\approx \gamma \cos\Delta A - \alpha_s$$

Hence $\theta' - \theta = \gamma' \cos\Delta A' - \gamma \cos\Delta A$

$$\delta\left(\frac{\partial u}{\partial y}\right) = \frac{1}{t}\sqrt{2}\,\delta\theta \qquad t \approx 1 \text{ year}$$

$$\delta\theta = \delta(\gamma \cos\Delta A)$$

$$= \cos\Delta A \cdot \delta\gamma + \gamma \sin\Delta A \cdot \delta(\Delta A)$$

$$\leq \delta\gamma + \gamma \cdot \delta(\Delta A)$$

Errors depend on the type of disc used in the inclinometer. The three cases are listed below.

Disc	4°	10°	26°
γ_{max}	4°	10°	20°
$\delta\gamma$	0.1°	0.25°	1°
$\delta(\Delta A)$	1°	1°	1°
$\delta\left(\frac{\partial u}{\partial y}\right)$	0.004	0.01	0.035

It is difficult to estimate the error in calculating $\frac{\partial u}{\partial y}$ by the third method described in section 3.6. So it has been assumed that the errors are the same as in the other methods.

The magnitudes of the terms in formulae (1) and (2) above will now be compared with these errors.

The first terms are

$$\tan\theta' - \tan\theta \approx \theta' - \theta + \tfrac{1}{3}(\theta'^3 - \theta^3)$$

$$(\theta' - \theta)\sec^2\bar{\theta} \approx (\theta' - \theta)\left[1 + \tfrac{1}{4}(\theta' + \theta)^2\right]$$

$$\text{Difference} \leqslant \tfrac{1}{12}(\theta' - \theta)(\theta' + \theta)^2$$

In hole 322 the maximum values occur at the bottom of the hole. They are $\theta' - \theta = 0.11$ and $\theta' + \theta = 0.35$. The difference term is 0.0015 which is negligible compared with the experimental error. In hole 209, the maximum values of the difference term are 0.0002 and 0.0075 when the 4° and 26° inclinometer discs are used respectively. In both cases then differences are less than the experimental error.

The difference in the second terms in formulae (1) and (2) is that between $\overline{\tan\theta}$ and $\tan\bar{\theta}$. The greatest difference occurs at the foot of hole 209. Its value is 0.01. When this is multiplied by $\frac{\partial u}{\partial x}$ (=0.02), it is negligible compared with the experimental error.

As was explained in section 3.6., three alternative values can be taken for $\frac{\partial u}{\partial x}$. These are zero (corresponding to laminar flow), the surface value (corresponding to Nye's assumption that $\frac{\partial u}{\partial x}$ is constant with depth), and a value which varies linearly with depth according to the relation obtained by differentiation of equation 14 of section 5.1. Relevant values at the surface and bed are

given in Table 21. The greatest difference between any of these values is 0.02. For hole 322, $\overline{\tan \theta}$ does not exceed 0.15 except for the bottom reading where it is 0.25. These values correspond to differences of 0.003 and 0.005 in computed values of $\frac{\partial u}{\partial y}$. These differences are slightly less than the standard errors for the appropriate inclinometer discs. In hole 209, $\overline{\tan \theta}$ does not exceed 0.2, except for the bottom value of 0.4. Corresponding differences in calculated values of $\frac{\partial u}{\partial y}$ for a difference of 0.02 in $\frac{\partial u}{\partial x}$ are 0.004 and 0.008. The latter value is negligible compared with the error for the 26° disc which was used. The other value is comparable with the error for the 4° disc.

The third term in formula (2) is negligible in all cases.

The fourth term on the right hand side of formula (2) is the correction for curvature of the pipe. Sections of borehole where inclinations were greater than and less than 10° will be considered separately. The maximum value of the term $(u \tan \theta + v) \sec \theta$ in any borehole was 5 m./yr. The maximum change in θ over a section of borehole of length 15.2 m. was 7.8°. This corresponds to a value of $\frac{\Delta \theta}{\Delta s}$ of 0.009. So the maximum value of the correction term was 0.045. This occurred in a section where the 26° disc was used in the inclinometer. The maximum value of the correction term in sections where 4° or 10° discs were used, was 0.0075. These correction terms are larger than

corresponding errors in measurement.

The conclusions to be drawn from this analysis are that the only difference between formulae (1) and (2) is the correction term for curvature of the pipe. This correction term should be applied, although there are many places in each borehole where its effect is negligible. The difference between a "laminar flow" analysis and one which makes allowance for the longitudinal strain rate is of little importance.

4.8. Ablation and Accumulation

The error in measuring the distance from the top of a marker to the ice surface should not exceed 2 cm. This is negligible compared with the sampling error inherent in the fact that ablation and accumulation can vary appreciably at points on the glacier only a few metres apart.

4.8.1. Ablation

Ablation was measured over a period of 5 weeks at 22 markers arranged in a longitudinal line of 200 m. Values varied between 95 and 133 cm. There was no systematic variation with position, and only 50 m. separated the markers at which greatest and least values were recorded. If these markers are regarded as a sample from an area where ablation was uniform, the standard error of the distribution is 9 cm. or about 10% of the mean. It has been assumed therefore that ablation measurements on single markers have a standard error of 10%.

4.8.2. Accumulation

Similar difficulties occurred in measurements of accumulation. Measurements at 15 markers in the lower part of the glacier ranged from 0 to 2.15 m. The range of values must have been greater than this because the majority of markers were completely buried by snow. The great variation can be largely attributed to the effect of wind. It was concluded that the measurements were insufficient to give any estimate of mean accumulation.

5. THEORY

5.1. Distribution of Stress and Velocity

The following theory is a slightly generalized form of that of Nye (1957). It is restated here from the beginning in order to make clear the assumptions which are involved at each stage.

Assumptions:

I. The ice is isotropic. This is probably a valid assumption for glacier ice.

II. The rate of flow depends only on the stress and not on the time for which it has been acting. In other words, a piece of ice remains under the same stress long enough for a steady state to be reached.

III. Hydrostatic pressure does not affect the flow law. This is an experimental result (Rigsby, 1958).

Consider a rectangular coordinate system fixed in space.

Let u, v, w be the velocity components.

Components of stress will be denoted by σ_{ij} or by σ_x, τ_{xy}, etc.

Components of the stress deviator will be denoted by σ'_{ij} or σ'_x etc.

Components of strain rate will be denoted by $\dot{\varepsilon}_{ij}$ or $\dot{\varepsilon}_x$, $\dot{\varepsilon}_{xy}$ etc.

Let E_2, ε'_2 be the second invariants of the strain rate

and stress deviator tensors respectively.

Let ρ be the density.

Relations of the following types therefore hold:

$$\sigma_x' = \sigma_x - \tfrac{1}{3}\sigma_{ii}$$

$$\sigma_{ij}' = \sigma_{ij} \qquad i \neq j$$

$$\dot{\varepsilon}_{xy} = \frac{1}{2}\left(\frac{\partial u}{\partial y} + \frac{\partial v}{\partial x}\right)$$

$$2E_2 = \dot{\varepsilon}_{ij}\,\dot{\varepsilon}_{ij}$$

$$2\xi_2' = \sigma_{ij}'\,\sigma_{ij}'$$

$$3\xi_3' = \sigma_{ij}'\,\sigma_{jk}'\,\sigma_{ki}'$$

Further Assumptions:

IV. The ice is incompressible. This implies that $\dot{\varepsilon}_{ii} = 0$.

V. The components of strain rate are proportional to the components of the stress deviator. The stress deviator is taken, not the stress, because of III. This is also consistent with IV. Let λ be the constant of proportionality. Then $E_2 = \lambda^2 \xi_2'$. It is shown by Glen (1958c, p. 174) that, under assumptions I to IV, the most general form of the relation between stress and strain rate is

$$\dot{\varepsilon}_{ij} = -\tfrac{2}{3}\xi_2' C\,\delta_{ij} + B\,\sigma_{ij}' + C\,\sigma_{ik}'\,\sigma_{kj}'$$

where B, C are functions of ξ_2', ξ_3'.

Assumption V implies that $C = 0$.

VI. The glacier is regarded as a block of ice of infinite extent resting on a rough bed. The upper surface is a plane inclined at angle α_s to the horizontal.

Take x axis in the surface, pointing down the line of greatest slope.

Take y axis normal to the surface, positive downwards.

The z axis is horizontal.

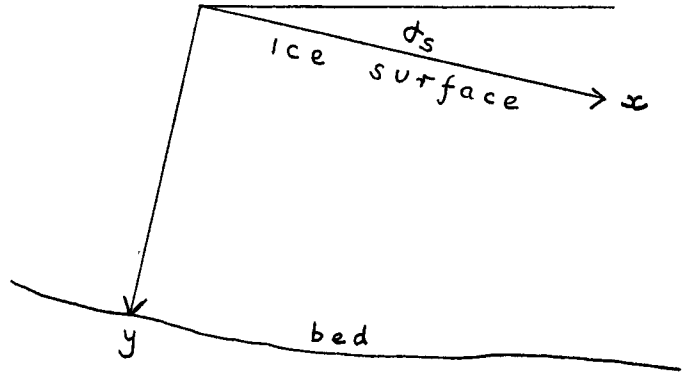

VII. Consider plane strain, in which movement is confined to the xy plane, i.e. w = 0, $\frac{\partial}{\partial z} = 0$.

Hence $\sigma_z' = 0$, $\tau_{xz} = 0$, $\tau_{yz} = 0$ by V.

Hence $$\sigma_z = \frac{1}{2}(\sigma_x + \sigma_y)$$

and $$\sigma_x' = -\sigma_y' = \frac{1}{2}(\sigma_x - \sigma_y) \qquad (1)$$

Also $$\varepsilon_3' = 0$$

The equations of equilibrium are

$$\frac{\partial \sigma_{ij}}{\partial x_j} + \rho g_i = 0$$

(g_i = component of acceleration along x_i axis due to gravity). In the present case these reduce to

$$\frac{\partial \sigma_x}{\partial x} + \frac{\partial \tau_{xy}}{\partial y} + \rho g \sin \alpha_s = 0 \qquad (2)$$

$$\frac{\partial \tau_{xy}}{\partial x} + \frac{\partial \sigma_y}{\partial y} + \rho g \cos \alpha_s = 0 \qquad (3)$$

To obtain a solution of these equations it is necessary to make another assumption.

VIII. Σ_2' and τ_{xy} are functions of y only.

By (1) $$\Sigma_2' = \frac{1}{4}(\sigma_x - \sigma_y)^2 + \tau_{xy}^2$$

Hence $$(\sigma_x - \sigma_y)\left(\frac{\partial \sigma_x}{\partial x} - \frac{\partial \sigma_y}{\partial x}\right) = 0$$

If $\sigma_x = \sigma_y$, $\sigma_x' = \sigma_y' = 0$, $\Sigma_2' = \tau_{xy}^2$.

This is a special case.

Thus $$\frac{\partial \sigma_x}{\partial x} = \frac{\partial \sigma_y}{\partial x} \qquad (4)$$

(2) and (3) have to be solved subject to the boundary conditions.

$$\begin{aligned} \sigma_y &= \pi \quad \text{(atmospheric pressure)} \\ \tau_{xy} &= 0 \end{aligned} \qquad (5)$$

for y = 0 and all x.

For this condition to be consistent with VIII, the x axis must be taken in the surface, rather than horizontal or parallel to the bed for example.

By VIII, (3) reduces to

$$\frac{\partial \sigma_y}{\partial y} + \rho g \cos \alpha_s = 0$$

whence $$\sigma_y = -\bar{\rho} g y \cos \alpha_s + \pi \qquad (6)$$

where $$\bar{\rho} = \frac{1}{y} \int_0^y \rho \, dy$$

It follows that $$\frac{\partial \sigma_y}{\partial x} = 0$$

Thus by (4) $$\frac{\partial \sigma_x}{\partial x} = 0$$

Hence (2) becomes

$$\frac{\partial \tau_{xy}}{\partial y} + \rho g \sin \alpha_s = 0$$

$$\tau_{xy} = -\bar{\rho} g y \sin \alpha_s \qquad (7)$$

Now $$\Sigma_2' = \frac{1}{4} (\sigma_x - \sigma_y)^2 + \tau_{xy}^2$$

Hence $$\sigma_x = \pi - \bar{\rho} g y \cos \alpha_s + 2\sqrt{\Sigma_2' - (\bar{\rho} g y \sin \alpha_s)^2} \qquad (8)$$

(6), (7), and (8) constitute the stress solution. It involves the function Σ_2' which is at present undetermined.

It is possible to relax the assumption of plane strain to a small extent by putting $\tau_{xz} = c_1 z$ so that $\frac{\partial \tau_{xz}}{\partial z} = c_1$, a constant. c_1 is added to the left hand side of equation (2) and the stress solution (equation 7) becomes

$$\tau_{xy} = -(\bar{\rho} g \sin \alpha_s + c_1) y \qquad (7')$$

Similarly one can put $\tau_{yz} = c_2 z$.

It has been assumed that ξ_2' is independent of x, and it was shown that $\xi_3' = 0$ for all x. So λ is independent of x. The velocity solution can now be obtained.

$$\frac{\partial^2 u}{\partial x^2} = \frac{\partial}{\partial x}(\dot{\varepsilon}_x) = \frac{\partial}{\partial x}(\lambda \sigma_x') = 0 \qquad (9)$$

Similarly $$\frac{\partial^2 v}{\partial x\, \partial y} = 0 \qquad (10)$$

$$\frac{\partial^2 u}{\partial x\, \partial y} + \frac{\partial^2 v}{\partial x^2} = 0 \qquad (11)$$

By IV $$\frac{\partial u}{\partial x} + \frac{\partial v}{\partial y} = 0$$

Hence (11) becomes $$\frac{\partial^2 v}{\partial x^2} = \frac{\partial^2 v}{\partial y^2} \qquad (12)$$

(10) has general solution

$$v = X(x) + Y(y)$$

By (12) $$X''(x) = Y''(y)$$

$$= -K, \text{ a constant.}$$

So $$v = v_0 + sx - ry - \tfrac{1}{2}K(x^2 + y^2) \qquad (13)$$

where $v = v_0$ at $x = 0, y = 0$

and r, s are constants.

$$\frac{\partial u}{\partial x} = -\frac{\partial v}{\partial y} = r + Ky$$

$$u = u_o + rx + Kxy + f(y) \qquad (14)$$

where $u = u_o$ at $x = 0$, $y = 0$

$f(0) = 0$

$r = \frac{\partial u}{\partial x}$ at $x = 0$, $y = 0$

$s = \frac{\partial v}{\partial x}$ at $x = 0$, $y = 0$

The boundary condition at the surface (y = 0) is $\tau_{xy} = 0$. By assumption V, this implies that

$$\dot{\varepsilon}_{xy} = 0$$

The boundary condition on the bed is

$$v_b = m u_b$$

where $m = \tan(\alpha_b - \alpha_s)$ where α_b is the slope of the bed at the point in question. It must be assumed that IX. α_b changes only slowly with x.

The first boundary condition leads to

$$f'(0) = -s$$

If h is the ice thickness at x = 0, the value of y on the bed can be approximated in the form $y = h + mx + \cdots$

Thus

$$u_b = u_o + rx + Kx(h + mx + \cdots) + f(h + mx + \cdots)$$

$$v_b = v_o + sx - r(h + mx + \cdots) - \tfrac{1}{2}K\left[(h + mx + \cdots)^2 + x^2\right]$$

where the subscript b denotes a value on the bed.

The second boundary condition gives

$$v_0 - \tau h - \tfrac{1}{2} K h^2 = m u_0 + m f(h)$$

But by (14)

$$f(h) = u_b - u_0 \quad \text{at } x = 0$$

Hence $$v_0 - \tau h - \tfrac{1}{2} K h^2 = m u_b$$

or
$$K = \frac{2}{h^2}\left(v_0 - m u_b - \tau h\right) \tag{15}$$

Again, by (14)
$$\frac{\partial u}{\partial x} = \tau + K y$$

Hence
$$\overline{\left(\frac{\partial u}{\partial x}\right)} = \frac{1}{h}\int_0^h \frac{\partial u}{\partial x}\, dy = \tau + \tfrac{1}{2} K h$$

So (15) can be written

$$h\overline{\left(\frac{\partial u}{\partial x}\right)} = v_0 - m u_b \tag{16}$$

where u_b, $\overline{\left(\frac{\partial u}{\partial x}\right)}$ refer to x = 0.

Equation (16) also follows directly from IV, VII, for

$$\frac{\partial u}{\partial x} = -\frac{\partial v}{\partial y}$$

$$\int_0^h \frac{\partial u}{\partial x}\, dy = -\int_0^h \frac{\partial v}{\partial y}\, dy$$

$$h\overline{\left(\frac{\partial u}{\partial x}\right)} = -m u_b + v_0$$

as before.

Another derivation of equation (16) is given in Appendix 1.

The function $f(y)$ in (14) can be expressed in terms of λ as follows:

$$\dot{\varepsilon}_{xy} = \frac{1}{2}\left(\frac{\partial u}{\partial y} + \frac{\partial v}{\partial x}\right) = \frac{1}{2}\left[f'(y) + s\right]$$

$$= \lambda \tau_{xy}$$

$$= -\lambda \bar{\rho} g y \sin \alpha_s \qquad \text{with} \quad \lambda^2 = \frac{E_2}{\Sigma_2'}$$

$$f(y) = -sy - 2\bar{\rho} g \sin \alpha_s \int_0^y y \lambda \, dy \qquad (17)$$

since $f(0) = 0$ (see equation 14).

For the solutions to be determinate, the flow law must be known. Moreover, it must be assumed that

X. The flow law does not involve the third invariant Σ_3'. In other words, λ is a function of Σ_2' only.

If the flow law is $E_2 = F(\Sigma_2')$, $\lambda^2 = \dfrac{F(\Sigma_2')}{\Sigma_2'}$

Now $\mathbf{E_2} = \lambda^2 \Sigma_2' = \dfrac{\dot{\varepsilon}_x^2 \, \Sigma_2'}{\sigma_x'^2}$

$$= \frac{(r + Ky)^2 \, \Sigma_2'}{\Sigma_2' - (\bar{\rho} g y \sin \alpha_s)^2} = F(\Sigma_2')$$

If r, K, $\rho(y)$, and the form of $F(\Sigma_2')$ are known, this last relation enables Σ_2' to be determined as a function of y. (It is not a function of x because Σ_2' is not.) The velocity and stress solutions can then be determined.

The essential difference between the foregoing analysis and that of Nye is that Nye assumes initially that $\alpha_b = \alpha_s$.

The boundary conditions for the velocity solution are then

$$\dot{\varepsilon}_{xy} = 0 \quad \text{on} \quad y = 0 \qquad \text{as before}$$

and $$v = 0 \quad \text{on} \quad y = h \qquad \text{for all } x.$$

Substitution of this second condition in (13) gives

$$s = 0, \quad K = 0, \quad v_o = rh$$

$$v = r(h - y) \qquad \text{which is Nye's solution.}$$

The corresponding solution for u is (putting K = 0 in (14))

$$u = u_o + rx + f(y)$$

Two consequences of Nye's solution should be noted.

1. $\dfrac{\partial v}{\partial x} = 0$

Nye (1957, p. 119) makes it appear that this is an additional assumption. But the preceding analysis shows that it follows from the other assumptions. Specifically, it is a consequence of assuming that Σ_2', τ_{xy} are independent of x and that the slopes of surface and bed are equal.

It follows that $\dot{\varepsilon}_{xy} = \frac{1}{2} \dfrac{\partial u}{\partial y}$. The solution (7) shows that τ_{xy} is always negative. But the rate of work

$\dot{\varepsilon}_{xy}\,\tau_{xy}$ must be positive. Hence $\frac{\partial u}{\partial y}$ must be negative.

2. $\frac{\partial u}{\partial x} = \dot{\varepsilon}$, a constant.

In other words, the longitudinal strain rate does not vary with depth.

For the case when $\alpha_b \neq \alpha_s$, Nye (1957, p. 126) adjusts the velocity solution to

$$v = \dot{\varepsilon}(h - y) + u(\alpha_b - \alpha_s)$$

This does not quite agree with equation (13), which for s = 0, K = 0, is

$$v = v_o - \dot{\varepsilon} y$$

Hence

$$v_b = v_o - \dot{\varepsilon} h$$

$$v = \dot{\varepsilon}(h - y) + v_b$$

$$= \dot{\varepsilon}(h - y) + u_b \tan(\alpha_b - \alpha_s)$$

This expression involves u_b, the velocity at the bed, not u, the velocity at depth y. The expression can also be derived from the condition of incompressibility which, for $\frac{\partial u}{\partial x} = \dot{\varepsilon}$, a constant, is

$$\frac{\partial v}{\partial y} = -\dot{\varepsilon}$$

Integrate both sides with respect to y between the limits y and h, and the expression is obtained.

In a further development, Nye assumes that τ_{xy} is constant on the bed. The following equation for the

longitudinal strain rate is then derived.

$$\tau = \frac{1}{h}\left(a + \frac{q}{R_s}\cot\alpha_s\right) \qquad (18)$$

where a = rate of accumulation or ablation.

q = flow rate = volume, per unit thickness in z direction, which flows in unit time through a cross-section perpendicular to Ox.

R_s = radius of curvature of surface, taken positive if convex.

The two respects in which the preceding theory differs from that of Nye, namely (1) $\frac{\partial u}{\partial y}$ always negative and (2) $\frac{\partial u}{\partial x}$ independent of depth, can be tested by field measurements. Equation (18) can also be tested in this way.

Some further attempts to generalize the theory of this section are given in Appendix 2.

5.2. Effect of Valley Sides

The assumptions of infinite width (VI) and plane strain (VII) are questionable. An alternative approach is to regard the glacier as one half of a circular cylinder. It is convenient to use cylindrical polar coordinates (r, θ, x) with origin at the surface on the centreline and x axis in the surface pointing down the glacier. The equations of equilibrium are

$$\frac{\partial \sigma_r}{\partial r} + \frac{1}{r}\cdot\frac{\partial \tau_{r\theta}}{\partial \theta} + \frac{\partial \tau_{rx}}{\partial x} + \frac{\sigma_r - \sigma_\theta}{r} + \rho g_r = 0$$

$$\frac{\partial \tau_{r\theta}}{\partial r} + \frac{1}{r}\cdot\frac{\partial \sigma_\theta}{\partial \theta} + \frac{\partial \tau_{\theta x}}{\partial x} + \frac{2\tau_{r\theta}}{r} + \rho g_\theta = 0$$

$$\frac{\partial \tau_{rx}}{\partial r} + \frac{1}{r}\cdot\frac{\partial \tau_{\theta x}}{\partial \theta} + \frac{\partial \sigma_x}{\partial x} + \frac{\tau_{rx}}{r} + \rho g_x = 0$$

Make the following simplifying assumptions

1. $\tau_{r\theta} = \tau_{\theta x} = 0$

2. σ_r, σ_x, τ_{rx} do not depend on θ .

3. σ_x does not depend on x.

The equations then reduce to

$$\frac{\partial \sigma_r}{\partial r} + \frac{\partial \tau_{rx}}{\partial x} + \frac{\sigma_r - \sigma_\theta}{r} + \rho g_r = 0$$

$$\frac{1}{r}\cdot\frac{\partial \sigma_\theta}{\partial \theta} + \rho g_\theta = 0$$

$$\frac{\partial \tau_{rx}}{\partial r} + \frac{\tau_{rx}}{r} + \rho g_x = 0$$

The last equation has solution

$$\tau_{rx} = -\frac{1}{2}\bar{\rho} g r \sin\alpha_s \qquad (19)$$

This can be compared with the corresponding solution in the rectangular coordinate system for the centreline of an infinitely wide glacier,

$$\tau_{xy} = -\bar{\rho} g y \sin\alpha_s$$

In the above derivation it has not been shown that solutions for the four non-zero stress components can be obtained from the three equations combined with the flow law. While the derivation is not rigorous, it does, however, suggest that allowance can be made for the finite width of the glacier by inserting a factor $\frac{1}{2}$ in the appropriate stress solution. This is for a semicircular cross-section. For arbitrary cross-section it seems natural to replace $\frac{1}{2}$ by the factor $\frac{S}{ph}$ where S is the area of cross-section, p is the perimeter (excluding the upper surface), and h is the ice thickness on the centreline. The same result was obtained from statical considerations by Nye (1952b, p. 85-86).

5.3. Reduction of Borehole Data

The formulae used in section 3.6. will be derived in this section.

It is assumed that $\frac{\partial u}{\partial x}$, $\frac{\partial u}{\partial y}$, $\frac{\partial v}{\partial x}$ are constant both in time and over the distance moved by the pipe between observations. It must also be assumed that ice slips freely along the pipe.

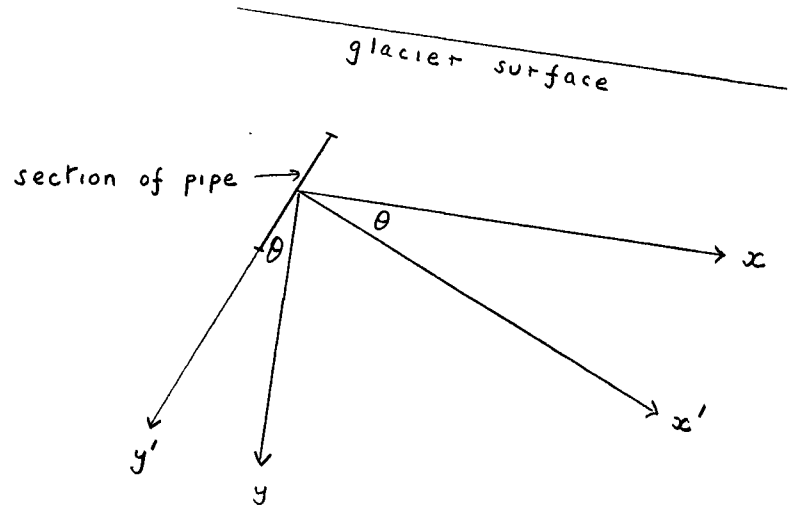

Let x', y' be axes perpendicular and parallel to the axis of the pipe, and x, y axes parallel and perpendicular to the glacier surface. x, x' are positive in the direction of glacier flow and y, y' are positive downwards. Let θ be defined by

$$\sin\theta = \frac{dx}{ds} \qquad \cos\theta = \frac{dy}{ds}$$

where s is distance measured along the pipe.

The relations between the coordinate systems are

$$x = x'\cos\theta + y'\sin\theta$$
$$y = -x'\sin\theta + y'\cos\theta$$
$$u' = u\cos\theta - v\sin\theta$$

A section of pipe will begin to tilt in proportion to twice the shear strain rate, as defined, i.e.

$$\frac{d\theta}{dt} = \frac{\partial u'}{\partial y'} + \frac{\partial v'}{\partial x'}$$

It is assumed that ice slips freely along the pipe, hence $\frac{\partial v'}{\partial x'}$ is zero.

Thus $$\frac{d\theta}{dt} = \frac{\partial u'}{\partial y'} = \frac{\partial u}{\partial y}\cos^2\theta + 2\sin\theta\cos\theta\,\frac{\partial u}{\partial x} - \sin^2\theta\cdot\frac{\partial v}{\partial x} \qquad (20)$$

Plane strain has been assumed so that

$$\frac{\partial u}{\partial x} + \frac{\partial v}{\partial y} = 0$$

by the assumption of incompressibility.

If $\theta = \theta_0$ at $t = 0$, and $\theta = \theta_1$ at $t = t$, then

$$t = \int_{\theta=\theta_0}^{\theta=\theta_1} \frac{d(\tan\theta)}{\frac{\partial u}{\partial y} + 2\frac{\partial u}{\partial x}\tan\theta - \frac{\partial v}{\partial x}\tan^2\theta}$$

Near the surface, $\frac{\partial v}{\partial x}$ and $\frac{\partial u}{\partial y}$ are comparable in magnitude but tan θ is small. At depth, where θ may be 30°, $\frac{\partial u}{\partial y}$ is large compared with $\frac{\partial v}{\partial x}$. Thus

$$\left|\frac{\partial v}{\partial x}\tan^2\theta\right| \ll \left|\frac{\partial u}{\partial y}\right|$$

Hence

$$t = \frac{1}{2\frac{\partial u}{\partial x}}\cdot\log\frac{\frac{\partial u}{\partial y} + 2\frac{\partial u}{\partial x}\tan\theta_1}{\frac{\partial u}{\partial y} + 2\frac{\partial u}{\partial x}\tan\theta_0}$$

or $$\frac{\partial u}{\partial y} = \frac{2\frac{\partial u}{\partial x}\cdot\left[\tan\theta_1 - \tan\theta_0\cdot\exp\left(2\frac{\partial u}{\partial x}t\right)\right]}{\exp\left(2\frac{\partial u}{\partial x}t\right) - 1} \qquad (21)$$

This equation was derived by Nye (1957, p. 130).

The maximum value of $\frac{\partial u}{\partial x}$ at the boreholes on the Athabaska Glacier was 0.023. In this case $\left(\frac{\partial u}{\partial x}\right)^2$ can be neglected and the formula reduces to

$$\frac{\partial u}{\partial y} = \frac{1}{t}\left(\tan\theta_1 - \tan\theta_0\right) - \frac{\partial u}{\partial x}\left(\tan\theta_1 + \tan\theta_0\right) \qquad (22)$$

It was suggested by Savage that this formula could be improved by taking account of the curvature of the pipe. This means that in equation (20) θ is a function of y'.

A term $\frac{\partial u'}{\partial \theta} \cdot \frac{d\theta}{dy'}$ must therefore be added.

$$\frac{\partial u'}{\partial \theta} \cdot \frac{d\theta}{dy'} = -\left(u \sin\theta + v \cos\theta\right) \frac{d\theta}{dy'}$$

and $$\frac{d\theta}{dy'} = \frac{d\theta}{ds}$$

Addition of this extra term means that the equation can no longer be integrated. The formula is therefore

$$\frac{\partial u}{\partial y} = \frac{d\theta}{dt} \sec^2\theta - 2\frac{\partial u}{\partial x}\tan\theta + \frac{\partial v}{\partial x}\tan^2\theta + \left(u\tan\theta + v\right)\left(\sec\theta\right)\frac{d\theta}{ds} \qquad (23)$$

Values averaged over the period are used for the various quantities.

6. RESULTS

6.1. General

This section consists of a brief review of the observational results. Detailed interpretation of certain aspects of these in terms of current theories of glacier flow is postponed to section 7.

6.2. Configuration of Surface

Positions and elevations of triangulation stations and markers are given in Tables 1 and 2. Table 3 and Figure 7 give the surface profile along the longitudinal line. Profiles along the transverse lines are given in Table 4 and Figures 8 to 14. All the data in Tables 3 and 4 and in Figure 7 were obtained from the present survey. In Figures 8 to 14 elevations of additional points have been added and the edges of the glacier and the extent of the debris cover at the sides have been indicated. This additional information has been taken from Kanasewich (1960). Any discrepancies between tabulated elevations and contours on the map can be ascribed to inaccuracies in plotting positions of markers on the map. All elevations measured in the survey check with those determined quite independently by Kanasewich.

The central parts of the transverse profiles show the convex shape typical of an ablation area. The sides are

relatively high because the thickness of the cover of debris is sufficient to reduce ablation appreciably.

The tables list the level of the surface in both 1959 and 1960. The change of thickness of the glacier in one year cannot be deduced from this data, however. Most of the apparent change is a result of the movement of the markers. In any case, to be of much value, such measurements of change of surface elevation should be made at the beginning or end of each ablation season. The surface level at the end of the 1959 season is known. Corresponding figures are not available for 1960, however, as the party left the glacier before the end of the ablation. Measurements were made during the winter but by this time the upward flow of ice had produced an appreciable change in surface level. Evidence regarding the change of thickness of the glacier over a long period is discussed in section 6.4.

The slope of the surface at each marker is given in Table 7. Values of surface curvature at points on the longitudinal line are listed in Table 9. Table 5 lists the width of the lower part of the glacier at different points. The maximum width is 1240 m. at L17; the minimum 890 m. at L30.

6.3. Configuration of Bed

Figure 5 is a map of the bedrock. Profiles of the bed along the longitudinal and transverse lines are shown in Figures 7 to 14. These figures were drawn on the basis of the measurements of ice thickness listed in Table 6. Direct measurements, either by the seismic or gravity method, were made at every point listed. It is noticeable that the gravity method gives a much smoother profile than does the seismic. Slope of the bed, as determined from the seismic records, is given in Table 8, and the curvature, obtained by differentiating the slope, in Table 9.

The configuration of the bed has already been described in section 1.2, and will be discussed further in section 7.

6.4. Surface Velocity

The horizontal component of surface velocity (U), its direction (A) measured in a horizontal plane, and the vertical component (V) are given in Tables 10, 11, and 14 respectively. Velocity normal to the ice surface (v) is also given in Table 14. Horizontal velocity was determined at weekly intervals in some cases. Inaccuracies of measurement make calculations of direction and vertical velocity over such periods of little value, however. Direction has not been calculated for periods of less than three weeks. For vertical velocity the minimum period was three months. The normal velocity v could not be calculated for a few

markers because they lay outside the area of the map. The surface slope was therefore unknown.

The quantities U, V, A determine the velocity vector. The component U was so much greater than V that the difference between U and the magnitude of the velocity vector was less than the standard error of measurement in nearly all cases. The only markers at which vertical velocity was measured where this did not hold were A6, A7, L38, and "D". The horizontal direction of the velocity vector at all markers on the longitudinal line never differed significantly from the direction of the line at that point.

Horizontal velocities along the longitudinal line are shown in Figure 15, and vertical and normal velocities in Figure 16. Each point has been plotted to correspond to the mean position of each marker at each period. Differences between the curves thus represent genuine seasonal differences in velocity, and are not merely a result of changes in position of each marker.

Horizontal velocity along the centreline decreases steadily from 74 m./yr. at L10 to 15 m./yr. at L39. This comparatively high value within 40 m. of the terminus can be explained by the high wastage of ice from this section as a result of calving into the terminal lake.

Figures 8 to 14 show horizontal velocities on the transverse lines. The average velocity for each line, calculated by the method described in section 3.2.4., is

given in Table 13. Velocities at the edge of the glacier on each transverse line are given in Table 12. These values were obtained by extending the curves in Figures 8 to 14 to the edges. This represents extrapolation of velocity over distances up to 300 m., so the results are very inaccurate. Velocities at the edge at the two locations where measurement was possible are also given in Table 12. These measurements were made 1 or 2 m. from the edge of the ice at points some 50 m. down glacier from the A line. The locations (A0, A10) are marked on Figure 2.

Near the icefall, the velocity at the edge is roughly 10% of the velocity on the centreline. Near the terminus (G line), the velocity at the edge is zero. The situation in the intervening region is not very clear. There are no great differences in velocity at the edge between lines C to F. The average velocity is between 80 and 90% of the maximum velocity on each of these lines. The most noticeable feature of the velocity profiles is their lack of symmetry. For lines C to F the velocity at the south-east edge is small or zero. At the north-west edge the velocity is about 60% of that on the centreline (except for line C). The reason for this asymmetry is not clear, but it could be a result of the shelf which appears to exist under the ice on this side of the valley (see Figures 5, 9, 10, 11). Alternatively, it is possible that an error was made in locating the edge of the glacier on one side. However, an

error of the order of 200 m. would be necessary to eliminate the effect. An error of this size seems improbable. Extrapolation of the velocity to the edge by a smooth curve may be unjustified, and it is not impossible that the velocity at the edge is zero everywhere below the icefall. The measured velocities at the edge do not show the asymmetry.

On all the transverse lines, the flow at each side diverges from the centreline. The divergence is seldom more than a few degrees, however. The divergence rises to 12° in the case of the F line where the glacier widens appreciably. Flow on the G line is complicated by the glacial lake at the north-west half of the terminus. Calving of ice into the lake produces a high wastage of ice and the markers above the lake (G5 to 7) flow towards it.

There is no discontinuity in velocity across the boundary between the debris-covered and comparatively clean areas of ice.

As is expected in the ablation area, ice flows upwards through the surface (i.e. v is negative) throughout the lower part of the glacier. In general, upward flow is greater towards the sides of the glacier than near the centreline. (In other words, near the sides v is more negative and U is smaller, so that the velocity vector is more steeply inclined to the surface.) But the effect is not very marked and the B line seems to be an exception. The value of v shows very little variation with distance

down the glacier. There is no significant deviation from a mean of -3.4 m./yr. along the longitudinal line between L11 and L35. The absolute value decreases between L35 and the terminus. A similar trend was observed on the Saskatchewan Glacier (Meier, 1960, p. 25).

The upward flow of ice compensates for the lowering of the surface by ablation. Comparison of v with the ablation rate thus determines whether the glacier is in equilibrium. Measurements of total ablation for a season are only available for one year, 1960. The mean value on the centreline was 4.2 m./yr. with very little variation over the lower part of the glacier (Table 27). If this ablation rate is typical one might conclude that the glacier is becoming thinner at a rate of about 0.8 m./yr. As was explained previously, no direct measurements of change of ice thickness were made in the present study. Some measurements over a long period are however available (see section 3.7.3.). Results are given in Table 15 and indicate a rate of decrease of thickness of 0.7 m./yr.

Agreement between the two figures is surprisingly good but may be fortuitous. It is by no means certain that 1960 was a typical ablation season. While ablation data for 1959 do not cover the whole season they certainly include the greater part of it. From these data (Table 27) it appears unlikely that the total ablation in 1959 exceeded 2.5 m. Ablation at similar altitudes on the Saskatchewan

Glacier averaged about 3.5 m. in 1953. This was considered to be a reasonably "normal" year (Meier, 1960, p. 8, 11). It thus seems quite likely that 4.2 m./yr. is an overestimate of the average ablation rate. The measurements of change of thickness refer to the region below L32. Variations in thickness of glaciers with time tend to be greatest near the terminus. The data of Table 15 suggest a lower rate of thinning at L32 than at L37. Thus 0.7 m./yr. is probably an overestimate of the mean value for the lower part of the glacier (i.e. below L10). While it is likely that the glacier is becoming thinner, its condition is probably considerably nearer to equilibrium than a change of 0.8 m./yr. would indicate.

Accurate information on the state of the glacier will eventually be available from the maps which the Water Resources Branch, Department of Northern Affairs and National Resources, plan to make every three years.

Over most of the lower part of the glacier values of V are also negative. This means that ice flows upwards relative to the horizontal. A similar result was found on the lowest 4.5 Km. of the Saskatchewan Glacier (Meier, 1960, p. 25).

Markers situated on debris-covered ice (e.g. B9, C2, C13, F9) have vertical velocities considerably smaller than those of other markers. Ablation is likewise reduced.

Horizontal velocities in the upper part of the glacier

are also given in Table 10. The maximum velocity recorded was 266 ± 25 m./yr. for marker J4 on the headwall. Difficulty of access prevented the setting of markers in the steeper parts of the headwall, where velocities are probably considerably greater than this. Marker A7 moved intact from top to bottom of the lowest icefall in two years. Measured velocity was about 130 m./yr., but this is the mean value over one year.

6.5. Strain Rate

Longitudinal strain rates along the centreline of the glacier are given in Table 16 and Figure 17. The strain rate changes steadily from about -0.1 per year below the icefall to approximately zero at L21. The strain rate is effectively zero between L21 and L27 and below this it becomes compressive again. Values below L35 were measured over a period of only six weeks and so are less accurate than the remainder. However, the positive value between L38 and L39 is probably genuine. L39 was some 40 m. from the edge of the ice cliff above the glacial lake and there were transverse crevasses nearby (see Figure 4). This value apart, the strain rate is never extending at any point along the longitudinal line. Apart from oblique crevasses along the margins and in the neighbourhood of the E line, there are no crevasses between L10 and L37.

Transverse strain rates calculated from the change in width of the glacier are listed in Table 18 along with

comparative measurements at the transverse lines. These measurements refer to the change in distance between the markers at each end of the line. Except at the E line (L27) agreement is surprisingly good. This method of estimating transverse strain rate in a valley glacier thus appears to be reasonably satisfactory. The only data required are the width of the glacier and the surface velocity along the centreline. It should be noted that estimation of transverse strain rates at intermediate points by linear interpolation between values measured at the transverse lines would not be satisfactory.

The discrepancy at the E line probably results from irregularity of the glacier bed. The variation of strain rates between individual markers is much greater on the E line than on the other transverse lines (see Table 17). This fact and the presence of crevasses oblique to the direction of flow between E4 and E6 suggest irregularities in the bed. This cannot be verified from seismic measurements as only two were made on the E line. The gravity profile does not show any irregularity. However, the ice thickness as determined by gravity at the intersection of the E and L lines was 215 m. The value obtained by a combination of seismic and borehole data was 248 m. (215 m. is the value given by Kanasewich (1960). Values for the E line in Table 6 have been adjusted to give 248 m.). This suggests that the gravity method is not very accurate in

this area.

Calculated transverse strain rates are shown in Figure 17.

6.6. Borehole Results

The inclinometer measurements are given in full in Table 20. Table 21 lists slope, velocity and other relevant information for each borehole. The configuration of each borehole in each year is plotted in Figures 18 to 20. Figures 21 to 23 show the variation of $\frac{\partial u}{\partial y}$ with depth y.

Values of $\frac{\partial u}{\partial y}$ computed by three methods described in section 3.6. are given in Table 22. This table supports the conclusions drawn from the error analysis of section 4.7. The difference between a "laminar flow" analysis and one which makes allowance for longitudinal strain rate and curvature of the pipe is not important in this instance. It could be very important of course for boreholes in regions where the longitudinal strain rate is high, or even for these boreholes in subsequent years when the distortion has increased . The difference between analysis by these methods and by the integrated method (column C of Table 22) does appear to be significant, however, at least in the case of hole 322. The discussion of section 7.1. indicates that the integrated method has a sounder theoretical basis than the other. Values of $\frac{\partial u}{\partial y}$ in column C of Table 22 have therefore been used in subsequent analyses. The broad conclusions drawn are however unaltered whether the values in columns A, B,

or C are used.

The most conspicuous feature of the results is that $\frac{\partial u}{\partial y}$ is positive in the upper parts of holes 322, 314, and 116. In hole 322, $\frac{\partial u}{\partial y}$ is positive down to a depth of about 100 m. and u is greater than its surface value down to about 180 m. Observations only extend down to 45 m. in hole 314 but $\frac{\partial u}{\partial y}$ is positive throughout. In hole 116, $\frac{\partial u}{\partial y}$ changes sign several times. This is presumably the result of experimental error which is somewhat greater in this hole than the others. But the velocity is greater than the surface velocity throughout (the borehole only extends to 116 m., but the ice thickness is 315 m.). The effect is not a very large one. In hole 322, for example, the surface and maximum velocities are 38.9 m./yr. and 39.5 m./yr. In few cases in fact do the individual values of $\frac{\partial u}{\partial y}$ exceed zero by more than twice their standard error. However, the general trend, and the fact that the effect is shown at three boreholes in the same area, seem to leave little doubt that the effect is a real one. A similar result for a borehole on the Blue Glacier is shown by Sharp (1960, p. 40) and other boreholes on the same glacier confirm it (Sharp, private communication). The theoretical implications of this are discussed in section 7.4.

The other conspicuous feature of the data is the much greater distortion in the lower part of hole 209 than in hole 322. The velocity at the bottom of hole 322 is 31.7 m./yr. or about 80% of the surface velocity. (The ice

thickness at this point was confirmed by seismic means. So it is considered virtually certain that this hole extends to bedrock.) In hole 209, the velocity at the bed is 7 m./yr. or about 25% of the surface velocity. This is an extrapolated value as measurements could not be made in the last 10 m. of this hole. It is possible that the velocity at the bed is less than 7 m./yr.

The difference between conditions at the two holes can perhaps be explained by the configuration of the glacier bed. Figure 7 shows a hollow in the bed near hole 209. This hollow might well be filled with ice which is semi-stagnant. The depth of the hollow appears to be of the order of 35 m. The velocity in hole 209 at this distance from the bed is about 21 m./yr. or 75% of the surface velocity. This is comparable with the figure at the bottom of hole 322.

The implications of the borehole data regarding the flow law of ice and current theories of glacier flow are discussed in detail in section 7.

6.7. Ablation and Accumulation

Ablation and accumulation data are given in Table 27. The ablation data are also shown in Figure 31.

Abnormally low values of ablation at C2, E1, F1, and G8 can be explained by the thick cover of debris on the ice at these points. At other markers where the cover was thinner (B9, C13, C14, D11, F9) the ablation is only

slightly less than the average for clean ice.

The most prominent feature of the data is the great difference in ablation between the two seasons. The data show no significant variation of ablation rate with distance along the glacier. Nor is any variation in total ablation clearly established for the part of the glacier below L10. The markers for which total ablation figures are available can be divided into two groups. The difference between the means of the two groups indicates a reduction of ablation of 1 cm. for each 4 m. rise in elevation. But it is quite possible that the difference between the two groups is merely a sampling fluctuation. The value is less than the gradient of 1 cm. per 3 m. measured at comparable elevations on the Saskatchewan Glacier (Meier, 1960, p. 11).

The net accumulation for the year 1959-60 as measured in a single snow pit on the crest between the drainage basins of the Athabaska and Saskatchewan Glaciers was 3 m. of firn. As was explained in section 4.8.2. no figure can be given for the mean accumulation on the lower part of the glacier. The number of measurements was insufficient.

7. DISCUSSION

7.1. Analysis of Borehole Data

Measurements in boreholes can be used to determine $\frac{\partial u}{\partial y}$, the gradient, in the direction normal to the surface, of the ice velocity parallel to the surface. Interpretation of measurements of inclination of the pipe in terms of ice velocity is not straightforward, however, and involves assumptions regarding the behaviour of the pipe. The distribution of velocity with depth plays a most important part in the subsequent discussion of glacier flow. These problems of interpretation will therefore be treated first. Methods used to analyse the data in various borehole experiments will first be reviewed briefly.

The first borehole experiment was that of Gerrard and others (1952). Their inclinometers did not measure azimuth, but were arranged to measure inclinations in a plane parallel to the direction of flow. This azimuth control was not satisfactory in the first year. This did not greatly affect the results, however, as the pipe was nearly vertical then.

Gerrard and others discuss possible sources of error. The couplings which joined the pipe sections were 2.5 cm. wider than the pipe itself. The length of the borehole changes in time due to deformation of the ice. The pipe cannot change its length and so it must slide in the borehole.

The protruding couplings oppose this. Gerrard and others state: "After about two weeks the ice in the borehole closed in around the pipe and gripped it firmly." Another source of error was the tendency of the pipe, which was of steel, to sag under its own weight. Aluminium pipe has been used in all subsequent borehole experiments.

Gerrard and others analysed their data on the assumption that flow was laminar. In other words, it was assumed that the pipe measured the deformation due to a simple shear stress acting parallel to the surface. Subsequent measurements showed that the longitudinal strain rate at the surface had the comparatively high value of 0.14 per year, however.

The borehole experiment on the Malaspina Glacier (Sharp, 1953a, b) was solely designed to test for "extrusion flow". The borehole was too far from any points on bedrock to permit measurement of surface movement. Surface strain rates were not measured. Analysis was therefore restricted to a plot of the deformation of the pipe over the two years.

Reduction of the borehole data from the Saskatchewan Glacier (Meier, 1960, p. 30) was also carried out under the assumption of laminar flow. Allowance for the longitudinal strain rate of -0.013 per year was made in calculation of the flow law, however. As this borehole only extended to a depth of 43 m., deformation was small. Errors due to ice

streaming past the pipe, sagging of the pipe, and resistance of the couplings to flow of ice along the pipe, were therefore regarded as negligible.

A laminar flow analysis was also used by Shreve for two boreholes on the Blue Glacier (Shreve, 1961). Surface measurements indicated that the longitudinal strain rate at these boreholes was "negligible".

The first analysis in which allowance was made for the longitudinal strain rate was the re-analysis of the data of Gerrard and others by Nye (1957, p. 128-132). Mathews (1959, p. 452) also took account of the longitudinal strain rate (0.07 per year) in his analysis of data from the Salmon Glacier. Nye calculated the value of $\frac{\partial u}{\partial y}$ at different depths by means of formula (21) of section 5.3. This procedure is subject to the assumptions that the pipe is straight, that $\frac{\partial u}{\partial x}$ and $\frac{\partial u}{\partial y}$ are constant in time and over the distance moved by the pipe in the year between observations, and that the ice slips freely along the pipe.

The need for the first assumption is eliminated if formula (23) of section 5.3. is used. All that can be determined from measurements of surface markers or in boreholes are values of velocity and strain rate meaned over the distance which the markers have travelled between observations. All measurements are also made under the assumption that the glacier is sufficiently near to a steady state so that the value of any of these quantities

at any point in space does not change appreciably between observations. This assumption, which seems a reasonable one, thus underlies all the measurements. The statement of Gerrard and others, that the pipe was gripped firmly by the ice, casts doubts on the assumption that ice slips freely along the pipe.

In the present study, horizontal and vertical movement of the top of each pipe was measured by triangulation. The following table lists the vertical velocities and those of nearby surface markers, arranged in order down the centreline. Holes 322 and 116 were some 100 m. off the longitudinal line. However, measurements on transverse lines indicated that the velocities varied little over this distance.

Vertical Velocities V
(m./yr., + downwards)
(standard error $\approx$ 0.15)

L16	0.24
L17	0.19
Hole 314	-0.42
Hole 322	-0.33
L18	-0.14
L19	-1.49
Hole 116	-1.70
L20	-2.34
L29	1.56
Hole 209	no data
L30	-0.19
Hole 194	-0.15

These data indicate that the vertical velocity of the top of each pipe was the same as that of the ice near the glacier surface. It is concluded that the pipe was gripped near the top. Difficulties experienced during drilling,

when the pipes were seized by the ice 5 to 10 m. below the surface, makes this supposition quite likely. It is attributed to the previous winter's "cold wave" not having been eliminated from the ice.

The pipe cannot, however, have been gripped along its whole length. The longitudinal strain rate at the surface was compressive at all boreholes. The transverse surface strain rate was in all cases numerically small compared with the longitudinal one. The strain rate $\dot{\varepsilon}_y$ in the direction normal to the surface was therefore extending. The length of the borehole also increases with time as a result of the shear deformation. The pipe cannot stretch. It is therefore concluded that the pipe was gripped by the ice near the surface and that the remainder of the pipe was dragged upwards along the line of the borehole. As was pointed out by Savage, this casts serious doubts on the validity of the analysis described previously.

Some data are also available as to whether ice tends to flow past the pipe rather than carry it along. Hole 314 was situated on the longitudinal line between markers L17 and L18. Figure 24 shows the distances moved by the pipe and adjacent markers over the period July 1959 to August 1960. The point on the graph for hole 314 does not deviate significantly from the curve for the markers. This indicates that there is no tendency for ice to flow past the pipe.

The foregoing discussion indicates that the basis of

the first two methods of analysis of borehole data, as described in section 3.6., is dubious. The third (integrated) method is therefore preferred. Values of $\frac{\partial u}{\partial y}$ computed by the different methods are given in Table 22. The conclusion, already stated in section 6.6. is that, for these boreholes and times of observation, values calculated by the integrated method are significantly different from values calculated by the other methods. The broad conclusions, drawn from the borehole data in subsequent sections, are, however, unaltered whichever method of analysis is used.

7.2. Validity of Assumptions

The theory of section 5.1. rests on many simplifying assumptions. There will be many places in real glaciers where these would not be expected to hold. The situation for the Athabaska Glacier will be examined in this section.

In section 5.1., assumptions I to V and X are general assumptions regarding the properties of ice. The only indication of whether or not these are valid comes from an overall comparison of field measurements with theoretical predictions.

Assumption VI, that the glacier is infinitely wide, is a poor assumption for valley glaciers. In the present case the width is only 3 or 4 times the depth. An alternative model, described in section 5.2., is to regard the glacier as half a circular cylinder. Comparison of these two models is

deferred to section 7.7.

The assumption of plane strain (VII) will be considered next. This implies that the transverse velocity w, the strain rates, $\dot{\varepsilon}_z$, $\dot{\varepsilon}_{xz}$, $\dot{\varepsilon}_{yz}$ and their first derivatives with respect to z (where z is the cross-glacier coordinate) are zero. Transverse surface strain rates ($\dot{\varepsilon}_z$) are listed in Table 18. The transverse strain rate does not exceed 0.01 per year except between L12 and L15 and between L33 and L35 where it rises to 0.02 per year. It is less than 0.005 per year at most places. The transverse strain rate was measured directly at the four boreholes (Table 19). Values were 0.002 (holes 322, 314), -0.001 (hole 116) and -0.0006 (hole 209). To neglect $\dot{\varepsilon}_z$ thus appears to be a valid first approximation.

Table 11 shows that, along the centreline, the direction of flow varies slowly from about 205° below the icefall to about 215° at L22 and back to 195° at the terminus. Thus the valley is effectively straight. Thus the transverse velocity w on the centreline should be zero by symmetry. Table 11 also shows that there is a region, roughly 250 m. wide, at the centre of each transverse line, across which the direction of surface velocity varies by not more than 1 or 2 degrees. In this region it is perhaps legitimate to assume that w and all its first derivatives are zero. Tables 10 and 14 give longitudinal and normal velocities on the transverse lines and show that $\frac{\partial u}{\partial z}$ and $\frac{\partial v}{\partial z}$ are small near the centreline. The shear strain rates $\dot{\varepsilon}_{xz}$ and $\dot{\varepsilon}_{yz}$

should thus be small. $\dot{\varepsilon}_{xz}$ was measured at the surface at holes 322 and 116. Values were small but, at least at hole 322, differed significantly from zero (Table 19). The implication of this is discussed further in section 7.4. It is not certain whether the first derivatives of the strain rates with respect to z are zero.

The longitudinal line of markers is everywhere within 100 m. of the centreline (i.e. line of greatest velocity). The two boreholes (322 and 116) which lie off the longitudinal line are as near the centreline as the markers are.

It is concluded that there is some doubt as to how good an approximation the assumption of plane strain is. In this respect the theory of section 5.2., which does not involve this assumption, may be preferable to that of section 5.1.

As regards the assumption (VIII) that $\dot{\varepsilon}_1'$ and τ_{xy} are independent of x it is useful to consider how rapidly such quantities as ice thickness, strain rates, and slopes vary with distance down the glacier. Profiles of surface and bed are shown in Figure 7. Ice thicknesses, and slopes and curvatures of surface and bed, are given in Tables 6 to 9.

At L10.5, a short distance below the icefall, the bed has a slope of 17°. Between L35 and the terminus the ice thickness is 100 m. or less and the slopes change quite rapidly in distances of this order. These areas will therefore be excluded from further consideration. Between L12 and L34 the surface slope varies gradually in the range

1.7° to 8.6°. Surface curvature is about 10^{-4} per m. at L25 and L27 and three times that amount at L34. Otherwise it is 5 x 10^{-5} per m. or less.

Between L12 and L21 the bed slope changes slowly. It never differs from the surface slope by more than 5°. Curvature of the bed does not exceed 4 x 10^{-4} per m. over this region. The bed slopes uphill at L21 and L23 and becomes more undulating below L27. There appears to be a rise with crest near L28, a depression near L30, and then a gradual rise to L32. Curvature of the bed increases to about 10^{-3} per m. at L29. For this reason, and because surface and bed slopes differ by 10°, hole 209 may not be very well sited. The surface curvature is very small there however (10^{-5} per m.).

Thus, throughout most of the lower section of the glacier, surface and bed slopes differ by only a few degrees and vary only slowly with distance x. More specifically, this is the case between L12 and L35 with the possible exception of the region between L27 and L32. The assumption should be particularly good in the area between L16 and L20 where boreholes 314, 322, and 116 are located.

Longitudinal strain rates at the surface are given in Table 16 and Figure 17. The strain rate is compressive throughout virtually the whole region and does not exceed -0.03 per year below L14. It varies only slowly with

distance x.

In general, the lower part of the Athabaska Glacier appears to be a very favourable region for which to make simplifying assumptions about the flow of valley glaciers. If the theory is found to be inapplicable in this case, one might conclude that the places in real glaciers to which it would apply are comparatively rare.

7.3. Variation of Longitudinal Strain Rate with Depth

As was explained in section 5.1., the longitudinal strain rate is expected, on Nye's theory, to be constant throughout the thickness of the glacier. Whether this is the case can be tested by two methods.

Method 1.

The hypothesis to be tested is that $\frac{\partial^2 u}{\partial x \partial y} = 0$.

Equation (16) of section 5.1 is

$$h\left(\overline{\frac{\partial u}{\partial x}}\right) = v_s - u_b \tan(\alpha_b - \alpha_s)$$

The method consists of using this equation to calculate $\left(\overline{\frac{\partial u}{\partial x}}\right)$, the longitudinal strain rate averaged over the thickness. This value is compared with $\left(\frac{\partial u}{\partial x}\right)_s$, the value measured at the surface.

The quantities above refer to the coordinate system of section 5.1. in which the x and y axes are respectively parallel and perpendicular to the surface. Measurements were made in the X, Y coordinate system in which the axes

are horizontal and vertical. The transformation equations are (for plane strain)

$$u = U \cos \alpha_s + V \sin \alpha_s$$

$$v = -U \sin \alpha_s + V \cos \alpha_s$$

$$\frac{\partial u}{\partial x} = \frac{\partial U}{\partial X} \cos 2\alpha_s + \frac{1}{2}\left(\frac{\partial U}{\partial Y} + \frac{\partial V}{\partial X}\right) \sin 2\alpha_s$$

The last equation can be simplified because

$$\frac{\partial u}{\partial y} + \frac{\partial v}{\partial x} = -\frac{\partial U}{\partial X} \sin 2\alpha_s + \left(\frac{\partial U}{\partial Y} + \frac{\partial V}{\partial X}\right) \cos 2\alpha_s$$

and $$\left(\frac{\partial u}{\partial y} + \frac{\partial v}{\partial x}\right)_s = 0$$

Hence, to a sufficient approximation,

$$\left(\frac{\partial u}{\partial x}\right)_s = \left(\frac{\partial U}{\partial X}\right)_s \cos 2\alpha_s$$

To avoid the assumption that $\dot{\varepsilon}_z = 0$, equation (16) was modified to

$$h\left(\overline{\frac{\partial u}{\partial x}}\right) = v_s - u_b \tan(\alpha_b - \alpha_s) - h\dot{\varepsilon}_z$$

The conclusions are unaltered whether or not $\dot{\varepsilon}_z$ is taken as zero, however.

The quantities h, α_s, α_b, U_s, V_s, $\left(\frac{\partial U}{\partial X}\right)_s$, and $\dot{\varepsilon}_z$ were

measured. Results are given in Tables 6, 7, 8, 10, 14, 16, and 18 respectively. U_b is known at boreholes 322 and 209. U_b was taken as the same fraction of U_s at holes 314 and 116 as at hole 322, as these three holes were in the same area. At other points the limiting values $U_b = 0$ and $U_b = U_s$ were taken. The calculation was carried out for the four boreholes, and the 11 points on the longitudinal line between L12 and L35 at which seismic measurements of h and α_b were made. Results are given in Table 23.

Accuracy of measurement must be taken into account. Standard errors of the various quantities are calculated in the relevant parts of section 4. They are also listed in the appropriate tables. As two extreme values were taken for U_b there is no need to consider further errors in the term $U_b \tan(\alpha_b - \alpha_s)$. Thus, from equation (16),

$$\frac{\delta\left(\overline{\frac{\partial u}{\partial x}}\right)}{\left(\overline{\frac{\partial u}{\partial x}}\right)} = \frac{\delta v_o}{v_o - m u_b} + \frac{\delta h}{h}$$

where $m = \tan(\alpha_b - \alpha_s)$

Errors and typical mean values are

$\delta v_o = 0.35$ m./yr.
$\delta h = 5$ m.

$u_b = 30$ m./yr.
$v_o = 3$ m./yr.
$m = -0.15$ to $+0.2$
$h = 250$ m.

Substitution of these values in the last formula gives a standard error of $\left(\overline{\frac{\partial u}{\partial x}}\right)$ of about 12%. Thus if $\left(\overline{\frac{\partial u}{\partial x}}\right)$ and $\left(\frac{\partial u}{\partial x}\right)_s$ differ by more than about 25% of their mean value, it is likely that the difference is a genuine one.

Inspection of Table 23 shows that only in two cases (L23 and L30.5) does $\left(\frac{\partial u}{\partial x}\right)_s$ fall between the two limiting values of $\left(\overline{\frac{\partial u}{\partial x}}\right)$. At L14 $\left(\frac{\partial u}{\partial x}\right)_s$ is not far from the value of $\left(\overline{\frac{\partial u}{\partial x}}\right)$ corresponding to $U_b = 0$. (L14 is, however, only about 600 m. from hole 322 where U_b is about 80% of U_s.) At all other points the discrepancies seem to be too large to be explained by experimental error.

From L12 to L21 the strain rate appears to be less compressive at depth than at the surface. At L25, L27, L32, L34, and hole 209, the reverse is true.

These data therefore show that there are few places along the centreline of the glacier where the longitudinal strain rate is constant with depth.

The modified theory of section 5.1. allows the longitudinal strain rate to vary (linearly) with depth. This theory cannot be verified numerically because the mean strain rate, as calculated by equation (16), is bound to agree with the value $r + \frac{1}{2} Kh$, with K given by equation (15). However, by equation (13), K is equal to $-\frac{\partial^2 v}{\partial x^2}$. This last quantity is constant with depth, according to the theory. It can in theory be calculated by numerical differentiation of the measured values of v. In practice, however, v is

about 3 $\pm$ 0.35 m./yr. and experimental errors are such that numerical values of its second derivative are of little value. However, the sign of $\frac{\partial^2 v}{\partial x^2}$ can be determined from the data. This is tabulated in Table 23. Signs are such that the mean strain rate should be greater or less than the surface strain rate according as $\frac{\partial^2 v}{\partial x^2}$ is negative or positive. Table 23 shows that only at L21 are the signs opposite to that predicted.

Method 2.

Boreholes 322 and 116 are on approximately the same flowline and about 160 m. apart. The distance between the pipes each year at different depths, and hence the longitudinal strain rate, can be calculated. Reduction of the pipe data has been treated in another section. The laminar flow analysis has been used in this case .

If, at a given depth, x_o, x_o' are the x coordinates of the pipes in 1960, x_1, x_1' the coordinates in 1961, ℓ_o, ℓ_1 the surface distance between the pipes in the two years, and t the time interval ($\approx$1 year), then

$$\frac{\partial u}{\partial x} = \frac{2}{t} \cdot \left\{ \frac{(\ell_1 + x_1' - x_1) - (\ell_o + x_o' - x_o)}{(\ell_1 + x_1' - x_1) + (\ell_o + x_o' - x_o)} \right\}$$

This method of analysis should be valid in the upper 100 m. of the pipe because $\frac{\partial u}{\partial y}$ is small there and the values in the two pipes appear to be comparable.

Results are shown in the following table:

y (m.)	$\frac{\partial u}{\partial x}$ (per yr.)
0	-.022
15.2	-.020
30.5	-.014
45.7	-.014
61.0	-.016
76.2	-.014
91.4	-.017
106.7	-.017

The experimental error is large. These results should therefore be treated with reserve until another year's observations have been obtained. Nevertheless they support the conclusion that longitudinal strain rate becomes less compressive with depth.

The observations of Glen (1956, p. 738) in the Austerdalsbre tunnel are of interest in this connection. The longitudinal strain rate decreased from 0.5 per year at the tunnel mouth to 0.15 per year at the end. The tunnel was approximately horizontal and of length 46 m. However, it was at the foot of an icefall and the surface slope was 26°. Nye's theory is not expected to hold under these circumstances.

To sum up, the data which have been presented in this section suggest that the modified theory of section 5.1. is

an improvement over the earlier version.

7.4. Variation of Velocity with Depth

As was mentioned in section 6.6., $\frac{\partial u}{\partial y}$ is positive down to a depth of roughly 100 m. in holes 322, 314, and 116. The data are given in Table 22. The very high value of 0.14 at 15.2 m. in hole 116 is probably the result of an original kink in the pipe. It is thus questionable. Other values are generally in the range 0.005 to 0.010. The standard error is 0.004. Few of the values differ from zero by more than twice the standard error. However, the general trend, and the fact that the effect is shown at three boreholes in the same area, seem to leave little doubt that the effect is genuine. A similar effect has been observed on the Blue Glacier (Sharp, private communication).

The stress solution (equation 7 of section 5.1) shows that τ_{xy} is always negative. The rate of work $\dot{\varepsilon}_{xy}\,\tau_{xy}$ must be positive. Hence $\frac{\partial u}{\partial y} + \frac{\partial v}{\partial x}$ must be negative. Positive values of $\frac{\partial u}{\partial y}$ are thus inconsistent with Nye's theory, in which $\frac{\partial v}{\partial x}$ is zero. On the revised theory (section 5.1.), however, $\frac{\partial v}{\partial x}$ is not zero. Hence $\frac{\partial u}{\partial y}$ may be positive provided that $\frac{\partial v}{\partial x}$ is negative and numerically greater than $\frac{\partial u}{\partial y}$. If it is assumed that components of strain rate and stress deviator tensors are proportional, $\frac{\partial u}{\partial y} + \frac{\partial v}{\partial x}$ must be zero at the surface because τ_{xy} is. Hence

a negative value of $\frac{\partial v}{\partial x}$ at the surface implies a positive value of $\frac{\partial u}{\partial y}$ there. Values of $\frac{\partial v}{\partial x}$ at the surface, calculated by numerical differentiation of measured values of v (see section 3.4.4.), are -0.0045, -0.0005, -0.0055, and -0.0011 at holes 322, 314, 116, and 209 respectively. The standard error is about 0.005. The values are all negative and are comparable in magnitude with the values of $\frac{\partial u}{\partial y}$ in the upper 100 m. of each borehole.

The magnitude of the errors makes it impossible to verify whether $\frac{\partial u}{\partial y} + \frac{\partial v}{\partial x}$ is in fact negative at all depths. But the results are not inconsistent with the revised theory.

There is also another factor which might explain this effect. According to equation (7') of section 5.1. the stress solution is

$$\tau_{xy} = -(\bar{\rho} g \sin \alpha_s + c_1) y$$

where

$$c_1 = \frac{\partial \tau_{xz}}{\partial z} \quad \text{at} \quad z = 0$$

$\dot{\epsilon}_{xz}$ was measured at the surface at holes 322 and 116. Values were .0034 and .0017 respectively (Table 19). Thus τ_{xz} is expected to be positive at these points. Axes were chosen so that holes 322 and 116 lie slightly on that side of the centreline where z is negative. τ_{xz} should be zero on the centreline by symmetry. Thus $\frac{\partial \tau_{xz}}{\partial z}$ is negative at the boreholes. Its value is unknown, but it will decrease the

numerical value of τ_{xy} and may even make τ_{xy} positive. In the latter case, values of $\frac{\partial u}{\partial y}$ would be positive even if $\frac{\partial v}{\partial x}$ were zero. In practice τ_{xz} may vary with depth y, although the theory given above does not permit this. Thus it is possible that the effect is only important near the surface.

It is hoped that a further series of measurements in the boreholes, combined with measurements of $\dot{\varepsilon}_{xz}$ at hole 209 (where $\dot{\varepsilon}_{xy}$ is always negative), will provide more information about this effect.

7.5. Numerical Check of Equation 18

Equation 18 of section 5.1. enables the longitudinal strain rate to be calculated from the ablation rate, ice thickness, flow, surface slope, and curvature. In Table 24, calculated and measured values are compared at the two boreholes and eleven other points on the longitudinal line where ice thickness was measured by seismic means. The flow q was calculated as the product of ice thickness and mean velocity. The latter was taken as 90% of the surface velocity, as explained in section 3.2.5. Surface curvature was calculated by the method of section 3.7.1.

Except at L21, there is no agreement. Equation 18 rests on the assumption that the shear stress on the bed of the glacier is constant, in addition to all the previous assumptions (I to X in section 5.1.). It has been shown in preceding sections that some of these assumptions are

questionable. The lack of agreement in this case is thus hardly surprising.

7.6. The Flow Law of Ice

The present study is concerned not so much with the flow law of ice itself as with its application to glaciers. However, the form of the flow law is important in the subsequent discussion. Work on this subject will therefore be reviewed briefly in this section.

Numerous laboratory experiments have been made to determine the flow law of ice, both in single crystals and polycrystalline aggregates. While some details remain uncertain, the general properties are now well established. Results have been summarized by Glen (1958a, c).

A single crystal deforms plastically only by gliding on the basal plane (McConnel, 1891; Mügge, 1895; Glen and Perutz, 1954; Steinemann, 1954; Nakaya, 1958). It has long been uncertain whether there was any preferred glide direction (Glen and Perutz, 1954; Steinemann, 1954). This question has recently been discussed by Kamb (1961). No yield stress, below which no deformation occurs, has been found (Glen, 1958c, p. 171).

The relation most frequently studied is that between strain and time for constant load. Experiments with single crystals have been carried out by Griggs and Coles (1954), Steinemann (1954), Jellinek and Brill (1956), Butkovich and

Landauer (1958, 1959), and Kamb (1961), among others. For a given stress, the strain rate increases with time. Eventually, however (after perhaps 10 or 20 hours), the strain rate reaches a steady value. Resting of the crystal in the middle of the test does not restore the original part of the curve. Nor does a change of glide direction. Similar behaviour is observed irrespective of whether the stress is applied as a tension, compression, or shear.

The flow law is of the form

$$\dot{\varepsilon} = k \tau^n$$

where $\dot{\varepsilon}$ is the effective shear strain rate and τ is the effective shear stress. (Thus for experiments with uniaxial compression or tension $\dot{\varepsilon}$ is $\sqrt{3}$ x uniaxial strain rate and τ is $(1/\sqrt{3})$x stress.) k and n are constants. Hydrostatic pressure does not affect the flow law provided that the difference between the temperature of the experiment and the melting point is kept constant (Rigsby, 1958). This experiment was carried out at pressures up to 350 bars. The pressure never reaches this value in any glacier or ice-sheet except in Antarctica. The value of k depends on the temperature; that of n does not. Values of n obtained in the experiments listed above range from 1.5 to 3.9 with a mean of about 2.5.

Experiments with randomly oriented polycrystalline ice have been carried out by Glen (1952, 1955), Steinemann

(1958a, b), Butkovich and Landauer (1958, 1959), Vialov (1958), and Mellor (1959), among others.

In contrast to the case of single crystals, the curve of strain against time under constant stress for polycrystals has an initial transient stage in which the strain rate decreases. Thereafter strain rate attains a steady value. However, if the stress is greater than 4 bars the strain rate finally increases again (this last figure refers to Glen's experiment, carried out near the melting point). All details of the relation between the properties of polycrystals and single crystals are not yet clear. However, the initial decrease of strain rate can be ascribed to interference between crystals with different orientations. Production, by recrystallization, of crystals more favourably oriented for glide in the direction of the stress produces the subsequent increase of strain rate (Glen, 1958a, c). Formation of complex interlocking grains makes intergranular slip very difficult.

The flow law of a randomly oriented polycrystalline aggregate appears to be of the same form as that of single crystals, and with about the same value of index n. The following values of n refer to the steady part of the creep curve. They exclude the initial transient part and also any possible final reacceleration under high stress. Glen (1954) obtained values of 3.2 or 4.2. Steinemann's (1958a, p. 25) values ranged from 1.9 at 1 bar to 4.2 at 15 bars. These values were for laboratory ice. Mellor (1959) obtained a

value of 4.2 for Antarctic glacial ice at -30°C for stresses between 2 and 15 bars.

Butkovich and Landauer (1958) carried out two series of experiments, one with shear stresses in the range of 0.5 to 3 bars, the other with uniaxial compressions from 7 to 28 bars. The temperature was -5°C. Both commercial and glacial ice were used. A simple power law with n = 2.96 fitted all the data. Two other proposed laws proved less satisfactory. These were

$$\dot{\varepsilon} = A \sinh \frac{\tau}{\tau_0}$$

and

$$\dot{\varepsilon} = a\tau + b\tau^3$$

These results at high stresses do not agree with those of Glen, quoted above, or of Vialov (1958, p. 389), who observed a great increase of strain rate at stresses above about 5 to 7 bars (at -8°C). This effect is not relevant to the present study because stresses on the glacier are certainly less than 2 bars.

The possibility of a change in the flow law at a stress of about 1 bar is of considerable importance to glacier flow however. The shear stress is less than this value throughout the greater part of a glacier. Glen (1955, p. 536) states that there may be a bend in the stress-strain rate curve at about 1 bar. Steinemann, as quoted above, obtained a value of 1.9 for n at 1 bar. Vialov (1958, p. 389) states that n

is reduced to 1.5 below 1 bar. Shoumskiy (1958, p. 248) states that only in the lowest layers of a glacier is n equal to 3 or 4. It has a lower value throughout the bulk of a glacier. He identifies the transition point as that at which primary recrystallization becomes the predominant mechanism of flow. Mellor (1959) also states that n is 1.5 below 1 bar, but gives no evidence in support. Glen (1958a) criticised Steinemann's results on the ground that, at low stresses, the stress was not maintained for a sufficiently long period. The steady state was thus never reached. It is not clear whether Vialov's results are free from this objection.

The experiments of Jellinek and Brill (1956) showed Newtonian viscous flow. The strains were very much smaller than those in any other experiment, however, and the time period was shorter (2 or 3 hours).

Weertman (1955, 1957a, b) has considered different dislocation mechanisms and derived theoretical creep laws. These are power laws with indices between 2.5 and 4.5

As was stated earlier, the constant k in the flow law depends on the temperature. Glen (1955, p. 532) showed that his data fitted a variation of the form $\exp\left(-\frac{Q}{RT}\right)$. R is the gas constant and T the absolute temperature. Glen obtained a value of 31.8 K cal./mole for Q, the creep activation energy. Lliboutry (1959) obtained a value of 35.4 K cal./mole from various data. More precise measurements (Jellinek and Brill, 1956; Raraty and Tabor, 1958)

indicate that the correct value is about 14 K cal./mole, however.

From a study of phase equilibrium within polycrystalline ice, Steinemann (1958c) has concluded that the behaviour of ice at the melting point can be obtained by extrapolation of results for cold ice. There are no specific mechanisms to modify the flow law near the melting point.

Certain difficulties arise in the application of these results to glacier flow. It must be assumed that crystals in glacier ice are randomly oriented so that the ice is isotropic. It must also be assumed that each piece of ice remains under the same stress long enough for a steady state to be reached (these are assumptions I and II of section 5.1.). Glen (1958c, p. 180) has shown that the first condition may be relaxed. The ice may become anisotropic as a result of the stress but the direction of stress must not change.

The complex stress systems which exist in a real glacier present greater difficulties. In all but one of the experiments described above the stress consisted either of uniaxial tension or compression, or of a simple shear. The sole exception was the experiment of Steinemann (1958a), in which uniaxial compression and shear were superimposed. Results have been interpreted by Glen (1958a, c). They appear to contradict the assumption (V and X of section 5.1.) that the relation between strain rates and stress deviators is of the form $\dot{\varepsilon}_{ij} = \lambda(\xi_2')\,\sigma_{ij}'$.

It is perhaps premature to reject this relation until further experiments have been carried out to confirm Steinemann's result. It seems unlikely that a general solution of the stress equations could be found for the case of a more general flow law which involves the third invariant Σ_3' of the stress deviator tensor.

Derivation of a flow law from measurements on glaciers will be discussed in more detail in following sections. Previous studies have shown broad agreement between field and laboratory results. Nye (1957, p. 130) concluded that the results of the Jungfraujoch borehole experiment (Gerrard and others, 1952) were consistent with a flow law of the form

$$\dot{\varepsilon} = 0.148\ \tau^{4.2}$$

Here $2\dot{\varepsilon}^2 = E_2$, $2\tau^2 = \Sigma_2'$, strains are measured in yr^{-1}, stresses in bars. The constants have the values determined by Glen (1955). Mathews (1959) calculated a value of 2.8 for n from borehole data from the Salmon Glacier. Shreve (1960) obtained a value of 2.6 for two boreholes on the Blue Glacier. Hansen and Landauer (1958) obtained a value of 3.77 from the rate of closure of a borehole in the Greenland ice-cap. The temperature in this case was -25°C.

Measurements of the rate of closure of tunnels dug in glaciers also give information on the flow law. Nye (1953) has analysed these data. He concluded that data from three tunnels (on Z'mutt Glacier, Vesl Skautbreen, and at

Jungfraujoch) were consistent with a power law with n = 3.07. Data from another tunnel (on Arolla Glacier) were not. Subsequent measurements in a tunnel on Austerdalsbre did not agree with the law either, (Glen, 1956). However, these last two tunnels were each located at the foot of an icefall, where the simplifying assumptions of the theory are not expected to hold. Landauer (1959) obtained a value of n of 2.8 from measurements of shear in two tunnels at the edge of the Greenland ice-cap. The shear stresses were considerably less than 1 bar. He obtained a value of 3.2 from measurements of the rates of closure of the same tunnels. The tunnel data cover a lower range of stresses than do most other measurements. They lend no support to the suggestion that n is about 1.5 for stresses below 1 bar.

Meier (1960, p. 43) has proposed a flow law which includes a viscous term. He analysed all available data from boreholes and tunnels and also included Glen's laboratory results. He concluded that the flow law deviated significantly from a simple power law, and fitted the relation

$$\dot{\varepsilon}_0 = 0{\cdot}018\ \sigma_0 + 0{\cdot}13\ \sigma_0^{4{\cdot}5}$$

Here $\dot{\varepsilon}_0 = \sqrt{\frac{E_2}{3}}$, $\sigma_0 = \sqrt{\frac{\xi_2'}{3}}$. Units of stress and strain rate are bars and yr^{-1} respectively.

Meier plotted the data from the Saskatchewan Glacier

twice, once for a laminar flow analysis and once with the longitudinal strain rate taken into account. He also included laminar flow analyses of data from boreholes at the Jungfraujoch and on the Malaspina Glacier. The measured strain rate at the Jungfraujoch was +0.14 per yr. Meier states that the Malaspina borehole was in a region of strong compressive flow. Elimination from Meier's graph of all points for which laminar flow was erroneously assumed, removes all points from the "viscous" part of his curve (i.e. all points for stresses less than 0.2 bars and most points for stresses less than 0.8 bars). The remaining points (except for the Austerdalsbre tunnel data which lie far from any other points on the graph) do not deviate significantly from a simple power law.

The conclusions from this section can be summarized as follows. The flow law for ice is of the form $\dot{\varepsilon} = k \tau^n$. This applies to single crystals or randomly oriented polycrystalline aggregates, under uniaxial compression or tension or simple shear. k but not n depends on the temperature. Neither depend on the hydrostatic pressure. Measured values of n vary between 2 and 4.5 with a mean of about 3. The value of k appears to be about 0.3 or 0.4 at 0°C, for $\dot{\varepsilon}$ in yr^{-1} and τ in bars. This relation holds for stresses between 1 and 5 bars and possibly over a wider range. It is also possible that n falls to about 1.5 for stresses below 1 bar. The extension of the equation to complex stress systems in the form $E_2 = k' \Sigma_2'^n$ is doubtful.

7.7. Effect of Valley Sides

In section 5.1. the shear stress was shown to be

$$\tau_{xy} = -\bar{\rho} g y \sin \alpha_s \qquad \text{(equation 7)}$$

It was assumed, among other things, that the width of the glacier was infinite. An alternative approach was adopted in section 5.2. The glacier was regarded as half of a circular cylinder. The shear stress in this case is

$$\tau_{xr} = -\tfrac{1}{2} \bar{\rho} g r \sin \alpha_s \qquad \text{(equation 19)}$$

For arbitrary cross-section it is approximately

$$\tau_{xr} = -F \bar{\rho} g r \sin \alpha_s \qquad \text{(19a)}$$

where the "shape factor" $F = \frac{A}{ph}$. A is the area of cross-section of the glacier, p is the perimeter excluding the upper surface, and h is the ice thickness at the centreline. On a vertical plane along the centreline r equals the depth y.

If a flow law, based on laboratory results, is assumed to be applicable in a glacier, the relative merits of these two assumptions can be assessed. Curves of $\frac{\partial u}{\partial y}$ against y are calculated from the flow law. They are then compared with the observed results from the two deep boreholes.

Glen's flow law for quasi-viscous creep was adopted, (Glen, 1955). Reasons for this choice will be given in section 7.9. In the present notation the law is

$$\sqrt{\tfrac{1}{2}E_2} = 0.148\left(\sqrt{\tfrac{1}{2}\Sigma'_2}\right)^{4.2}$$

Units of $\sqrt{\frac{1}{2}E_2}$ and $\sqrt{\frac{1}{2}\Sigma'_2}$ are yr.$^{-1}$ and bars respectively. It is sufficiently accurate for the present purpose to use an analysis in which the longitudinal strain rate is zero. This simplifies calculation of the theoretical curves. In this case

$$\sqrt{\tfrac{1}{2}E_2} = \tfrac{1}{2}\frac{\partial u}{\partial y}$$

$$\sqrt{\tfrac{1}{2}\Sigma'_2} = F\bar{\rho}\,g\,y\,\sin\alpha_s$$

The surface slope α_s was measured at each borehole. Values of F for each transverse line were determined from the profiles of Figures 10 to 13. Values at the boreholes were found by linear interpolation between these. The values were 0.58 and 0.62 for holes 322 and 209 respectively. Curves were also drawn for F = 1, the case of an infinitely wide glacier.

Calculated and observed curves are compared in Figure 25. Strain rates calculated without the shape factor are 10 to 20 times greater than those observed. The assumption that the glacier is infinitely wide is thus invalid in this case.

Adoption of a flow law with a lower index than 4.2 would have reduced the separation between the theoretical curves. The conclusion would not have been altered, however.

A more complicated calculation which makes allowance for the longitudinal strain rates also leaves the conclusion unchanged.

The general solution of the stress equations in cylindrical coordinates has not been obtained. The solution for the case of the infinite sheet, as given in section 5.1., has therefore been adopted, with the stress solution modified by the shape factor. The shear stress is $\tau_{xy} = -F \bar{\rho} g y \sin \alpha_s$. In effect, every component of the stress deviator tensor is multiplied by F, because the measured strain rates are unchanged whether F is inserted or not, and it is assumed that components of strain rate and stress deviator tensors are proportional. The constant of proportionality is thus effectively multiplied by $1/F$.

When the glacier is regarded as a cylinder, measurements of change of surface velocity on transverse lines provide information about the flow law. In equation (19a) r can be taken as z, the distance measured across the glacier surface from the centreline. It must be assumed that the longitudinal and transverse strain rates and the velocity normal to the surface are zero, and that the surface is a plane.

In this case,

$$\sqrt{\tfrac{1}{2} E_2} = \tfrac{1}{2} \frac{\partial u}{\partial z}$$

$$\sqrt{\tfrac{1}{2} \Sigma'_2} = F \bar{\rho} g z \sin \alpha_s$$

All quantities on the right-hand sides of these equations are known. Thus the relation between $\frac{1}{2}E_2$ and $\frac{1}{2}\xi_2'$ can be derived.

For the D and E lines, $\frac{\partial u}{\partial x}$ at the surface on the centreline has values -0.004 and +0.005 respectively (Table 16). Corresponding values of $\frac{\partial w}{\partial z}$ are -0.002 and +0.003 (Table 18). These are small compared with values of $\frac{\partial u}{\partial z}$, except near the centreline. The case of the E line is slightly doubtful because there are diagonal crevasses a short distance down glacier from it. The assumption that the glacier surface is a plane is reasonable, but the assumption that v is zero is at best a rough approximation. One practical difficulty is accurate location of the centreline. Its position was determined by interpolation between the two markers in each line where the velocity was greatest. Its position and thus the values of z may be in error by perhaps 25 metres. Values of τ_{xz} for markers near the centreline are thus inaccurate.

Values of $\frac{\partial u}{\partial z}$ and τ_{xz} on the D and E lines are given in Table 25 and their logarithms are plotted in Figure 28. Agreement with the linear relation predicted by the flow law is considered to be satisfactory in view of the inaccuracy of the data.

If on the other hand the glacier is regarded as an infinite sheet, and if the flow is laminar (i.e. if the surface and bed are parallel planes and if the velocity vector is at all points parallel to the surface and directed down the direction of greatest surface slope) the velocity

at any point on the surface is

$$u = A (\bar{\rho} g h \sin \alpha_s)^m$$

The index m depends on the relative proportions of differential movement in the ice and slip on the bed (Nye, 1959c, p. 497). The ice thickness at the point is h. A linear relation between log u and log(h sin α_s) is thus expected. These values for the D and E lines are plotted in Figure 29. No relationship is apparent. However, failure of the assumption of laminar flow may account for this.

Figures 28 and 29 can be regarded as additional evidence for regarding the glacier as a cylinder, rather than an infinite sheet.

7.8. Stress and Strain Rate at Boreholes

The second invariants of the strain rate and stress deviator tensors were evaluated for each point at which inclinations were measured in the two deep boreholes. The formulae are given below. Their derivation and the meanings of the symbols are given in section 5.1.

$$\frac{1}{2} E_2 = \left(\frac{\partial u}{\partial x}\right)^2 + \frac{1}{4}\left(\frac{\partial u}{\partial y} + \frac{\partial v}{\partial x}\right)^2$$

$$\frac{\partial u}{\partial x} = \tau + Ky$$

$$\frac{\partial v}{\partial x} = s - Kx$$

$$K = \frac{2}{h^2}\left[v_s - u_b \tan(\alpha_b - \alpha_s) - \tau h\right]$$

$$\tau_{xy} = -F\bar{\rho} g y \sin\alpha_s$$

$$\lambda = \frac{\frac{1}{2}\left(\frac{\partial u}{\partial y} + \frac{\partial v}{\partial x}\right)}{\tau_{xy}}$$

$$\frac{1}{2}\Sigma_2' = \frac{1}{2}E_2/\lambda^2$$

α_s, $\tau = \left(\frac{\partial u}{\partial x}\right)_s$, $S = \left(\frac{\partial v}{\partial x}\right)_s$ were measured at the surface.

$\frac{\partial u}{\partial y}$ was measured at various depths y.

h, u_b, and the value of x corresponding to a given value of y were also derived from the borehole data.

F was obtained by interpolation between values on the transverse lines.

$\bar{\rho}$ was taken as 0.91.

The upper part of hole 322 (above 150 m.), in which $\frac{\partial u}{\partial y}$ differs from zero by less than twice its standard error, has been excluded from the analysis. Values of $\frac{1}{2}E_2$ and $\frac{1}{2}\Sigma_2'$ are given in Table 26. Their logarithms are plotted in Figures 26 and 27.

It should be noted that the data have not been smoothed. It is difficult to make a precise error analysis of these data. The errors may be roughly assessed as follows.

In the upper part of each borehole the major part of

$\frac{1}{2}E_2$ is $\left(\frac{\partial u}{\partial x}\right)^2$. The standard error of $\frac{\partial u}{\partial x}$ is about 10% (see section 4.5.). Hence the standard error of $\frac{1}{2}E_2$ is about 20%. In the lower part of each borehole the major part of $\frac{1}{2}E_2$ is $\left(\frac{\partial u}{\partial y}\right)^2$. The error of $\frac{\partial u}{\partial y}$ is again of the order of 10% in hole 209, but somewhat greater than this in hole 322 (see Table 22). A 20% error in $\frac{1}{2}E_2$ will cause an error of 0.2 in log $\frac{1}{2}E_2$. The error in y is small. Although F and α_s are subject to errors of the order of 5%, these will affect all values for the one borehole equally. The error in τ_{xy} is thus negligible. There will be an error in $\frac{1}{2}\dot{\varepsilon}_2'$ however, because this quantity is calculated from $\frac{1}{2}E_2$.

A linear relation between log $\frac{1}{2}E_2$ and log $\frac{1}{2}\dot{\varepsilon}_2'$ is regarded as a satisfactory fit at each borehole, within the accuracy of the present data. This does not, of course, exclude the possibility that measurements over a period of several years will reveal significant deviations from a linear relationship.

The data from both boreholes and the transverse lines are all plotted on Figure 30. Within the experimental error, all the points for the boreholes and some of those for the transverse lines appear to lie on the same straight line. This is interpreted as an indication that the basic assumptions of Nye's theory are reasonable approximations. The important assumptions are that τ_{xy} varies only slowly with x, that components of strain rate and stress deviator tensors are proportional, and that the constant of proportion-

ality depends only on ξ_2' .

The question of the optimum value of the index in the power law is discussed in the next section.

7.9. Comparison of Data with Different Flow Laws

Two slightly different approaches can be used to obtain information about the flow law from glacier data. Different forms of flow law can be assumed, and the optimum values of the numerical constants in these laws can be deduced from the data. Alternatively, one can test whether the data deviate significantly from a flow law determined in the laboratory. Both approaches will be considered here.

A simple power law was assumed and the value of the index n calculated as the regression coefficient of $\log \frac{1}{2} E_2$ on $\log \frac{1}{2} \xi_2'$. Results for the four sets of data were as follows:

Data	n	number of points
D line	1.4	5
E line	2.2	4
Hole 322	2.3	12
Hole 209	5.2	12

It will be explained later why values of n determined from the transverse lines might be less than those determined from boreholes.

The standard error of n, as determined from the regression

analysis, is about 0.8 for the two boreholes. Errors of the other data will be considerably greater. As was explained in section 6.6, conditions in the lowest 35 m. of hole 209 may be unusual as a result of the configuration of the bed. If the last three points are omitted from the regression, the value of n for this hole is reduced to 2.8. The fact that the value can be almost halved by omitting three points reinforces the view, suggested by the large standard error, that values of n derived by this method are unreliable.

The inclinometer used in these experiments reads to 0.1°. Considerable care was taken in making the measurements. The overall accuracy could be improved slightly by reduction of the spacing between measurement points in the pipe. This will be done in future measurements. However, it is considered unlikely that the standard of accuracy can be improved to any great extent. The accuracy of the data from the transverse lines could be improved considerably by a considerable increase in the number of markers.

Apart from inaccuracies in measurement, the complex stress systems which exist in glaciers make interpretation of observations difficult. The most that one can expect to do is to demonstrate whether glacier measurements are consistent with a flow law determined in the laboratory.

It is desirable to know the value of k, the multiplying constant in the flow law, as well as the index n. The constant k depends on the temperature. A value determined

at the same temperature as the glacier, or else one adjusted for the temperature difference, must therefore be used. Two of the most extensive series of laboratory experiments are those of Glen (1955) and Butkovich and Landauer (1958). Their values have been taken. It is not absolutely certain that the Athabaska Glacier is at the pressure melting temperature. Flow laws for -1.5°C as well as 0°C have therefore been used. The constants are given below. They refer to a flow law of the form $\sqrt{\frac{1}{2} E_2} = k \left(\sqrt{\frac{1}{2} \Sigma_2'} \right)^n$. Units of $\sqrt{\frac{1}{2} E_2}$, $\sqrt{\frac{1}{2} \Sigma_2'}$, and k are $yr.^{-1}$, bars, and $yr^{-1}\ bar^{-n}$ respectively.

Source	k	n	T°C
Glen ("quasi-viscous creep")	0.148	4.2	0
	0.020	4.2	-1.5
Glen ("minimum observed creep")	0.854	3.2	0
	0.116	3.2	-1.5
Butkovich and Landauer	0.435	2.96	0
	0.372	2.96	-1.5

The temperature correction is somewhat uncertain. Glen measured the "minimum observed creep" at four different temperatures. He assumed that k varied with temperature according to the Boltzmann law $\exp. \left(- \frac{Q}{RT} \right)$, and obtained the value of Q which best fitted his data. The point corresponding to measurements at -0.02°C did not lie on the curve, however. Thus the change in the value of k, as

tabulated, for a temperature change from -1.5°C to 0°C is much greater than predicted by the Boltzmann law with $Q = 31.8$ K cal./mole. Moreover, this value of Q is now considered to be too high (see section 7.6.). In the table above, the values of k for the minimum observed creep at the two temperatures are Glen's values. Glen only gives a value of k at 0°C for the case of quasi-viscous creep. The value at -1.5°C in the table was calculated so that the ratios of k at the two temperatures were the same for the two creep laws.

The experiments of Butkovich and Landauer were carried out at -5°C. The value of k at 0°C has been calculated by the Boltzmann law with a value of Q of 14 K cal./mole, as has been done by Weertman (1961, p. 960). The value at -1.5°C has been calculated in the same way. The change of k with temperature is very much smaller in this case than in Glen's results. However, it has not been clearly established that k does vary with temperature according to the Boltzmann Law, especially near the melting point. Thus Glen's determinations of k which were made at the two temperatures in question are to be preferred.

These six flow laws are plotted in the form $\log \frac{1}{2}E_2$ against $\log \frac{1}{2}\xi'_2$ in Figure 30. All points from the two deep boreholes and the two transverse lines are also shown.

If the points at the lower end of the curve (i.e. for stresses less than 1 bar) are disregarded, Glen's law for quasi-viscous creep ($n = 4.2$) provides the best fit to the

data. All the borehole points lie between the two lines which correspond to this law. The fit would be very satisfactory if the glacier had a mean temperature of about -0.75°C rather than the pressure melting temperature. Unfortunately, no temperature measurements are available. It is to be hoped that some will be made at some future date.

The possibility that n may be reduced for stresses below 1 bar was discussed in section 7.6. The deviations from the straight lines at low stresses in Figure 30 might be taken to support this theory. In addition, the values of n calculated from the D and E lines are 1.4 and 2.2. The mean stresses are 0.33 and 0.66 bars respectively. The interpretation is doubtful however. The points which show this trend are all derived from the transverse surface profiles and at points within 200 m. of the centreline. The position of the centreline was not determined to better than $\pm$25 m. Thus the calculated shear stresses at the points are not very reliable. Also the shear strain rate in this region is little greater than the longitudinal and transverse strain rates. Thus the assumption on which the calculation rests is dubious.

In addition, measurements of surface velocity include both differential motion within the ice and slipping of the glacier on its bed. At hole 322, which is about 500 m. up glacier from the D line, slipping represents about 80% of the total velocity. Weertman (1957c) has put forward a

theory of the slipping of a glacier on its bed. There is little experimental evidence for or against it. According to this theory the velocity of slipping is proportional to $R^{n+1} \tau^{\frac{1}{2}(n+1)}$ where τ is the shear stress on the bed, R measures the roughness of the bed, and n is the index in the flow law. When the glacier is regarded as a cylinder, as here, τ should be constant along a transverse line. In this case only differential motion within the ice would contribute to $\frac{\partial u}{\partial z}$, the rate of change of velocity with distance from the centreline. But the theory may be an oversimplification. In addition, the roughness of the bed might be smaller near the sides of the glacier than near the centre. This might result either from the nature of the bed or because meltwater was more plentiful at the sides than near the centre. This would reduce the value of n derived from measurements of variation of $\frac{\partial u}{\partial z}$ with z.

The question might be resolved by measurements of surface velocity at several points near the middle of a transverse line in a region where longitudinal and transverse strain rates were small and the glacier was not slipping on its bed. An alternative method would be to make measurements in the upper part of a borehole where longitudinal and transverse strain rates were less than about 0.005 per yr. None of the present boreholes meet this requirement.

APPENDIX 1

Alternative Derivation of Equation (16)

The following alternative derivation of equation (16) in section 5.1. is due to Savage.

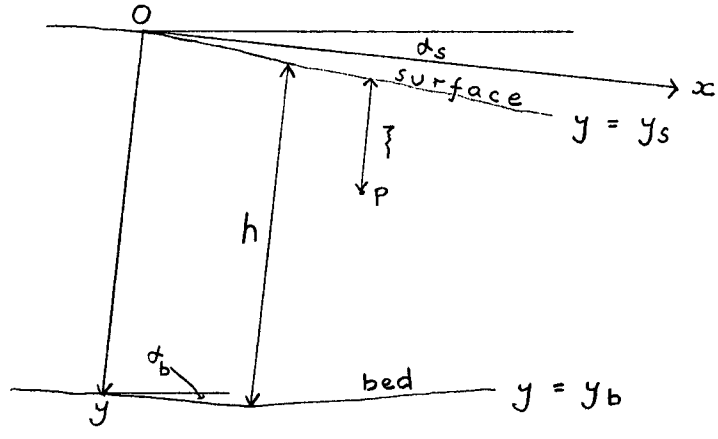

Take x, y axes in directions of tangent and normal to the surface at the origin.

Let $y = y_s(x,t)$ be the surface

$y = y_b(x)$ be the bed.

Consider a particle of ice just below the surface. Let D denote differentiation following the particle.

Let $u = \frac{Dx}{Dt}$, $v = \frac{Dy}{Dt}$ (Velocities are measured following the particle.)

Let ζ denote distance below ice surface, and h ice thickness.

$$\zeta(x, y, t) = y - y_s(x, t)$$

$$h(x, t) = y_b(x) - y_s(x, t)$$

$$= y_b(x) - y + \zeta(x, y, t)$$

$$\frac{\partial h}{\partial x} = \frac{dy_b}{dx} - \frac{\partial y_s}{\partial x}$$

$$\frac{\partial h}{\partial y} = 0$$

$\frac{dy_b}{dx} = m = \tan(\alpha_b - \alpha_s)$ where $\alpha_b - \alpha_s$ = slope of bed relative to x axis.

The continuity equation can be written as

$$\frac{\partial q}{\partial x} + \frac{\partial h}{\partial t} = \psi$$

where ψ is the rate of accumulation (or ablation).

The flow $$q = \int_{y_s}^{y_b} u \, dy$$

$$\frac{\partial q}{\partial x} = \int_{y_s}^{y_b} \frac{\partial u}{\partial x} dy + u_b \frac{dy_b}{dx} - u_s \frac{\partial y_s}{\partial x}$$

$$= h\left(\overline{\frac{\partial u}{\partial x}}\right) + m u_b - u_s \frac{\partial y_s}{\partial x}$$

$$\frac{\partial h}{\partial t} = \frac{Dh}{Dt} - u\frac{\partial h}{\partial x} \qquad \text{since } \frac{\partial h}{\partial y} = 0$$

$$= \frac{Dh}{Dt} - mu + u\frac{\partial y_s}{\partial x}$$

But $$\frac{Dh}{Dt} = mu - v + \frac{D\zeta}{Dt}$$

and $$\frac{D\zeta}{Dt} = \psi$$

The particle in question is just below the surface. So $u = u_s$ and $v = v_s$ in the last two equations. Substitution in the continuity equation yields

$$\psi = h\left(\overline{\frac{\partial u}{\partial x}}\right) + mu_b - u_s\frac{\partial y_s}{\partial x} - v_s + \psi + u_s\frac{\partial y_s}{\partial x}$$

i.e. $$h\left(\overline{\frac{\partial u}{\partial x}}\right) = v_s - mu_b$$

which is equation (16).

It is important to note that the ablation (or accumulation) rate does not occur in the final equation (16).

APPENDIX 2

Generalizations of the Theory

Some possible generalizations of the theory of section 5.1. will be outlined here. The results appear to be of little practical value, however.

First, a three-dimensional treatment will be considered. In this, assumptions I to VI and X of the previous section stand. VII (plane strain) is not made. VIII is replaced by the assumption that every component of the stress deviator tensor is independent of x. IX is replaced by the assumption that the glacier is of constant thickness h.

The equations for the velocities are obtained as follows. The incompressibility condition gives

$$\frac{\partial u}{\partial x} + \frac{\partial v}{\partial y} + \frac{\partial w}{\partial z} = 0$$

The stress deviator components being independent of x give

$$\frac{\partial^2 u}{\partial x^2} = 0$$

$$\frac{\partial^2 v}{\partial x \partial y} = 0$$

$$\frac{\partial^2 w}{\partial x \partial z} = 0$$

$$\frac{\partial^2 u}{\partial x \partial y} + \frac{\partial^2 v}{\partial x^2} = 0$$

$$\frac{\partial^2 w}{\partial x \partial y} + \frac{\partial^2 v}{\partial x \partial z} = 0$$

$$\frac{\partial^2 u}{\partial x \partial z} + \frac{\partial^2 w}{\partial x^2} = 0$$

The boundary conditions are that v = 0 on y = h for all x and z. Also $\dot{\varepsilon}_{xy} = \dot{\varepsilon}_{yz} = 0$, on y = 0 for all x and z.

It is also necessary to make the simplifying assumption that the variation of each velocity with z is linear.

The following velocity solutions are obtained

$$u = u_0 + a_1 x + a_2 z + a_1 a_2 xz + \varphi_1(y)$$

$$v = -(a_1 + a_3 + a_1 a_2 z)(y - h)$$

$$w = w_0 + a_4 x - \frac{1}{2} a_1 a_2 x^2 + a_3 z - a_1 a_2 hy + \varphi_2(y)$$

The constants are the values of the following quantities at the origin.

$$a_1 = \frac{\partial u}{\partial x} \qquad a_2 = \frac{\partial u}{\partial z} \qquad a_3 = \frac{\partial w}{\partial z} \qquad a_4 = \frac{\partial w}{\partial x}$$

$$\varphi_1(0) = \varphi_1'(0) = \varphi_2(0) = \varphi_2'(0) = 0$$

The functions can be evaluated if the flow law is known.

The stress equations reduce to

$$\frac{\partial \sigma_x}{\partial x} + \frac{\partial \tau_{xy}}{\partial y} + \rho g_x = 0$$

$$\frac{\partial \sigma_y}{\partial y} + \rho g_y = 0$$

$$\frac{\partial \tau_{yz}}{\partial y} + \frac{\partial \sigma_z}{\partial z} = 0$$

The boundary conditions are

$$\left.\begin{aligned} \sigma_y &= \pi \text{ (atmospheric pressure)} \\ \tau_{yz} &= \tau_{xy} = 0 \end{aligned}\right\} \text{on } y = 0 \text{ for all } x, z.$$

The solutions are

$$\sigma_x = \pi - \bar{\rho} g_y y + \frac{1}{\lambda}(2a_1 + a_3 + 2a_1 a_2 z)$$

$$\sigma_y = \pi - \bar{\rho} g_y y$$

$$\sigma_z = \pi - \bar{\rho} g_y y + \frac{1}{\lambda}(a_1 + 2a_3 + a_1 a_2 z)$$

$$\tau_{xy} = -\bar{\rho} g_x y$$

$$\tau_{yz} = \frac{1}{2\lambda}(-a_1 a_2 y + \varphi_2'(y))$$

$$\tau_{zx} = \frac{1}{2\lambda}(a_4 + a_2)$$

One objection to this solution is that in it $\frac{\partial u}{\partial x}$ is independent of y.

An alternative approach is to consider plane strain but to attempt to eliminate the assumptions that ε_z' and τ_{xy} are functions of y only. If it is assumed instead that σ_x' is independent of x (i.e. $\frac{\partial \sigma_x}{\partial x} = \frac{\partial \sigma_y}{\partial x}$), the equations for

the stresses become

$$\frac{\partial \sigma_y}{\partial x} + \frac{\partial \tau_{xy}}{\partial y} + \rho g_x = 0$$

$$\frac{\partial \tau_{xy}}{\partial x} + \frac{\partial \sigma_y}{\partial y} + \rho g_y = 0$$

Hence

$$\frac{\partial^2 \sigma_y}{\partial x^2} = \frac{\partial^2 \sigma_y}{\partial y^2}$$

$$\frac{\partial^2 \tau_{xy}}{\partial x^2} = \frac{\partial^2 \tau_{xy}}{\partial y^2}$$

Solutions are

$$\sigma_y = f_1(x-y) + f_2(x+y) + \pi$$

$$\tau_{xy} = g_1(x-y) + g_2(x+y)$$

The boundary conditions for a plane surface are

$$\left.\begin{aligned} \sigma_y &= \pi \\ \tau_{xy} &= 0 \end{aligned}\right\} \quad \text{on } y = 0 \text{ for all } x.$$

To satisfy these

$$f_1 = -f_2, \qquad g_1 = -g_2$$

Hence

$$\frac{\partial \sigma_y}{\partial x} = 0, \qquad \frac{\partial \tau_{xy}}{\partial x} = 0 \qquad \text{and thus}$$

$$\frac{\partial \sigma_x}{\partial x} = 0, \qquad \frac{\partial \varepsilon_2'}{\partial x} = 0$$

Thus the assumption that σ_x' is independent of x implies that ε_2' and τ_{xy} are also.

The single assumption that τ_{xy} is independent of x leads to a more general case. In this case

$$\sigma_y = \pi - \bar{\rho} g_y y \qquad \text{as before,}$$

but τ_{xy} is an arbitrary function of y, and σ_x is a function of both x and y. Further simplifying assumptions are necessary.

An alternative approach is to consider plane strain and assume that $\sigma_x' = \sigma_y' = 0$, without assuming that any of the stress components are independent of x.

Since $\sigma_x' = \sigma_y' = 0$, $\sigma_x = \sigma_y$, $\frac{\partial \sigma_x}{\partial x} = \frac{\partial \sigma_y}{\partial x}$

and this case is included in one which was treated before.

BIBLIOGRAPHY

The following abbreviations are used.

I.A.S.H. 46 - International Association of Scientific Hydrology, Publication 46; Proceedings of General Assembly at Toronto, 1957, Vol. IV, Snow and Ice.

Similarly, Publication 47; Proceedings of Symposium at Chamonix, 1958, Physics of the movement of ice.

Publication 54; Proceedings of General Assembly at Helsinki, 1960, Snow and Ice.

Publication 55; Proceedings of Symposium on Antarctica, Helsinki, 1960.

J. Glac. - Journal of Glaciology.

P.R.S. - Proceedings of Royal Society (London), Series A.

Butkovich, T.R., and Landauer, J.K. 1958. The Flow Law for Ice. I.A.S.H. 47, p. 318-25.

Butkovich, T.R., and Landauer, J.K. 1959. The Flow Law for Ice. U.S. Snow, Ice and Permafrost Research Establishment, Research Report 56.

Collier, E.P. 1960. Study of Glaciers in Banff and Jasper National Parks 1960. Water Resources Branch, Department of Northern Affairs and National Resources.

Demorest, M. 1941. Glacier Flow and its Bearing on the Classification of Glaciers. Bulletin of Geological Society of America, Vol 52, p. 2024-25.

Demorest, M. 1943. Ice Sheets. Bulletin of Geological Society of America, Vol. 54, p. 363-400.

Field, W.O., and Heusser, C.J. 1953. Glacier and Botanical Studies in the Canadian Rockies 1953. Canadian Alpine Journal, Vol. 37, p. 128-40.

Finsterwalder, S. 1897. Der Vernagtferner. Wissenschaftliche Ergänzungshefte zur Zeitschrift der deutsch und österreich. Alpenvereine, Vol. 1, No. 1, p. 1-112.

Gerrard, J.A.F., and others. 1952. Measurement of the Velocity Distribution along a Vertical Line through a Glacier, by J.A.F. Gerrard, M.F. Perutz and A. Roch. P.R.S., Vol. 213, No. 1115, p. 546-58.

Glen, J.W. 1952. Experiments on the Deformation of Ice. J. Glac., Vol. 2, No. 12, p. 111-15.

Glen, J.W. 1955. The Creep of Polycrystalline Ice. P.R.S., Vol. 228, No. 1175, p. 519-38.

Glen, J.W. 1956. Measurement of the Deformation of Ice in a Tunnel at the Foot of an Icefall. J. Glac., Vol. 2, No. 20, p. 735-45.

Glen, J.W. 1958a. The Mechanical Properties of Ice. 1. The Plastic Properties of Ice. Advances in Physics, Vol. 7, No. 26, p. 254-65.

Glen, J.W. 1958b. The Slip of a Glacier past its Side Walls. J. Glac., Vol. 3, No. 23, p. 188-92.

Glen, J.W. 1958c. The Flow Law of Ice. I.A.S.H. 47, p. 171-83.

Glen, J.W. 1961. Measurement of the Strain of a Glacier Snout. I.A.S.H. 54, p. 562-67.

Glen, J.W., and Perutz, M.F. 1954. The Growth and Deformation of Ice Crystals. J. Glac., Vol. 2, No. 16, p. 397-403.

Griggs, D.T., and Coles, N.E. 1954. Creep of Single Crystals of Ice. U.S. Snow, Ice and Permafrost Research Establishment. Report II.

Hansen, B.L., and Landauer, J.K. 1958. Some Results of Ice-Cap Drill Hole Measurements. I.A.S.H. 47, p. 313-17.

Heusser, C.J. 1956. Postglacial Environments in the Canadian Rocky Mountains. Ecological Monographs, Vol. 26, p. 263-302.

Jellinek, H.H.G., and Brill, R. 1956. Viscoelastic Properties of Ice. Journal of Applied Physics, Vol. 27, No. 10, p. 1198-1209.

Kamb, W.B. 1961. The Glide Direction in Ice. J. Glac., Vol. 3, No. 30, p. 1097-1106.

Kanasewich, E.R. 1960. An Interpretation of Some Gravity Measurements in the Canadian Cordillera. Thesis, University of Alberta.

Lagally, M. 1934. Mechanik und Thermodynamik des stationären Gletschers. Leipzig.

Landauer, J.K. 1959. Some Preliminary Observations on the Plasticity of Greenland Glaciers. J. Glac., Vol. 3, No. 26, p. 468-74.

Lliboutry, L. 1961. Température des couches inférieures et vitesse d'un inlandsis. Comptes Rendus, Vol. 252, No. 12, p. 1818-20.

Mathews, W.H. 1959. Vertical Distribution of Velocity in Salmon Glacier, British Columbia. J. Glac., Vol. 3, No. 26, p. 448-54.

McConnel, J.C. 1891. On the Plasticity of an Ice Crystal. P.R.S., Vol. 49, No. 299, p. 323-43.

Meier, M.F. 1960. Mode of flow of Saskatchewan Glacier, Alberta, Canada. U.S. Geological Survey Professional Paper No. 351.

Mellor, M. 1959. Creep Tests on Antarctic Glacier Ice. Nature, Vol. 184, No. 4687, p. 717.

Mügge, O. 1895. Uber die Plasticität der Eiskrystalle. Neues Jahrbuch für Mineralogie, Geologie und Palaeontologie, Vol. 2, p. 211-28.

Nakaya, U. 1958. The Deformation of Single Crystals of Ice. I.A.S.H. 47, p. 229-40.

Nizery, A. 1951. Electrothermic Rig for the Boring of Glaciers. Transactions of the American Geophysical Union, Vol. 32, No. 1, p. 66-72.

Nye, J.F. 1951. The Flow of Glaciers and Ice-Sheets as a Problem in Plasticity. P.R.S., Vol. 207, No. 1091, p. 554-72.

Nye, J.F. 1952a. A Method of Calculating the Thickness of the Ice-Sheets. Nature, Vol. 169, No. 4300, p. 528-30.

Nye, J.F. 1952b. The Mechanics of Glacier Flow. J. Glac., Vol. 2, No. 12, p. 82-93.

Nye, J.F. 1953. The Flow Law of Ice from Measurements in Glacier Tunnels, Laboratory Experiments, and the Jungfraufirn Borehole Experiment. P.R.S., Vol. 219, No. 1139, p. 477-89.

Nye, J.F. 1957. The Distribution of Stress and Velocity in Glaciers and Ice-Sheets. P.R.S., Vol. 239, No. 1216, p. 113-33.

Nye, J.F. 1958a. Surges in Glaciers. Nature, Vol. 181, No. 4621, p. 1450-51.

Nye, J.F. 1958b. A Theory of Wave Formation in Glaciers. I.A.S.H. 47, p. 139-54.

Nye, J.F. 1959a. The Deformation of a Glacier below an Icefall. J. Glac., Vol. 3, No. 25, p. 387-408.

Nye, J.F. 1959b. A Method of Determining the Strain Rate Tensor at the Surface of a Glacier. J. Glac., Vol. 3, No. 25, p. 409-19.

Nye, J.F. 1959c. The Motion of Ice-Sheets and Glaciers. J. Glac., Vol. 3, No. 26, p. 493-507.

Nye, J.F. 1960. The Response of Glaciers and Ice-Sheets to Seasonal and Climatic Changes. P.R.S., Vol. 256, No. 1287, p. 559-84.

Raraty, L.E., and Tabor, D. 1958. The Adhesion and Strength Properties of Ice. P.R.S., Vol. 245, No. 1241, p. 184-201.

Reid, I.A. 1961. Triangulation Survey of the Athabaska Glacier July 1959. Water Resources Branch, Department of Northern Affairs and National Resources.

Rigsby, G.P. 1958. Effect of Hydrostatic Pressure on Velocity of Shear Deformation of Single Ice Crystals. J. Glac., Vol. 3, No. 24, p. 273-78.

Seligman, G. 1947. Extrusion Flow in Glaciers. J. Glac., Vol. 1, No. 1, p. 12-21.

Sharp, R.P. 1953a. Deformation of a Vertical Borehole in a Piedmont Glacier. J. Glac., Vol. 2, No. 13, p. 182-84.

Sharp, R.P. 1953b. Deformation of Borehole in Malaspina Glacier, Alaska. Bulletin of the Geological Society of America, Vol. 64, No. 1, p. 97-99.

Sharp, R.P. 1960. Glaciers. Eugene, Oregon, University of Oregon Press.

Shoumskiy, P.A. 1958. The Mechanism of Ice Straining and its Recrystallization. I.A.S.H. 47, p.244-48.

Shoumskiy, P.A. 1961a. On the Theory of Glacier Motion. I.A.S.H. 55, p. 142-49.

Shoumskiy, P.A. 1961b. The Dynamics and Morphology of Glaciers. I.A.S.H. 55, p. 152-61.

Shreve, R. 1961. The Borehole Experiment on Blue Glacier, Washington. I.A.S.H. 54, p. 530-31.

Somigliana, C. 1921. Sulla profondita dei ghiacciai. Rendiconti della accademia nazionale dei Lincei, No. 30.

Stacey, J.S. 1960. A Prototype Hotpoint for Thermal Boring on the Athabaska Glacier. J. Glac., Vol. 3, No. 28, p. 783-86.

Steinemann, S. 1954. Results of Preliminary Experiments on the Plasticity of Ice Crystals. J. Glac., Vol. 2, No. 16, p. 404-13.

Steinemann, S. 1958a. Experimentelle Untersuchungen zur Plastizität von Eis. Beiträge zur Geologie der Schweiz, Geotechnische Serie, Hydrologie, No. 10.

Steinemann, S. 1958b. Resultats experimentaux sur la dynamique de la glace et leurs correlations avec le mouvement et la petrographie des glaciers. I.A.S.H. 47, p. 184-98.

Steinemann, S. 1958c. Thermodynamics and Mechanics of Ice at the Melting Point. I.A.S.H. 47, p. 254-65.

Streiff-Becker, R. 1938. Zur Dynamik des Firneises. Zeitschrift für Gletscherkunde, Vol. 26, p. 1-21.

Stutfield, H.E.M., and Collie, J.N. 1903. Climbs and Explorations in the Canadian Rockies. London, Longmans, Green and Co.

Vialov, S.S. 1958. Regularities of Ice Deformation. I.A.S.H. 47, p. 383-91.

Ward, W.H. 1958. Surface Markers for Ice Movement Surveys. I.A.S.H. 47, p. 105-10.

Weertman, J. 1955. Theory of Steady State Creep based on Dislocation Climb. Journal of Applied Physics, Vol. 26, No. 10, p. 1213-17.

Weertman, J. 1957a. Steady State Creep through Dislocation Climb. Journal of Applied Physics, Vol. 28, No. 3, p. 362-64.

Weertman, J. 1957b. Steady State Creep of Crystals. Journal of Applied Physics, Vol. 28, No. 10, p. 1185-89.

Weertman, J. 1957c. On the Sliding of Glaciers. J. Glac., Vol. 3, No. 21, p. 33-38.

Weertman, J. 1958. Travelling Waves on Glaciers. I.A.S.H. 47, p. 162-68.

Weertman, J. 1961. Equilibrium Profile of Ice-Caps. J. Glac., Vol. 3, No. 30, p. 953-64.

TABLE 1

POSITIONS AND ELEVATIONS OF TRIANGULATION STATIONS.

Units of coordinates are cm.

Elevation is cm above datum of 6000 feet (= 182880 cm).

Station	E	N	Elevation
1	200000	200000	14266
2	not used		
3	200000	249276	14942
4	294909	246037	11658
5	191724	288699	21020
6	313580	317056	25677
7	201720	347205	28749
8	313822	365583	32921
9	218963	409146	32850
10	314319	383070	34092
11	241414	466335	42414
12	330010	401102	33193
13	264965	510239	47076
14	364695	439354	40326
15	285971	549786	58838
16	412254	504918	45952
17	325728	591070	42191
18	453176	583609	52152
19	337211	616872	51617
20	468119	626003	56232
21	356578	660399	57652

TABLE 2

INITIAL POSITIONS AND ELEVATIONS OF MARKERS.

Units of coordinates are cm.
Elevation is cm above datum of 6000 feet (= 182880 cm).
Reference point is top of marker.
Results are corrected if marker was leaning.
Standard errors of position and elevation are 10 cm except for markers with an asterisk. The standard errors of these are 50 cm.

Marker	Date	E	N	Elevation
A 1	17.8.59	376159	669537	53996
2	21.7.59	382423	668065	54346
3	"	388080	666335	54562
4	"	399644	663342	54593
5	"	410393	659676	54391
6	17.8.59	421059	656290	53774
7	21.7.59	426304	655238	53878
B 1	"	362237	625508	44122
2	"	368327	622594	43840
4	"	381878	616212	44271
6	"	397065	609073	44684
7	"	406433	604664	44683
9	"	423536	596233	44060
C 2	"	327198	577054	40814
3	"	335941	573617	40425
5	"	350967	567929	40920
7	"	365048	562631	41241
9(L17)	22.7.59	378699	557469	41388
11	21.7.59	392803	552240	41274
13	"	408996	546219	41158
D 2	14.8.59	307593	524141	37123
3	20.7.59	315271	520687	37986
4	"	324501	516392	38135
5	23.7.60	332347	509167	38187
6	20.7.59	343303	507661	38276
7(L21)	"	349235	505024	38212
8	"	352641	503345	38243
9	23.7.60	359389	496568	38191
10	20.7.59	369902	495414	38331
11	23.7.60	378427	489019	38583

Table 2 continued

E	1	20.7.59	268814	472319	34429
	2	20.7.59	274921	467962	33584
	3	"	285106	460789	34352
	4	"	293529	454889	34464
	5	14.8.59	302245	448480	34414
	6	20.7.59	309703	443544	34489
	7	"	317936	437833	34332
F	1	19.7.59	228112	394732	25878
	2	"	236131	391234	25676
	3	"	243622	388053	26183
	4	"	252673	384233	26576
	6	"	271098	376473	27360
	7(L32)	"	276030	374433	27221
	8	"	279638	372903	27168
	9	"	294702	366639	26712
G	1	"	221009	338423	17970
	2	"	229605	334046	18640
	3	"	237917	329878	18657
	4	"	247032	325332	18611
	5	"	256145	320811	18536
	6(L37)	"	259816	319001	18130
	7	"	270082	313913	16863
	8	"	284279	306905	17433
L	1	1.9.59	405594	678070	54877
	2	21.7.59	408845	667827	54953
	10	"	406815	627770	46054
	11	"	404380	619947	45385
	12	"	401427	610572	44895
	13	"	398480	601161	44382
	14	"	395459	591500	43841
	15	"	392566	582208	43309
	16	22.7.59	385715	569979	42421
	17(C9)	"	378699	557469	41388
	18	"	371415	544494	40262
	19	"	364783	532638	39391
	20	"	357255	519261	38716
	21(D7)	20.7.59	349235	505024	38212
	22	22.7.59	341615	491522	37740
	23	18.8.59	334092	478143	36940
	24	"	327123	465763	36169
	25	22.7.59	320162	453234	35498
	26	"	315974	445787	34970
	27	"	312451	439455	34324
	28	2.9.59	307552	430720	33030
	29	22.7.59	300721	418524	31635
	30	19.7.59	292060	403046	29731
	31	"	283274	387371	28262
	32(F7)	"	276030	374433	27221

Table 2 continued

L33	19.7.59	271369	366109	26373
34	"	266754	357879	25177
35	"	262771	350773	23896
36	"	260782	331803	20760
37(G6)	"	259816	319001	18130
38	"	260356	307726	14520
39	"	261054	303763	13236
J 2*	3.8.60	467773	668030	60561
3*	"	466827	761382	72920
4*	"	474135	778249	79804
5*	"	484673	794154	84501
6*	"	426469	812361	90947
7*	"	441050	815973	88588
9*	"	502652	805554	87370
10*	"	432071	770318	69436
11*	"	392464	727440	64750
12*	"	394704	697026	57886
"B"*	5.8.59	475513	768687	77221
"D"*	"	424019	717000	63649
"E"*	"	460635	691757	63392
Hole 314	23.7.60	373519	547471	40664
Hole 10	31.7.60	360917	544838	40286
Hole 322	23.7.60	359034	548077	40289
Hole 116	25.7.60	352884	532393	39318
Hole 209	19.7.61	297176	412612	30647
Hole 194	"	288849	400103	29306
Hole 73	12.8.60	236365	350206	21861

TABLE 3

LONGITUDINAL SURFACE PROFILE.

Distances are in metres from the 1959 position of L10.
Elevations refer to ice surface measured in cm above datum.
Standard error of distance 15 cm, of elevation 10 cm.

Date	27.7.59		24.7.60	
Marker	Distance	Elevation	Distance	Elevation
L10	0	45897	75	45239
11	82	45208	149	44860
12	180	44727	240	44445
13	279	44214	335	43969
14	380	43691	432	43434
15	477	43134	527	42863
16	618	42243	664	41932
17	761	41236	804	40927
Hole 314	832		873	40408
18	910	40107	950	39846
19	1046	39211	1083	39052
20	1199	38566	1234	38486
21	1362	38055	1396	38002
22	1517	37598	1551	37518
23	1669	36922	1701	36798
24	1811	36164	1843	36069
25	1951	35313	1989	35151
26	2042	34818	2074	34586
27	2115	34151	2146	33868
28	2211	33096	2243	32758
29	2354	31495	2385	31092
30	2531	29589	2560	29303
31	2711	28103	2738	27937
32	2859	27023	2886	26830
33	2954	26213	2981	25942
34	3049	24994	3074	24629
35	3130	23718	3155	23305
36	3321	20611		
37	3450	17993		
38	3562	14371		
39	3603	13067		

TABLE 4

TRANSVERSE SURFACE PROFILES.

Distances are between adjacent markers. Units are metres. Elevations refer to ice surface. Units are cm above datum. Standard error of distance 15 cm, of elevation 10 cm.

Date		27.7.59		24.7.60	
Marker		Distance	Elevation	Distance	Elevation
A	1		54006		53656
	2	64	54167		53636
	3	59	54413		
	4	119	54392		
	5	114	54195		
	6	112	53563		51198
	7	53	53663		51146
B	1		43939		43408
	2	67	43636	68	43201
	4	150	44084	151	43713
	6	168	44469	170	44195
	7	104	44486	105	44259
	9	191	43875	193	43521
C	2		40698		40690
	3	94	40171	93	40047
	5	161	40749	159	40611
	7	150	41059	151	40830
	9	146	41236	147	40927
	11	150	41119	151	40866
	13	173	41012	173	40856
D	2		37112		37094
	3	84	37822	83	37729
	4	102	37958	101	37865
	5	107		107	38037
	6	100	38088	100	38020
	7	65	38055	65	38002
	8	38	38077	38	37990
	9	95		95	38013
	10	95	38152	95	38162
	11	110		110	38391

Table 4 continued

E	1		34305	34070
	2	75	33413	77 33234
	3	125	34141	124 33879
	4	103	34280	101 34066
	5	108	34358	110 34152
	6	89	34305	90 33998
	7	100	34187	101 33918
F	1		25807	
	2	88	25468	
	3	81	26000	
	4	98	26398	26164
	6	200	27177	201 26895
	7	53	27023	54 26830
	8	39	26988	40 26765
	9	163	26598	168 26304
G	1		17787	
	2	96	18442	18098
	3	93	18505	
	4	102	18445	
	5	102	18404	
	6	41	17993	
	7	115	16708	
	8	158	17308	17130

TABLE 5

WIDTH OF GLACIER.

Units are metres.

Marker	Width	Marker	Width	Marker	Width
L 10	1060	L 20	1190	L 30	890
11	1050	21	1175	31	915
12	1045	22	1165	32	955
13	1080	23	1140	33	1015
14	1175	24	1125	34	1080
15	1180	25	1110	35	1115
16	1220	26	1080	36	1210
17	1240	27	1075	37	1210
18	1235	28	1040	38	1210
19	1220	29	955	39	1210

TABLE 6

ICE THICKNESS.

Units are metres.
Standard errors are 5 m for seismic measurements, -10% +15% for gravity.
Direct measurements were made at all points listed.
Positions of markers are those of July 1959.
Location of points S1 to S6 and H5 are shown in Figure 2.
L10.5 is half-way between L10 and L11.
L30.5 is half-way between L30 and L31.

Marker	Thickness	Method	Marker	Thickness	Method
A 1	38	Gravity	D 8	290	Gravity
2	71	"	10	192	Seismic
3	97	"	E 1	87	Gravity
4	134	"	2	130	"
5	160	"	3	197	"
6	164	"	4	231	"
7	155	"	5	249	Seismic
B 1	112	"	6	249	Gravity
2	194	"	7	246	"
4	282	"	8	178	"
6	308	"	9	87	"
7	301	"	F 1	56	"
9	238	"	2	90	"
C 2	115	"	3	103	"
3	141	Seismic	4	113	"
4	257	Gravity	5	118	"
5	271	Seismic	6	122	"
6	302	Gravity	7	122	"
7	312	Seismic	8	113	"
9(L17)	314	Gravity	9	85	"
10	300	"	10	30	"
11	262	Seismic	G 1	35	"
12	242	Gravity	2	46	"
13	206	"	3	54	"
D 2	162	Seismic	4	54	"
3	235	Borehole	5	54	"
4	276	Gravity	6	50	"
6	311	Seismic	7(L37)	42	"
7(L21)	310	"	8	50	"

Table 6 continued

L 1	199	Seismic	H 5	187	Seismic
10.5	312	"	S 1	334	"
12	323	"	2	299	"
14	317	"	3	278	"
16	322	"	4	279	"
Hole 314	317	Borehole	5	92	"
L19	310	Seismic	6	187	"
21	310	"			
23	273	"			
25	248	"			
27	248	"			
29	186	"			
Hole 209	209	Borehole			
Hole 194	194	"			
L30.5	167	Seismic			
32	118	"			
34	113	"			

TABLE 7

SURFACE SLOPE.

Units are degrees. Standard error is 0.3°.
Measurements always made in direction of maximum slope.
Positions refer to July each year.

Marker	Slope 1959	Slope 1960	Marker	Slope 1959	Slope 1960
A 1	6.1	7.2	E 5	3.8	4.5
2	5.4	6.1	6	3.9	3.9
6	5.7	18.7	7	5.2	5.3
7	5.7	18.7	F 2	8.6	
B 1	9.8	9.0	3	7.0	
2	6.1	4.9	4	5.8	6.1
4	4.0	4.2	6	5.4	5.8
6	3.2	3.5	7	5.0	5.0
7	2.9	3.0	8	5.4	6.1
9	4.4	3.0	9	7.2	9.5
C 2	1.7	1.7	G 1	14.9	
3	3.4	3.4	2	13.6	13.6
5	2.6	2.8	3	14.8	
7	3.7	3.7	4	15.0	
9	4.3	4.4	5	14.7	
11	4.0	4.0	6	14.6	
13	2.5	2.5	7	25.5	
D 2	1.8	1.8	L 1	3.0	3.7
3	2.6	2.8	2	3.7	
4	2.5	2.5	10	4.5	4.0
5		2.5	11	4.0	2.6
6	2.0	2.0	12	2.8	2.8
7	1.7	1.7	13	2.8	3.0
8	1.7	1.7	14	3.1	3.3
9		1.6	15	3.6	3.7
10	1.6	1.6	16	4.1	4.1
11		1.4	17	4.3	4.4
E 1	7.6	8.0	18	4.2	4.1
2	5.2	4.8	19	3.2	2.9
3	5.2	5.4	20	1.9	1.9
4	4.5	4.8	21	1.7	1.7

Table 7 continued

L22	2.2	2.2	Hole 314	4.3	4.3
23	2.8	2.8	Hole 10		3.6
24	3.2	3.4	Hole 322		3.6
25	3.8	3.8	Hole 116		3.0
26	4.2	4.8	Hole 209		6.4
27	5.2	5.8	Hole 194		5.9
28	6.2	6.2	"B"	19.3	
29	6.4	6.4	"D"	9.3	17.6
30	5.9	5.9	"E"	13.0	
31	4.4	4.4	J 2		13.6
32	5.0	5.0	3		23.0
33	6.8	7.2	4		20.0
34	8.6	9.0	5		9.6
35	9.8	9.8	10		19.9
36	9.8		11		10.7
37	14.6		12		15.0
38	21.2	21.2			
39	23.0				

TABLE 8

SLOPE OF BED.

These slopes were determined from seismic records.
Slope measured relative to surface.
Units are degrees. Standard error is 20%.
U, D, L, R indicate that ice is getting thicker in that direction (up, down, left, right, looking down glacier).
E, G, F, P indicate grade of record (excellent, good, fair, poor).
Spread - trans. and long. indicate that split spread cable was used and shot point centred.
up, down, left, right indicate that shot point was at one end of cable and spread was in indicated direction from shot point.
Positions of markers refer to July 1959.
Location of points S1 to S6 and H5 are shown in Figure 2.
L10.5 is half-way between L10 and L11.
L30.5 is half-way between L30 and L31.

Marker	Spread	Slope	Grade
C 3	up	0	P
	trans	13 L	P
C 5	long	2 D	G
	trans	24 L	G
C 7	long	0	G
	trans	16 L	G
C11	trans	30 R	G
D 2	long	9 U	P
	trans	6 L	P
D 6	up	6 U	E
	left	15 R	G
	right	1 R	G
D10	up	1 D	F
	left	33 R	F
E 5	up	3 U	P
	right	8 L	G
L 1	up	14.5D	P
	down	1.5U	G
	left	6 L	P
	right	10 R	P
L10.5	up	13.5D	E
	down	11 D	G
	left	10.5L	G
	right	8 R	G

Table 8 continued

L12	long	4	U	G
	trans	5	R	G
L14	long	5	U	E
	trans	22	R	E
L16	long	1	U	G
	left	30	R	G
Hole 314	up	1.5	U	E
	down	2.5	D	E
	left	22	R	E
	right	5	R	E
L19	long	0		E
	trans	4	R	E
L21	long	4.5	U	G
	trans	13	R	G
L23	long	7	U	G
	trans	7	R	G
L25	up	2	D	G
	trans	26	R	F
L27	long	6	D	P
	trans	6	R	G
L29	long	10.5	D	G
	trans	6	R	G
L30.5	long	4	U	G
	trans	9	R	F
L32	up	1	D	P
	long	1	D	G
	right	5	L	P
L34	long	3	D	G
	trans	5	L	P
L37	long	1	U	F
	trans	0		F
Hole 322	long	2	D	E
	trans	2	L	E
H 5	up	7	D	G
	down	7	D	P
	left	2	L	P
	right	15	L	P
S 1	left	1	R	G
	right	2	L	E
S 2	down	9	D	G
	left	28	R	G
	right	16	R	G
S 3	down	4	D	E
	left	17	L	E
	right	9	R	E

Table 8 continued

S 4	up	12	D	G
	down	9	D	G
	left	18	L	G
	right	18	L	P
S 5	long	0		G
	trans	3	R	F
S 6	long	0		F
	trans	35	L	G

TABLE 9

CURVATURE OF SURFACE AND BED.

These were obtained by numerical differentiation of slope data in Tables 7 and 8. (Table 8 data were transformed to slopes relative to horizontal.)
Positions of markers refer to July 1959.
Units are per 10^5 m.
Minus sign means concave surface.

Marker	Curvatures Surface	Bed
L 10.5		
	- 19	- 232
12		
	12	- 6
14		
	7	37
16		
	1.5	18
Hole 314		
	- 10	- 18
19		
	- 8	- 33
21		
	6	- 8
23		
	6	63
25		
	15	58
27		
	9	41
29		
	- 11	- 111
30.5		
	2	39
32		
	33	52
34		
	26	9
37		

Table 10

HORIZONTAL SURFACE VELOCITY (U).

Units are m./yr.

Periods are			Standard error (m./yr.)
	A	21. 7.59 - 15. 8.59	2.5
	B	15. 8.59 - 1. 9.59	3
	C	1. 9.59 - 24. 7.60	0.15
	D	24. 7.60 - 31. 7.60	4
	E	31. 7.60 - 7. 8.60	4
	F	7. 8.60 - 13. 8.60	4
	G	13. 8.60 - 14.11.60	1
	H	14.11.60 - 10. 4.61	0.6
	J	10. 4.61 - 19. 7.61	0.6

This is the horizontal component of velocity. Its direction is given in Table 11. The vertical velocity component is in Table 14.
The difference between U and the magnitude of the velocity vector is negligible for nearly all markers.
There are variations of two or three days from these periods in individual cases.
Positions are the mean positions of the marker at each period.
A horizontal line means that the velocity is an average value for the periods covered by the line.

Marker	A	B	C	D	E	F	G	H	J
A 1		49.0	46.1						
2	69.0	69.3 ———							
3	94.3	85.5							
4	126.5	119.2							
5	135.8	131.8							
6		125.9	134.4	129.0 ———					
7	128.0 ———		131.7	127.1 ———			129.2 ———		

Table 10 continued

B	1		38.2	———	40.0				
	2		45.5	———	47.4				
	4		55.3	———	55.7				
	6		57.2	———	57.8				
	7		55.5	———	57.3				
	9		48.8	———	50.3				
C	2		13.7	———	13.4				
	3		29.7	———	———				
	5		34.0	———	38.8				
	7		38.0	———	42.7				
	9	see	L17						
	11		42.5	———	———				
	13		33.1	———	35.3				
D	2			23.8	———	33.0	———		
	3		29.0	29.1	———	57.7	28.9	25.5	25.6 26.5
	4		32.6	21.6	32.8	42.8	24.4	30.5	27.1
	5					66.4	30.8	29.0	29.0
	6		30.2	26.7	34.2	63.6	32.5	28.6	27.3
	7	see	L21						
	8		35.5	19.3	34.6	54.4	26.6	28.0	28.8
	9					46.6	32.4	30.4	25.9
	10		27.8	———	32.0	32.0	28.9	25.1	
	11					27.5	19.7		
E	1		18.2	13.3	18.7				
	2		27.7	24.5	———				
	3		31.6	———	———				
	4		34.0	24.8	28.9	35.8	———		
	5			24.0	33.2	31.0	———		
	6		30.1	32.8	———	31.4	———		
	7		30.8	———	32.6				32.9
F	1		7.9						
	2		18.2	12.8					
	3		23.6	17.6					
	4		27.1	21.7	26.5				
	6		25.2	23.5	27.4				
	7	see	L32						

Table 10 continued

F 8	24.4	20.4	25.8				
9	22.8	17.5	21.9				
G 1	4.8	2.8					
2	10.0	10.1	11.4				
3	21.0	13.3					
4	22.9	16.6					
5	20.8	16.1					
6	see L37						
7	19.9	11.0					
8	7.9	6.8	7.2				
L 1			112.0				
2	116.3	117.1					
10	78.8	73.4	74.0	72.0		66.0	63.1
11	68.5	63.5	66.2	65.8		58.6	58.7
12	63.1	53.5	59.3	61.4		55.0	53.9
13	59.4	45.8	55.3	53.7		50.9	50.8
14	52.8	46.2	51.9	50.5		48.0	
15	46.5	39.1	49.6				
16	46.4	35.8	46.5	46.1			
17	37.8	32.9	43.6	47.4			
18	37.9	33.0	40.7	43.4		37.0	
19	35.7	37.5		39.4		31.6	
20	32.8	21.9	35.2	36.2		30.3	
21	32.7	25.2	34.4		35.3 25.5	28.6	
22	32.3	25.4	34.4	30.2		30.4	29.7
23		33.4		28.7			
24		33.0		31.6		27.8	29.4
25	34.1	23.8	33.2	31.8		29.9	29.6
26	27.8		33.2	30.9		27.6	28.9
27	32.5			32.3			
28			32.8	31.7		30.6	
29	26.4		31.7	32.9		31.3	
30	29.9	22.0	28.5	32.7			
31	27.2	21.6	27.0	32.2		24.6	
32	29.8	26.1		32.5			
33	26.8	22.1	26.8				

Table 10 continued

L34	26.8	22.3	26.5	27.2					
35	26.9	21.3	25.6	26.1					
36	22.6	19.0							
37	22.6	13.9							
38	16.7	13.7	15.7						
39	15.1	15.7							
Hole 314	41.5			47.1	38.3	39.7	37.1	38.6	47.7
Hole 10					38.3	42.6	39.9	37.1	
Hole 322				45.1	37.6	33.2	35.7	40.0	
Hole 116				44.7	34.3	36.5	33.0	32.4	41.4
Hole 209							28.6		
Hole 194									31.9
"D"		128.7	147.7	154.0					
"E"		100.8							

Period August 3-14, 1960 Standard error = 25 m./yr.

J 2	52	J 7	11
3	200	9	171
4	266	10	91
5	188	11	30
6	11	12	88

Period 14.8.60 - 19.7.61 Standard error = .7 m./yr.

J 6	11.9
9	142.1

TABLE 11

HORIZONTAL DIRECTION OF SURFACE VELOCITY.

Periods are			Standard errors	
	AB	21. 7.59 - 1. 9.59		10°
	C	1. 9.59 - 24. 7.60		1°
	DEF	24. 7.60 - 13. 8.60		15°
	G	13. 8.60 - 14.11.60		4°
	H	14.11.60 - 10. 4.61		2°
	J	10. 4.61 - 19. 7.61		4°

There are variations of 2 or 3 days from these periods in individual cases.
These directions are measured clockwise from the base line which had azimuth 189.4° relative to true north.
A horizontal line means that the azimuth is an average value for the periods covered by the line.

Marker	AB	C	DEF	G	H	J
A 1		204				
2		200				
3	199					
4	195					
5	195					
6		197	197			
7	196	198	199	224	———	———
B 1	214	212				
2	211	211				
4	209	209				
6	207	206				
7	204	205				
9	202	202				
C 2	204	205				
3	207					

Table 11 continued

C 5	211	208			
7	208	207			
9	see L17				
11	206				
13	206	207			
D 2		212	207		
3		212	214	208	214
4	220	213	212	208	
5			216	211	
6	216	214	207	210	
7	see L21				
8	218	213	209	212	
9			221		
10	218	214	209		
11					
E 1	217	220			
2		216			
3	216				
4	215	220	215		
5		215	224		
6		213	211		
7	212	212			
F 1					
2	207				
3	201				
4	202	205			
6	202	202			
7	see L32				
8	201	201			
9	190	189			
G 1	209				
2	198	203			
3	196				
4	196				
5	184				
6	see L37				

Table 11 continued

G 7	182				
8	199	201			
L 1		197			
2		196			
10	203	203	206		
11	204	205	205		
12	204	206	206		
13	205	206	207		
14	207	206	205		
15	209	206			
16	210	206	208		
17	205	207	206		
18	209	208	208		
19		209	199		
20	213	210	212		
21	215	213		211	
22	217	214	214	215	
23		216	213		
24		216	208	214	216
25	219	214	211	214	
26	212	213	214	213	
27	214		205		
28		213	210	213	
29	210	212	218	209	
30	210	210	211		
31	204	205	207	204	
32		202	204		
33	199	199			
34	197	196	193		
35	195	194	192		
36	192				
37	185				
38	189	190			
39	183				

Table 11 continued

Hole 314	206 ———		207	206	208	208
Hole 10				209 ———		
Hole 322			208	207	208 ———	
Hole 116			209	208	209	210
Hole 209				210 ———		
Hole 194						211
"D"		203	199			
"E"	204					
J 6				196 ———		
9				228 ———		

TABLE 12

HORIZONTAL VELOCITY AT EDGE OF GLACIER.

Units are m./yr.

These are rough values obtained by extrapolation.

	Velocities		
Line	S.W. Edge	Centre	N.E. Edge
A	20	134	
B	17	58	36
C	0	44	15
D	6	35	21
E	7	33	22
F	0	27	16
G	0	20	0

The following values were measured directly. The location was about 50 m. down glacier from the A line. Units are m./yr. The standard error is 1 m./yr.

S.W. Edge	N.E. Edge
10.7	10.8

TABLE 13

MEAN VELOCITY ON TRANSVERSE LINES.

The ratio is that of the mean surface velocity to the maximum surface velocity.

Line	Ratio
B	0.86
C	0.81
D	0.87
E	0.85
F	0.87
G	0.69

TABLE 14

VERTICAL VELOCITY AND NORMAL VELOCITY.

V = vertical velocity (measured directly).
v = velocity normal to ice surface (calculated from V, horizontal velocity, and surface slope).
Positive direction is downwards.
Units are m./yr.

Periods are		Standard errors are	
		V	v
C	1. 9.59 - 24. 7.60	0.15	0.35
G	13. 8.60 - 14.11.60	0.6	1.4
H	14.11.60 - 10. 4.61	0.4	0.9
J	10. 4.61 - 19. 7.61	0.6	1.4

There are minor variations from these periods in individual cases. Other periods are too short for results to be of sufficient accuracy.
A horizontal line means that the velocity is an average for the periods covered by the line.
Positions are those of the marker at each period.
Velocities are those of a particle of ice just below the surface (i.e. at foot of marker), except at boreholes where the velocity is that of the top of the pipe.

	C		G		H		J	
Marker	V	v	V	v	V	v	V	v
A 1	0.85	-4.46						
2	2.60	-4.37						
6	26.20	-2.86						
7	24.81	-3.66						
B 1	2.46	-4.15						
2	1.27	-3.26						
4	0.10	-3.90						
6	-0.99	-4.34						
7	-1.05	-4.02						
9	0.97	-2.26						
C 2	-1.28	-1.67						
3	-3.83	-5.63						
5	-2.14	-3.97						
7	-1.15	-3.86						

Table 14 continued

C 9	see L17					
11	0.43	-2.50				
13	-1.09	-2.64				
D 3	-3.24	-4.61	-3.29	-4.54	-3.21	-4.55
4	-2.61	-4.06	-3.57	-4.77		
5			-2.66	-3.92		
6	-1.94	-3.12	-3.25	-4.19		
7	see L21					
8	-2.66	-3.67	-3.29	-4.13		
9			-2.86	-3.56		
10	-2.94	-3.80				
E 2	-2.43	-4.57				
3	-1.45	-4.37				
4	-1.56	-3.90				
5	-1.57	-3.99				
6	-1.12	-3.35				
7	-0.15	-3.15				
F 4	-1.49	-4.25				
6	-1.22	-3.93				
7	see L32					
8	-1.87	-4.45				
9	1.41	-1.72				
G 2	0.66	-1.95				
L 1	0.49	-6.06				
10			-1.93	-6.51	-1.41	-5.29
11	0.14	-3.68	-2.69	-5.39	-1.97	-4.73
12	-0.80	-3.62	-2.53	-5.15	-2.05	-4.65
13	-0.77	-3.58	-1.85	-4.57	-1.60	-4.34
14	-0.34	-3.24	-1.52	-4.31		
15	0.04	-3.07				
16	0.24	-3.08				
17	0.19	-3.13				
18	-0.14	-3.11	-0.48	-3.15		
19	-1.49	-3.48	-0.87	-2.48		
20	-2.34	-3.49	-0.60	-1.59		
21	-3.16	-4.20	-2.98	-3.84		
22	-2.55	-3.89	-2.42	-3.60	-2.49	-3.68
23	-1.82	-3.45				
24	-2.01	-3.93	-2.47	-4.15	-2.22	-4.01
25	-1.94	-4.14	-0.93	-2.93	-1.27	-3.30
26	-1.21	-3.83	-0.08	-2.42	-1.46	-3.95
27	-0.18	-3.32				
28	0.11	-3.48	0.82	-2.53		
29	1.56	-1.99	2.67	-0.84		
30	-0.19	-3.13				
31	-2.23	-4.32	-0.94	-2.86		
32	-2.08	-4.37				

Table 14 continued

L33	-0.88	-4.17			
34	0.53	-3.58			
35	1.57	-2.86			
38	5.44	-0.65			
Hole 314			-0.40	-0.44	-0.40
Hole 10			-0.53		
Hole 322			-2.18	0	
Hole 116			-1.58		-1.97
Hole 209					
Hole 194				-0.49	-0.15
"D"	29.8	-5.6			
J 6		2.8*			
J 9		21.6*			

* Standard error = 0.7 m./yr.

TABLE 15

RATE OF THINNING.

See section 3.7.3 for details of method of calculation.

Location	Thinning(m)	Period(yr)	Rate(m./yr.)	Source
L36	9.5	13	0.73	Water Resources survey.
L32	76	130	0.58	Height of stn.9 above ice.
L37	107	130	0.83	Height of stn.7 above ice.

TABLE 16

LONGITUDINAL SURFACE STRAIN RATE.

Strain rates are measured in a horizontal plane.
Positions are the mean positions of the markers at each period.
Units are per year.

Periods are	Standard errors are
AB 21. 7.59 - 1. 9.59	.015
C 1. 9.59 - 24. 7.60	.002
G 13. 8.60 - 14.11.60	.008
H 14.11.60 - 10. 4.61	.005

There are variations of 2 or 3 days in individual cases.

Markers	AB	C	G	H
L10-11		-.103	-.103	-.062
11-12		-.074	-.040	-.054
12-13		-.042	-.043	-.034
13-14		-.034	-.030	
14-15		-.023		
15-16		-.022		
16-17		-.021		
17-18		-.019		
18-19		-.022	-.041	
19-20		-.018	-.008	
20-21		-.007	-.010	
21-22		-.001	+.012	
22-23		-.004	-.008	-.002
23-24		-.003		
24-25		-.001	+.016	0
25-26		+.001	-.027	-.008
26-27		-.002	+.016	
27-28		+.003		
28-29		-.007	+.004	
29-30		-.018		
30-31		-.009		
31-32		-.004		
32-33		-.002		
33-34		-.006		
34-35		-.014		
35-36	-.017			
36-37	-.016			
37-38	-.031			
38-39	+.010			

TABLE 17

TRANSVERSE SURFACE STRAIN RATE (MEASURED).

Strain rates are measured in a horizontal plane.
Positions are the mean positions of the markers at each period.
Units are per year.

Periods are		Standard errors are
AB	21.7.59 - 1.9.59	.015
C	1.9.59 - 24.7.60	.002

There are variations of 2 or 3 days in individual cases.

Markers	AB	C	Markers	AB	C
B 1- 2		+.003	G 1-2	+.02	
2- 4		+.010	2-3	+.02	
4- 6		+.016	3-4	+.01	
6- 7		+.016	4-5	+.03	
7- 9		+.014	5-6	0	
C 3- 5		-.009	6-7	0	
5- 7		0			
7- 9		+.004			
9-11		+.001			
11-13		+.004			
D 2- 3		-.008			
3- 4		-.010			
4- 6		-.003			
6- 7		+.005			
7- 8		-.006			
8-10		0			
E 2- 3		-.002			
3- 4		-.014			
4- 5		+.022			
5- 6		+.011			
6- 7		+.007			
F 2- 3	+.02				
3- 4	0				
4- 6		+.006			
6- 7		+.003			
7- 8		+.014			
8- 9	+.02				

TABLE 18

TRANSVERSE SURFACE STRAIN RATE (CALCULATED).

Units are per year.
Measured values are between the two end markers in each transverse line.
Calculated values are obtained from the change in width of the glacier. They are thus average values across the whole glacier.
Markers refer to their mean position over winter 1959-60.
Standard error of measured values is .002.

Marker	Transverse strain rate. Calculated	Measured
L 10	-.008	
11	-.002	
12	+.017	+.012
13	+.024	
14	+.010	
15	+.006	
16	+.004	
17	+.001	0
18	-.002	
19	-.003	
20	-.003	
21	-.002	-.002
22	-.003	
23	-.003	
24	-.002	
25	-.004	
26	-.004	
27	-.007	+.003
28	-.012	
29	-.011	
30	0	
31	+.004	
32	+.009	+.014
33	+.013	
34	+.011	
35	+.008	
36	+.003	
37	0	
38	0	
39	0	

TABLE 19

SURFACE STRAIN RATES AT BOREHOLES.

Units are per year.
Measurements refer to the plane of the glacier surface.
x, z directions are down and across glacier respectively.

	Strain rates		
Borehole	x	z	xz
314	-.0196	+.0015	
322	-.0229	+.0019	+.0034
116	-.0168	-.0012	+.0017
209	-.0114	-.0006	
	Standard errors		
314		undetermined	
322	.0007	.0007	.0006
116	.0017	.0017	.0014
209		undetermined	

TABLE 20

BOREHOLE DATA.

Standard errors - Inclination 0.1°, 0.25°, 1° for 4°, 10°, 26° discs respectively.
Azimuth 1°.
"Distance" measured along pipe from top in 1960.

Hole 322

Direction of surface flow N 12 E

	18-20 July, 1960.			7-12 July, 1961.		
Distance(m)	Inclination	Azimuth	Disc (if not 4°)	Inclination	Azimuth	Disc (if not 4°)
0						
3.96				0.4	S 09 W	
7.62	0.9	S 26 W		0.1	N	
15.24	0.3	S 82 W		0.3	N 06 W	
22.86	0.9	N 65 W		0.7	N 30 W	
30.48	0.5	N 31 W		0.8	N 30 W	
38.10	0.0			0.3	N 08 W	
45.72	1.4	S 62 W		1.0	S 61 W	
53.34				0.9	N 52 W	
60.96	0.7	S 11 W		0.4	S 30 E	
68.58				1.9	S 44 W	
76.20	1.7	N 73 W		1.3	N 73 W(?)	
83.82				0.2	N 80 W(?)	
91.44	6.0	S 20 W	10	4.8	S 28 W	
99.06				5.6	S 33 W	10
106.68	4.1	S 28 W		4.3	S 28 W	
114.30				4.4	S 26 W	10

Table 20 continued

121.92	4.1	S 26 W	10	4.9	S 27 W	
129.54				4.1	S 09 W	10
137.16	4.0	S 21 W	10	4.8	S 20 W	
144.78				3.5	S 26 W	10
152.40	3.8	S 16 W		4.0	S 21 W	
160.02				5.2	S 12 W	10
167.64	2.9	S 43 W		4.1	S 33 W	
175.26				3.0	S 23 W	10
182.88	4.4	S 07 E		4.9	S 10 E	
190.50				5.0	S 20 W	10
198.12	1.6	S 63 W		3.5	S 43 W	
205.74				2.0	S 22 W	10
213.36	2.8	S 44 W		4.1	S 27 W	
220.98				3.2	S 56 W	10
228.60	2.9	S 75 W		4.7	S 47 W	
236.22				4.2	S 52 W	10
243.84	2.1	S 74 W		5.0	S 39 W	10
251.46				4.3	S 56 W	10
259.08	3.2	N 71 W		3.7	S 73 W	10
266.70				4.9	S 46 W	10
274.32	1.6	N 62 W		3.9	S 43 W	10
281.94				5.0	S 47 W	10
289.56	6.0	N 87 W	10	8.9	S 73 W	10
297.18				6.8	S 63 W	10
304.80	11.3*	S 73 W	10	13.5	S 60 W	26
312.42				13.0	S 48 W	26
320.04	11.9*	S 42 W	10	20.0	S 31 W	26
320.95				20.0	S 31 W	26

* Standard error = 0.5°

Table 20 continued

Hole 209

Direction of flow at surface N 14 E.

	9-10 August, 1960.			10-11 July, 1961.		
Distance(m)	Inclination	Azimuth	Disc (if not 4°)	Inclination	Azimuth	Disc (if not 4°)
0	0.6	S 48 W				
1.83				0.7	S 40 W	
7.62				0.4	S 40 W	
15.24	0.2	N 43 W		0.3	N 20 E	
22.86				1.0	S 57 W	
30.48	1.0	S 56 W		1.0	S 46 W	
38.10				1.0	S 42 W	
45.72	0.6	S 84 W		1.0	S 52 W	
53.34				1.0	S 40 W	
60.96	0.6	S 72 W		1.1	S 50 W	
68.58				1.3	S 41 W	
76.20	0.7	S 73 W		1.3	S 45 W	
83.82				1.7	S 35 W	
91.44	0.2	S 43 W		1.5	S 33 W	
99.06				1.5	S 28 W	
106.68	1.7	N 83 W		1.7	S 38 W	
114.30				2.1	S 40 W	
121.92	2.2	N 68 W		3.0	S 54 W	
129.54				4.0	S 43 W	
137.16	0.7	N 40 W		4.6	S 37 W	
144.78				4.6	S 40 W	10
152.40	1.7	N 75 W		6.2	S 28 W	10
160.02				8.9	S 17 W	10
167.64	2.0	S 55 W		10.0	S 21 W	10
175.26				13.0	S 21 W	26
182.88	1.5	N 89 W		17.0	S 19 W	26
183.79				17.0	S 20 W	26

Table 20 continued

195.07			32.5*
198.12	1.4	S 56 W	
201.47			24.8*
207.26	1.9	S 36 W	

* Readings with acid bottle S.E. = 1°

Hole 116

Direction of flow at surface N 13 E

Disc = 10° throughout

	24 July, 1960.		13 July, 1961.	
Distance(m)	Inclination	Azimuth	Inclination	Azimuth
0	1.0	N		
7.62			1.7	N 05 E
15.24	3.5	S 16 W	3.1	N 46 W
22.86			4.3	N 40 W
30.48	5.0	N 55 W	5.0	N 46 W
38.10			5.2	N 40 W
45.72	6.2	N 44 W	5.0	N 52 W
53.34	6.0	N 52 W	5.9	N 47 W
60.96	3.0	N 22 W	3.4	N 28 W
68.58			3.8	N 09 W
76.20	4.2	N 36 W	4.7	N 41 W
83.82			4.0	N 36 W
91.44	4.3	N 27 E	4.5	N 36 E
99.06			4.0	N 08 E
106.68	3.4	N 04 W	4.0	N 03 W
114.30	3.3	N 08 E	3.1	N 08 E

Table 20 continued

Hole 314

Direction of flow at surface N 12 E

Disc = 4° throughout

	3 August, 1960.		14 July, 1961.	
Distance(m)	Inclination	Azimuth	Inclination	Azimuth
0	1.0	E		
7.62			1.4	N 86 E
15.24	1.3	N 87 E	1.6	N 71 E
22.86			1.1	N 45 E
30.48	0.9	N 68 E	1.0	N 55 E
38.10			0.9	S 79 E
45.72	1.0	S 85 E	1.1	S 59 E

TABLE 21

SLOPES, VELOCITIES, STRAIN RATES AT BOREHOLES.

See section 5.1 for definition of symbols.

Symbol	Units	Hole 322	Hole 209	Hole 314	Hole 116
h	m.	321	209	314	315
α_s	degrees	3.5	6.3	4.2	2.9
α_b	"	5.3	16.9	5.3	2.9
U_s	m./yr.	38.9	28.8	40.8	35.2
U_b	"	31.7	7.0		
V_s	"	-0.46	1.25	0	-1.60
V_b	"	3.02	2.12		
v_s	"	-2.84	-1.94	-2.98	-3.36
v_b	"	1.03	1.29		
$\left(\frac{\partial u}{\partial x}\right)_s$	per yr.	-0.0229	-0.0114	-0.0196	-0.0168
$\left(\frac{\partial u}{\partial x}\right)_b$	"	-0.0012	-0.0213		
$\left(\frac{\partial v}{\partial x}\right)_s$	"	-0.0045	-0.0011	-0.0005	-0.0055
$\left(\frac{\partial w}{\partial z}\right)_s$	"	0.0019	-0.0006	0.0015	-0.0012
K	$m.^{-1}$ $yr.^{-1}$	0.000068	-0.000048		

TABLE 22

BOREHOLE RESULTS.

The tabulated quantity is $\frac{\partial u}{\partial y}$ the rate at which the velocity parallel to the surface changes with depth. Units are per year. Results of 3 different methods of analysis are given:

A "Laminar flow" (see part 1a of section 3.6.)
B Addition of corrections for longitudinal strain rate (variable with depth) and curvature of pipe (part 2 of section 3.6.)
C Integrated method (part 3 of section 3.6.)

Hole 322

y(m.)	A	B	C	Standard error
4.0	+.006	+.007		
7.6	18	20	+.009	
15.2	7	10	16	
22.8	5	8	6	
30.5	4	6	5	
38.1	5	8	5	
45.7	4	6	9	.004
61.0	+.007	+.009	0	
76.2	-.024*	-.022*	+.003	
91.4	+.028*	+.023*	-.013	
106.6	-.004	-.004	4	
121.8	14	16	8	
137.0	14	15	6	
152.2	4	5	15	.01
167.4	23	23	16	
182.6	7	8	19	
197.8	36	36	27	.004
213.0	29	28	21	
228.2	47	47	35	
243.4	63	63	47	
258.7	40	38	58	
273.9	69	70	69	.01
289.0	60	63	55	
304.1	65	57	46	.035
318.9	-.117	-.076	76	

* These values are doubtful.

Table 22 continued.

Hole 209

y(m.)	A	B	C	Standard error
1.8	-.002	+.001		
15.2	+.004	5	+.003	
30.5	-.004	-.002	-.006	
45.7	12	8	9	
61.0	12	9	13	
76.2	13	11	18	.004
91.4	23	20	24	
106.7	25	22	31	
121.9	50	49	55	
137.1	90	90	85	
152.3	115	117	121	.01
167.4	160	163	189	
182.5	320	320	335	.035
196.9	-.638	-.623	526	

Hole 116

y(m.)	A	B	Standard error
15.2	+.181*	+.140*	
30.4	-.012	-.012	
45.6	+.023	+.023	
53.2	-.009	-.009	.01
60.8	0	0	
76.0	0	0	
91.2	-.002	-.002	
106.4	-.009	-.009	
114.0	+.003	+.003	

* These values are questionable.

Hole 314

y(m.)	A	Standard error
15.2	+.008	
30.4	2	.004
45.6	10	

TABLE 23

COMPARISON OF MEAN AND SURFACE STRAIN RATES.

	measured $\left(\frac{\partial u}{\partial x}\right)_s$	calculated $\left(\frac{\overline{\partial u}}{\partial x}\right)$			sign of $\frac{\partial^2 v}{\partial x^2}$
		$u_b = 0$	u_b measured	$u_b = u_s$	
L12	-.068	-.019		-.005	-
14	-.032	-.029		-.015	-
16	-.021	-.015		-.012	-
Hole 314	-.0196		-.013		-
Hole 322	-.0229		-.014		-
L19	-.021	-.007		-.007	-
Hole 116	-.0168		-.010		-
L21	-.021	-.013		-.004	+
23	-.003	-.009		+.006	-
25	+.002	-.013		-.017	+
27	-.001	-.020		-.038	+
Hole 209	-.0114		-.016		+
L305	-.011	-.014		-.003	+
32	-.004	-.046		-.050	+
34	-.011	-.048		-.059	+

TABLE 24

COMPARISON OF MEASURED AND CALCULATED STRAIN RATES.

These values of $\frac{\partial u}{\partial x}$ were calculated by equation 18 of section 5.1. For details of the comparison see section 7.5.

	calculated	measured
L12	-.105	-.068
14	+.031	-.032
16	+.011	-.021
Hole 314	-.038	-.020
L19	-.070	-.021
21	-.024	-.021
23	+.023	-.003
25	+.029	+.002
27	+.023	-.001
Hole 209	-.022	-.011
L30.5	-.038	-.011
32	+.007	-.004
34	+.008	-.011

TABLE 25

STRAIN RATES AND STRESSES ON TRANSVERSE LINES.

See section 7.7. for explanation of symbols and method of calculation.

Units are z - metres
u - m./yr.
$\frac{\partial u}{\partial z}$ - yr^{-1}
τ_{xz} - bars

F = 0.56, 0.61 for D and E lines respectively.

Marker	u	$\frac{\partial u}{\partial z}$	z	τ_{xz}
D 2	23.82			
		-0.0627	434.5	-0.642
3	29.10			
		-0.0363	341.7	-0.504
4	32.78			
		-0.0070	187.6	-0.276
6	34.22			
		-0.0025	51.4	-0.076
7	34.38			
			0	0
8	34.56			
		-0.0135	113.9	-0.168
10	31.99			
E 1	18.66			
		-0.0770	318.5	-1.174
2	24.49			
		-0.0572	218.4	-0.805
3	31.62			
		-0.0144	100.5	-0.370
5	33.22			
			0	0
6	32.82			
		-0.0027	95.1	-0.350
7	32.55			

TABLE 26

STRAIN RATES AND STRESSES AT BOREHOLES.

See sections 5.1. and 7.8. for explanation of symbols and method of calculation.
Units of strain rate and stress are $yr.^{-1}$ and bars respectively.

$\frac{\partial v}{\partial x}$ = -.004 and -.001 for holes 322 and 209 respectively.

Hole 322

y	$\dot{\varepsilon}_x$	$\dot{\varepsilon}_{xy}$	τ_{xy}	$\frac{1}{2}E_2$	$\frac{1}{2}\xi'_2$
152.2	-0.013	-0.010	-0.481	2.69×10^{-4}	0.621
167.4	12	10	.530	2.44	.684
182.6	11	12	.577	2.65	.612
197.8	10	16	.625	3.56	.544
213.0	8	13	.673	2.33	.626
228.2	7	20	.723	4.49	.586
243.4	6	26	.769	7.12	.588
258.7	5	31	.819	9.86	.691
273.9	4	37	.866	13.85	.760
289.0	3	30	.914	9.09	.845
304.1	2	25	.962	6.29	.931
318.9	01	40	-1.008	16.01	1.015

Hole 209

y	$\dot{\varepsilon}_x$	$\dot{\varepsilon}_{xy}$	τ_{xy}	$\frac{1}{2}E_2$	$\frac{1}{2}\xi'_2$
30.5	-0.013	-0.004	-0.185	1.85×10^{-4}	0.396
45.7	14	5	.278	2.21	.682
61.0	14	7	.370	2.45	.694
76.2	15	10	.462	3.25	.696
91.4	16	13	.554	4.25	.770
106.7	17	16	.646	5.45	.886
121.9	17	28	.739	10.73	.749
137.1	18	43	.831	21.73	.814
152.3	19	61	.924	40.82	.935
167.4	19	95	1.016	93.86	1.071
182.5	20	.168	1.108	286.24	1.245
196.9	21	.263	1.195	696.10	1.439

TABLE 27

ABLATION AND ACCUMULATION.

Ablation measured in cm. of ice, accumulation in cm. of snow. Positions are mean position of each marker at each period. Periods:

Ablation	1959	17 July - 27 August (end of season)
	1960(a)	Start of season - 4 August
	1960(b)	Start - end of season
Accumulation	1960-1	End of summer 1960 - 10 April, 1961.

Standard error is about 10%.

Marker	Ablation 1959	Ablation 1960a	Ablation 1960b	Accumulation 1960-1
A 2	174			
3	152			
4	175			
5	182			
6	146			
7	217	116		
B 1	160	324		
2	175	260		
3	201	257		
4	210			
5	192	338		
6	207	309		
7	214	265		
9	171			
C 2	74			
3		409		
4	138	300		
5	145	292		
6	161	260		
7	157	296		
8	173	191		
9(L17)	131	229		
10	146	156		
11	165	175		
12	144	173		
13	127	213		
14	121			

Table 27 continued.

D	3	166	306	438	0
	4	147	273	405	112
	5	154	262	406	132
	6	133			
	7(L21)	187	218		
	8	167	288		
	9	189	261		
	10		245		
	11	147	187		
E	1	88			
	2	181	315		
	3	207	363		
	4	179			
	5	210	273		
	6	181	316		
	7	168	211		
	8	144	126		
F	1	47	122		
	2		322		
	3	182	324		
	4	170	302		
	5	193	326		
	6	162	326		
	7(L32)	173	331		
	8	156	334		
	9	108	127		
G	1	217			
	3	222			
	4	162			
	5	152			
	6(L37)	166			
	7	194			
	8	74	66		
L	1	142	284		
	2	154			
	10	150	317	437	43
	11	196	289	418	44
	12	196	321	441	43
	13	217	272	396	128
	14	218	262	364	131
	15	173	241		
	16	168	220		
	17	131	229		
	18	184	194		
	19	187	184		

Table 27 continued.

L20	138	267		
21	187	218		
22	142	272	411	81
23	165	260		
24	158	258	434	131
25	188	271	425	160
26	176	282	451	76
27	190	253		
28	220	269		
29	152	191		
30	182	226		114
31	185	304		102
32	147	331		122
33	178	292		
34		234		
35	201	184		
36	171			
37	166			
38	166			
39	217			
Hole 314				215
Hole 116				168
Hole 194				142

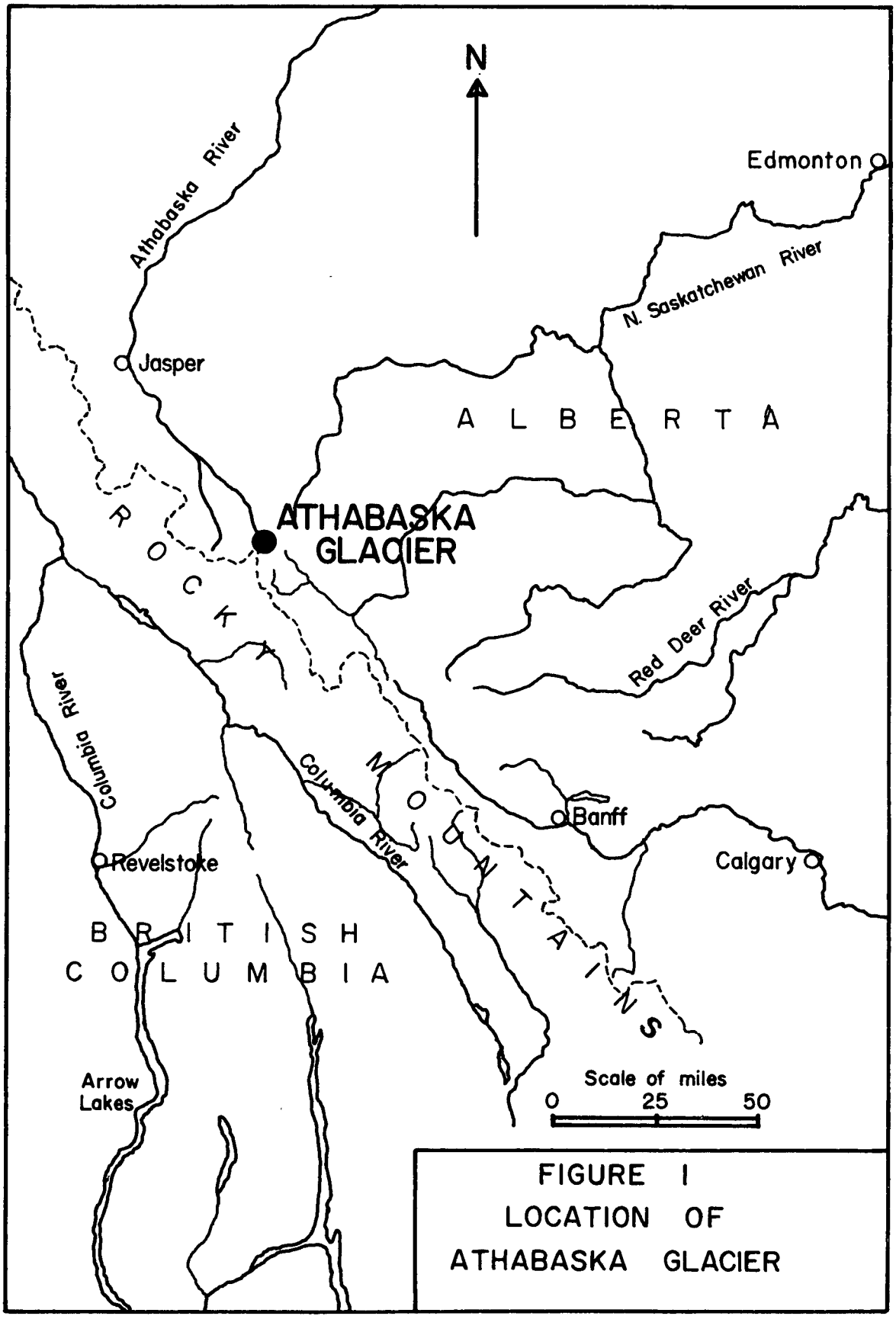

FIGURE 1
LOCATION OF
ATHABASKA GLACIER

Figure 3 ATHABASKA GLACIER

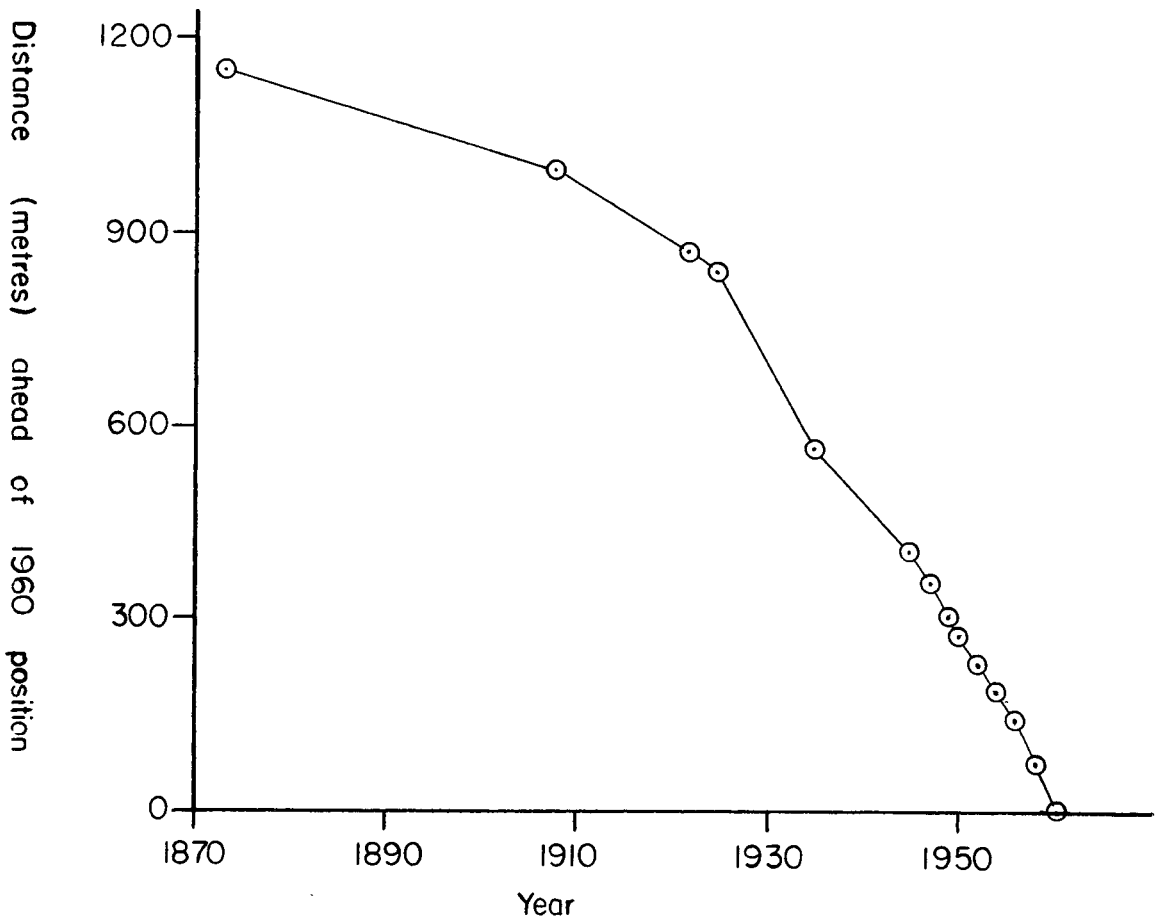

FIGURE 6 RECESSION OF GLACIER TERMINUS

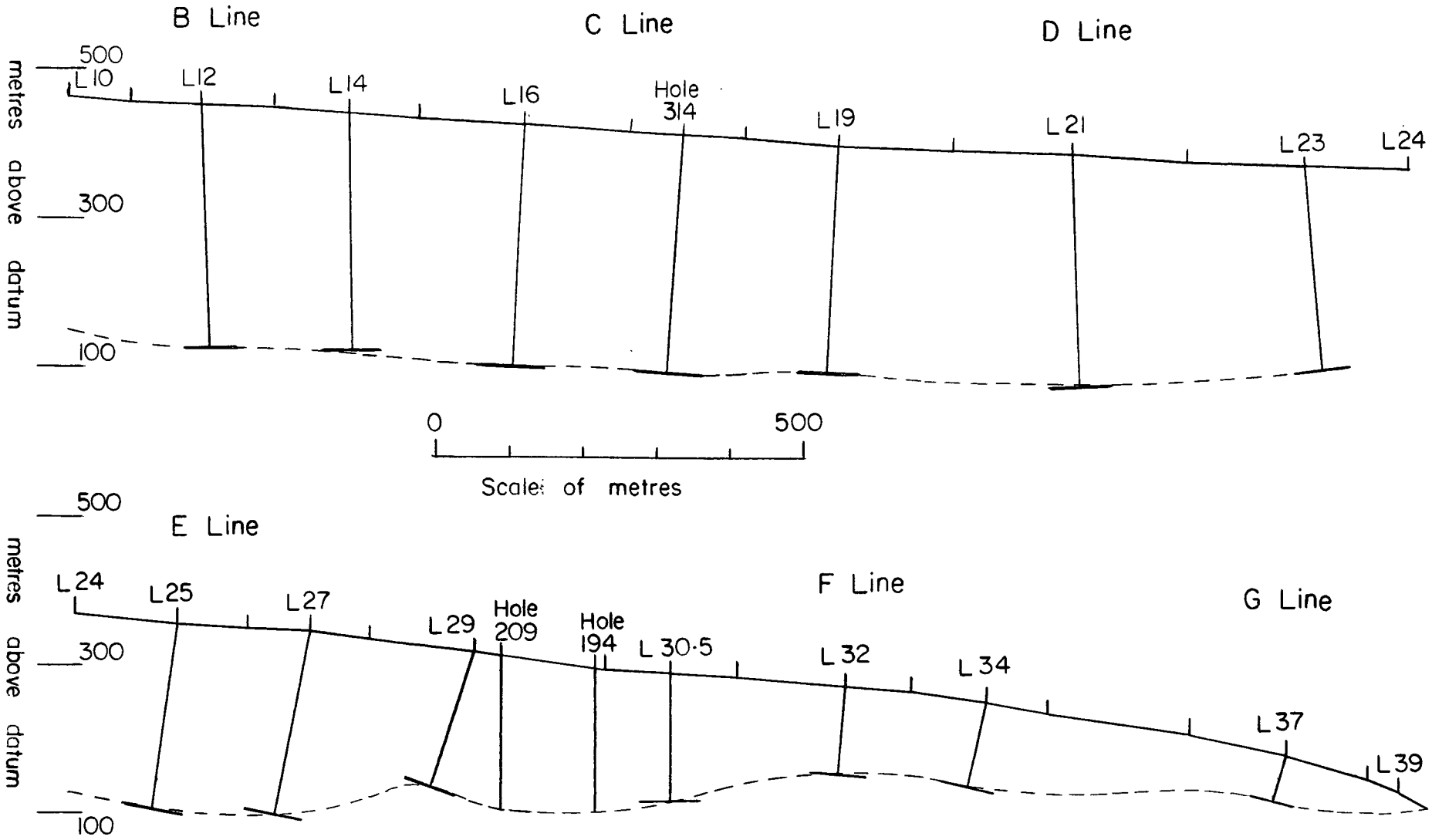

FIGURE 7 LONGITUDINAL PROFILE

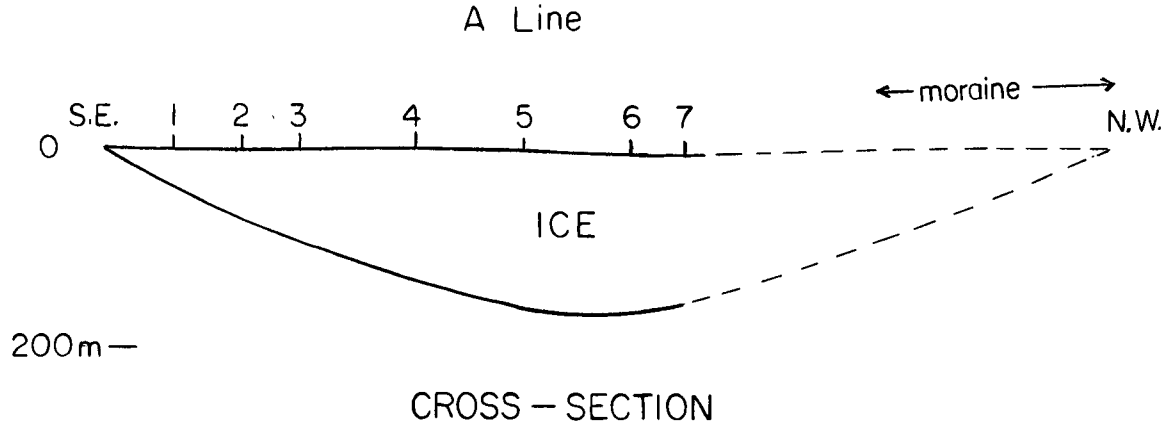

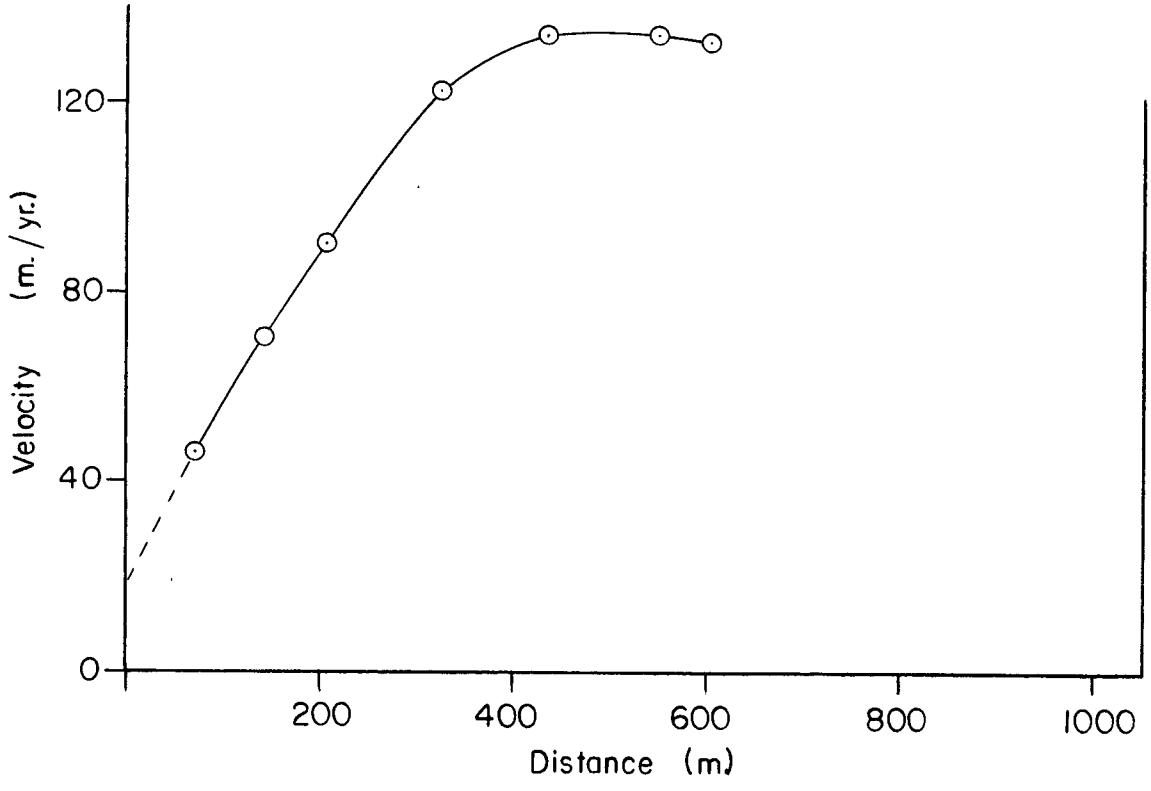

FIGURE 8 HORIZONTAL SURFACE VELOCITY

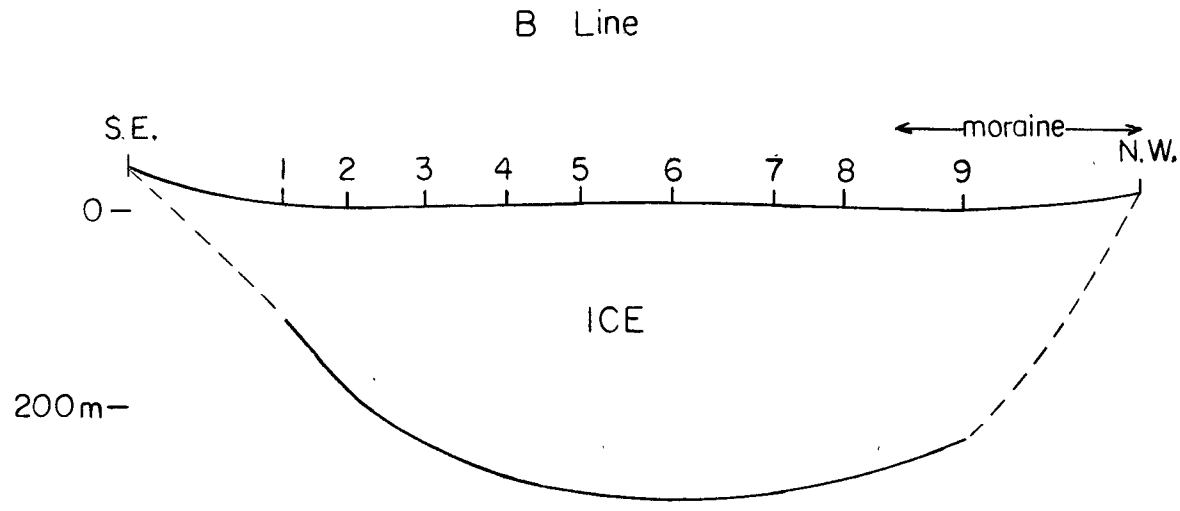

CROSS-SECTION

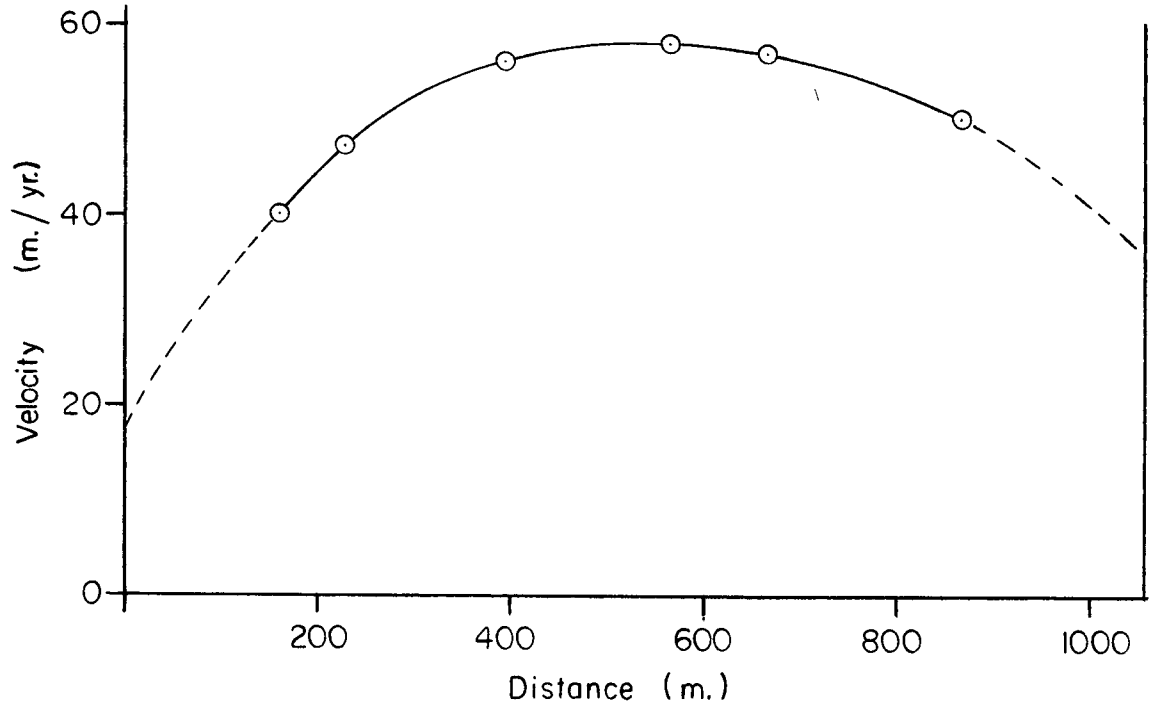

FIGURE 9 HORIZONTAL SURFACE VELOCITY

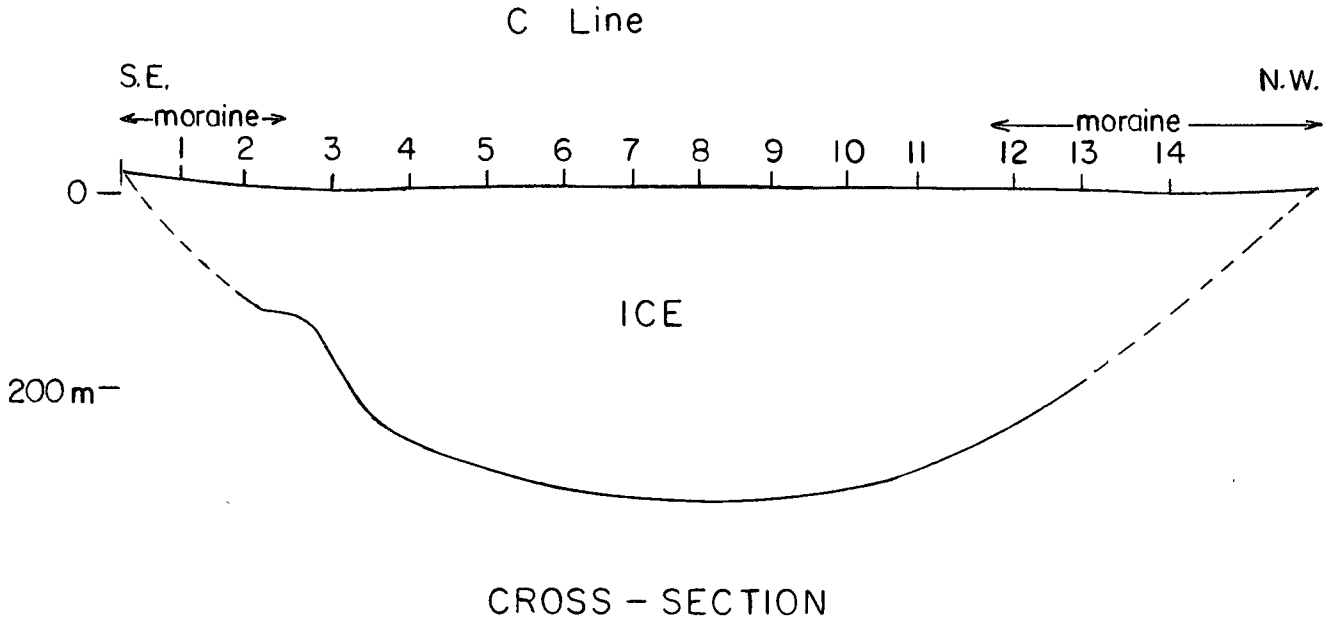

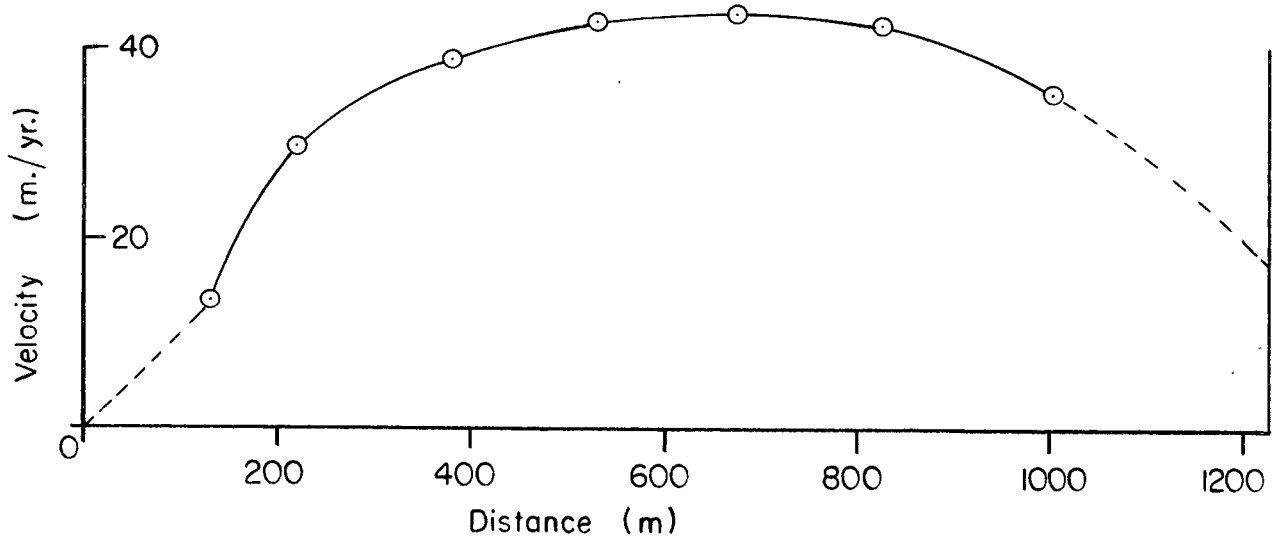

FIGURE 10 HORIZONTAL SURFACE VELOCITY

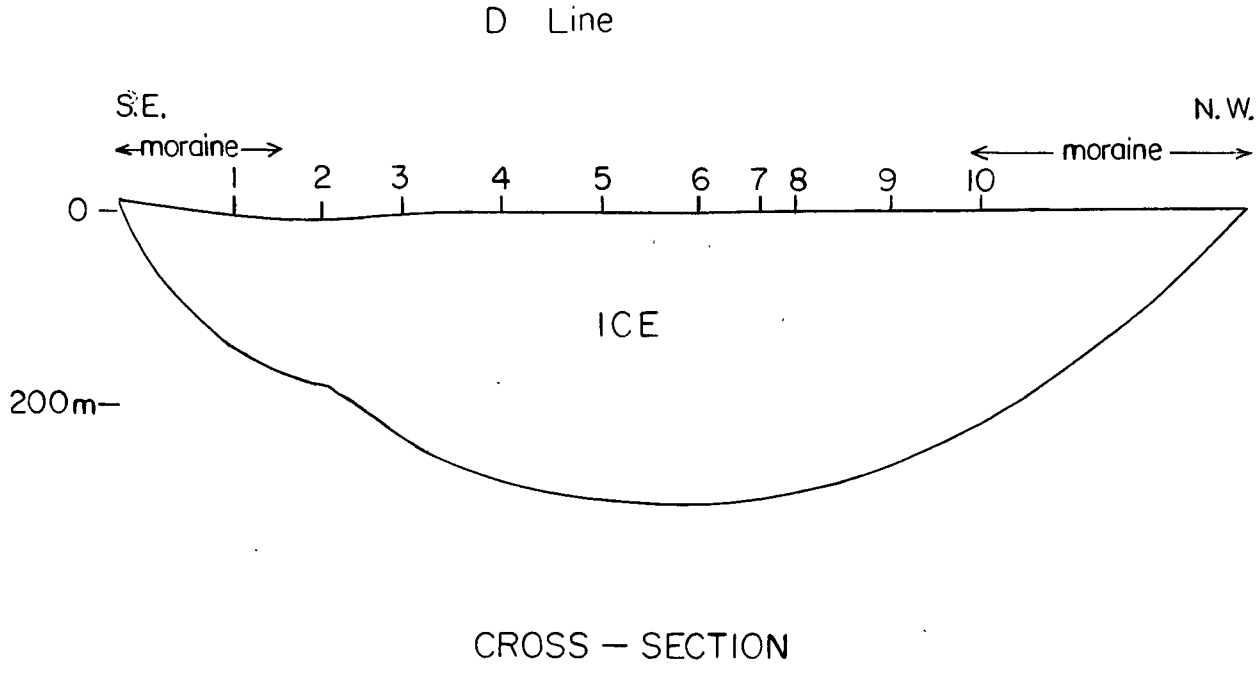

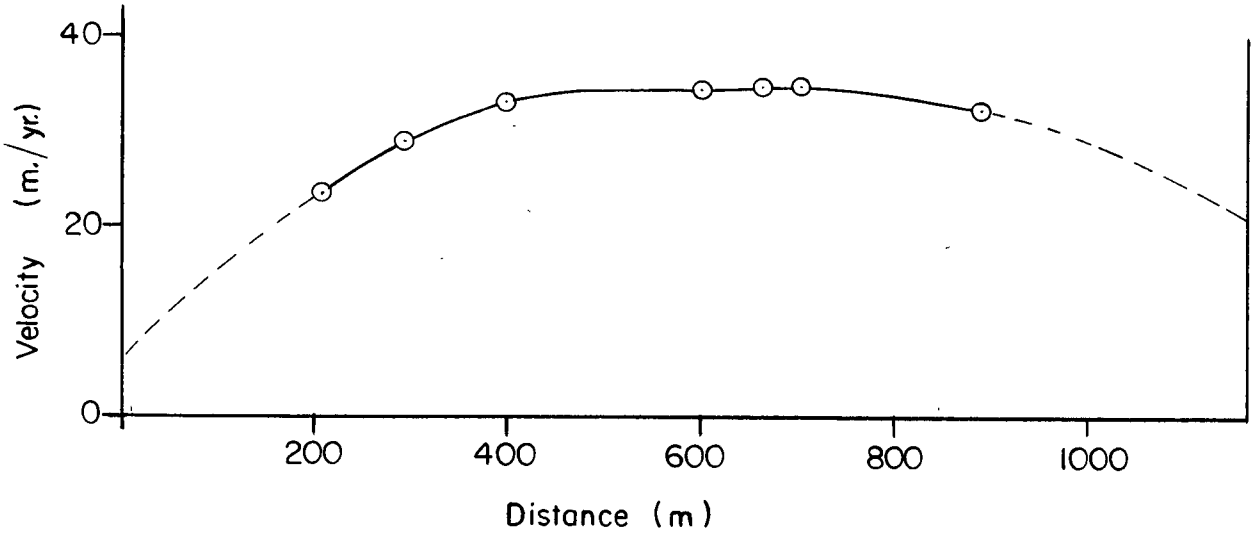

FIGURE 11 HORIZONTAL SURFACE VELOCITY

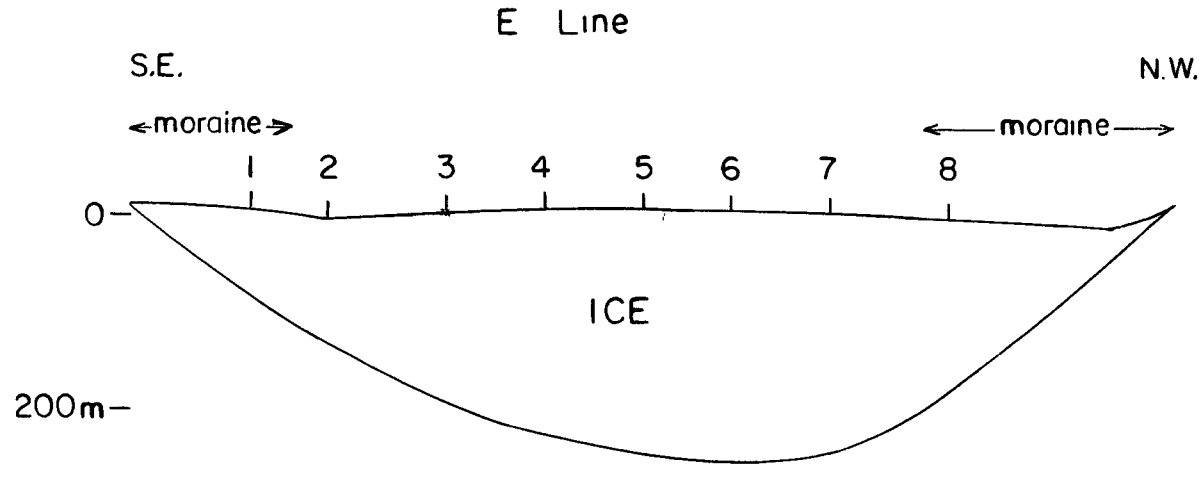

CROSS-SECTION

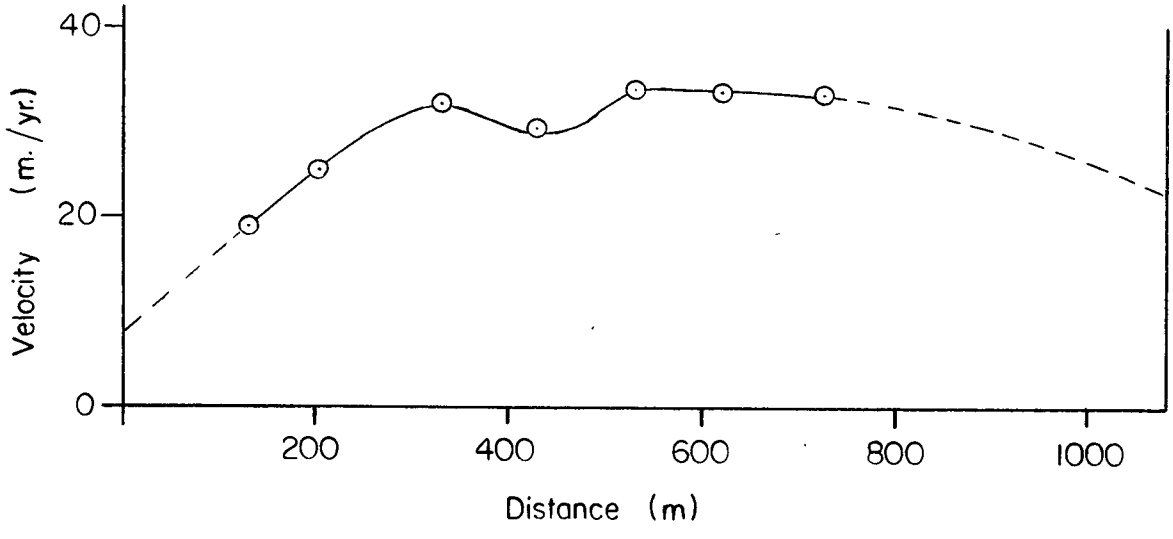

FIGURE 12 HORIZONTAL SURFACE VELOCITY

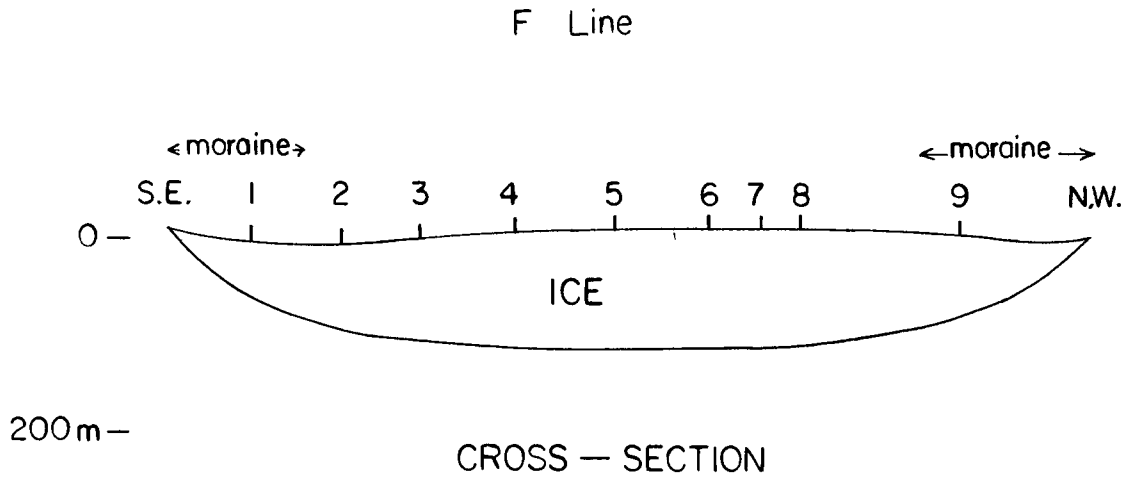

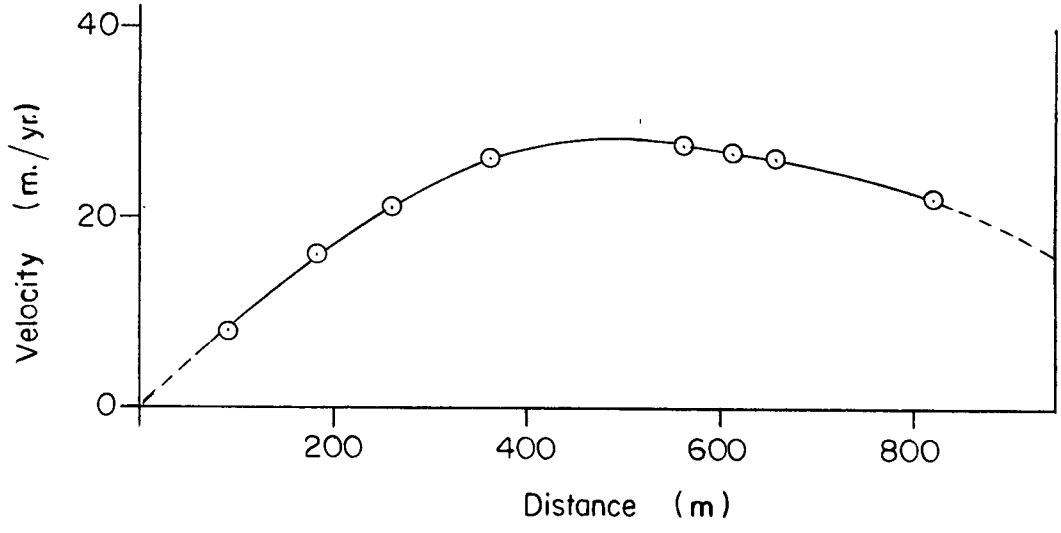

FIGURE 13 HORIZONTAL SURFACE VELOCITY

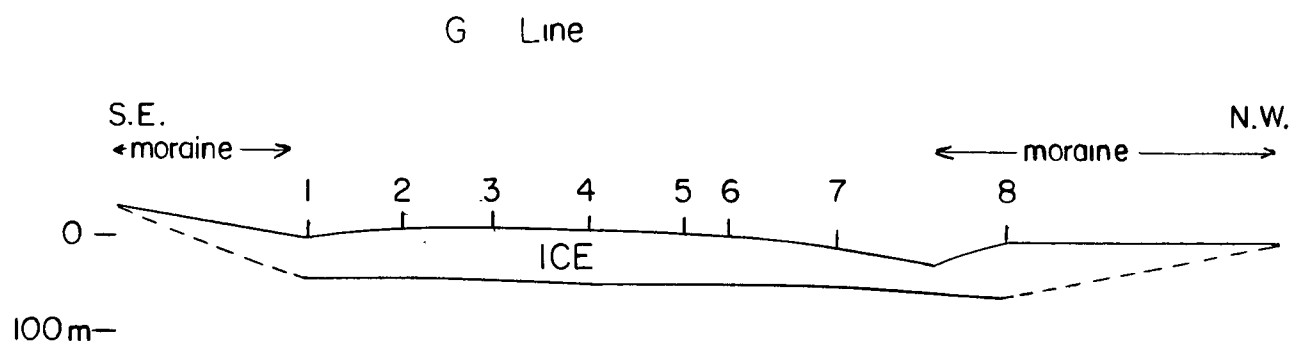

CROSS-SECTION

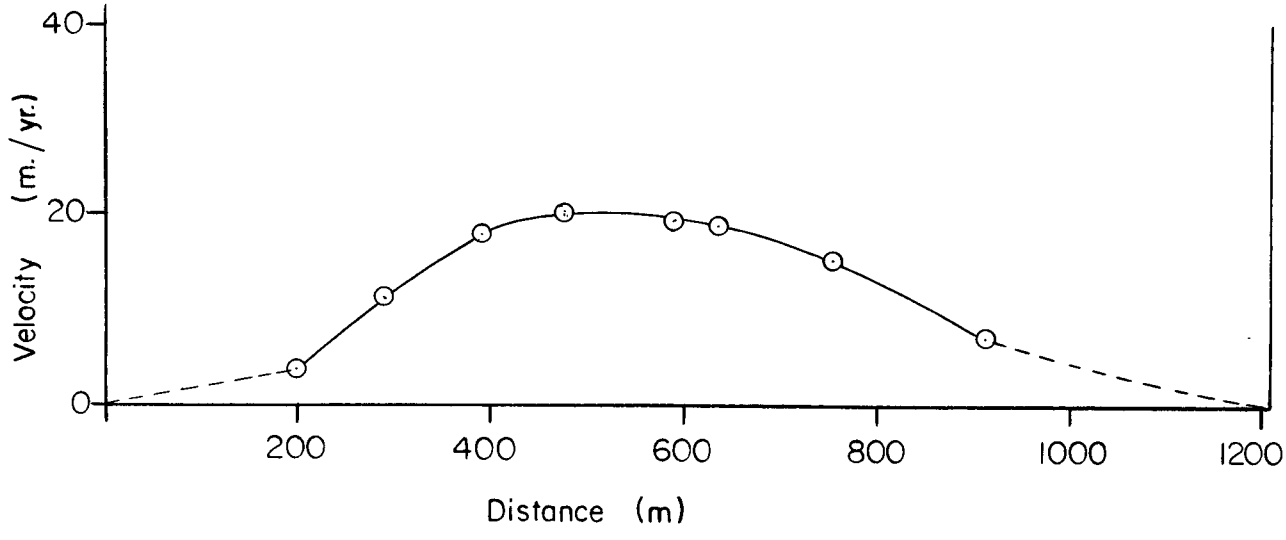

FIGURE 14 HORIZONTAL SURFACE VELOCITY

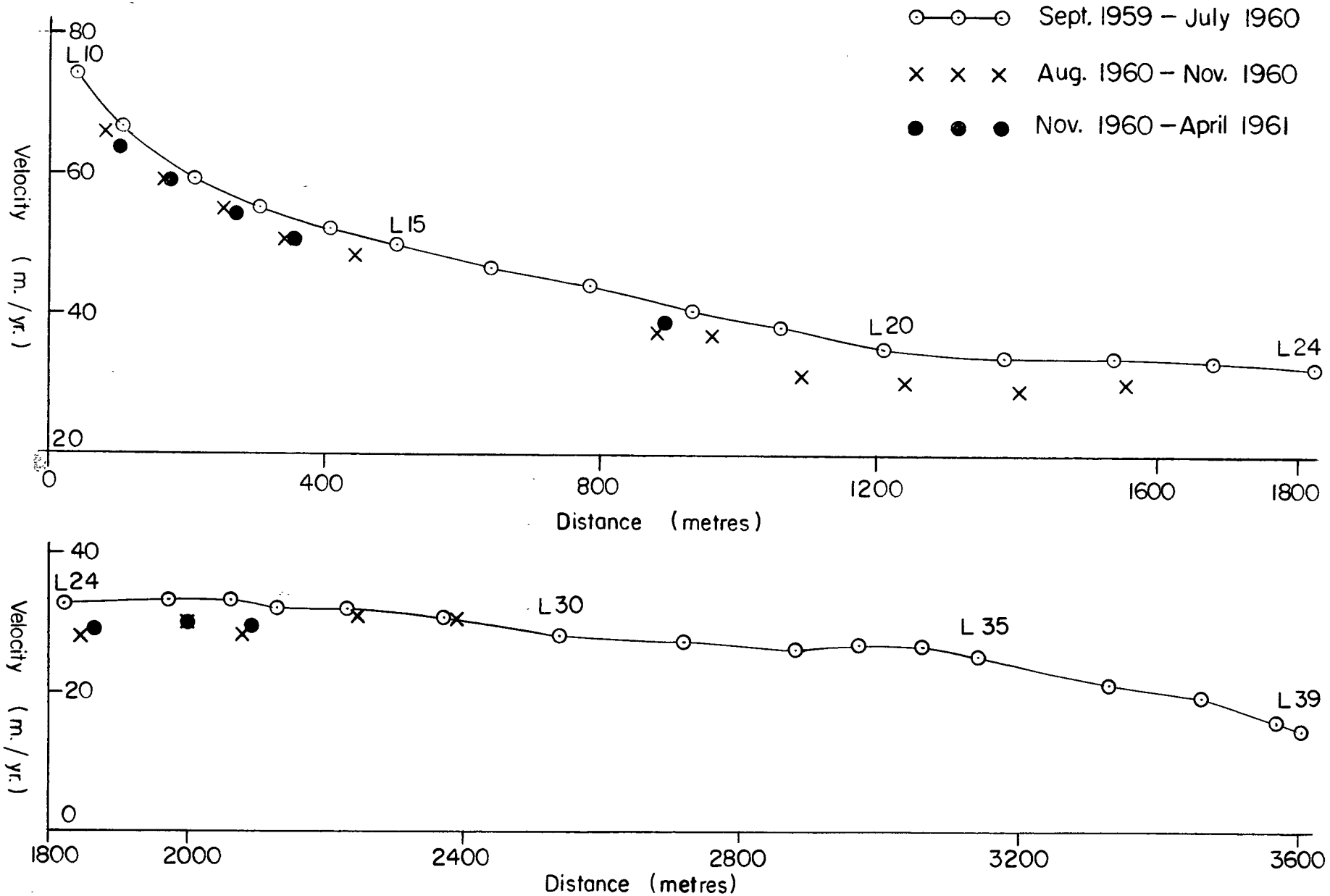

FIGURE 15 SURFACE VELOCITY ON LONGITUDINAL LINE

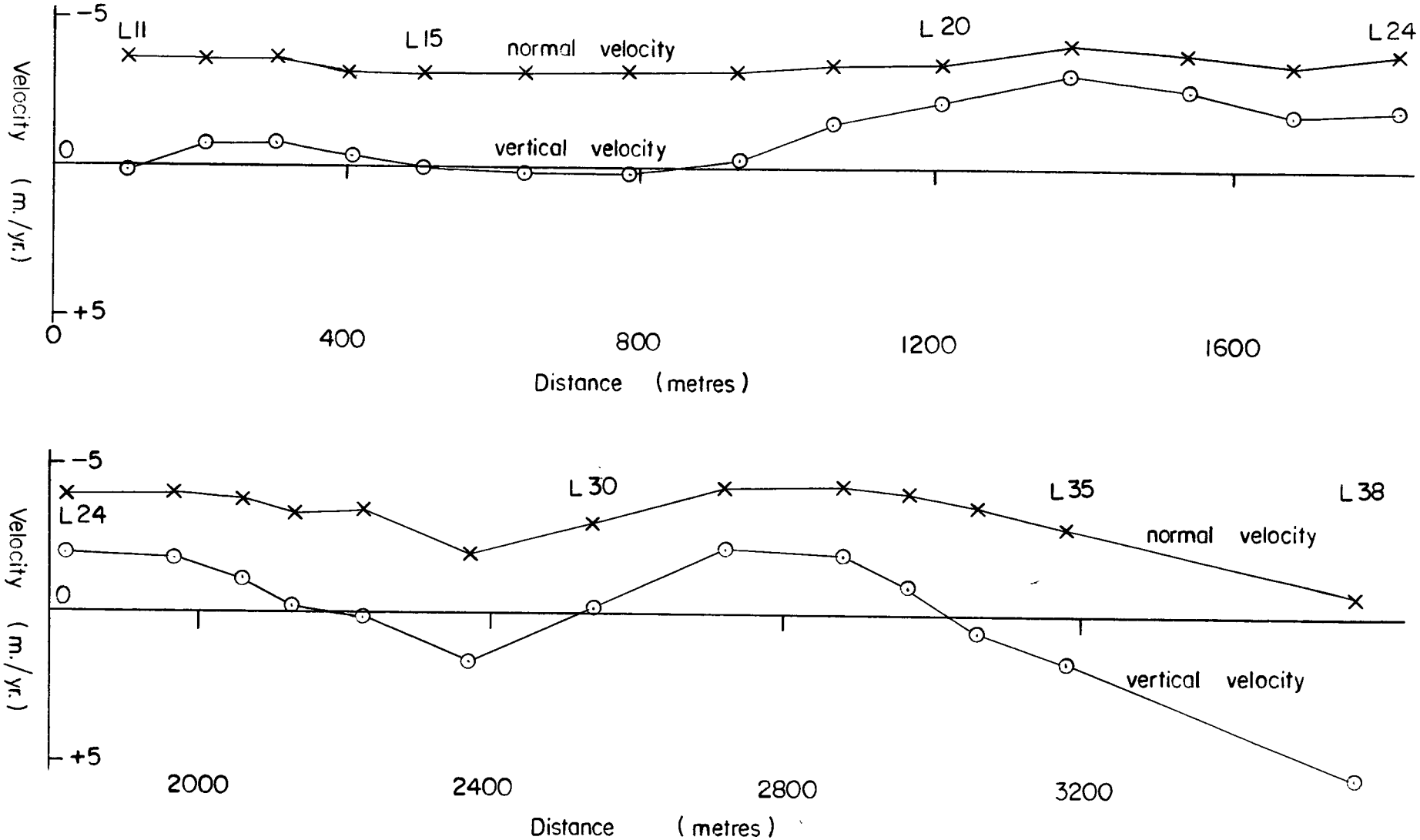

FIGURE 16 VERTICAL VELOCITY AND VELOCITY NORMAL TO SURFACE ON LONGITUDINAL LINE

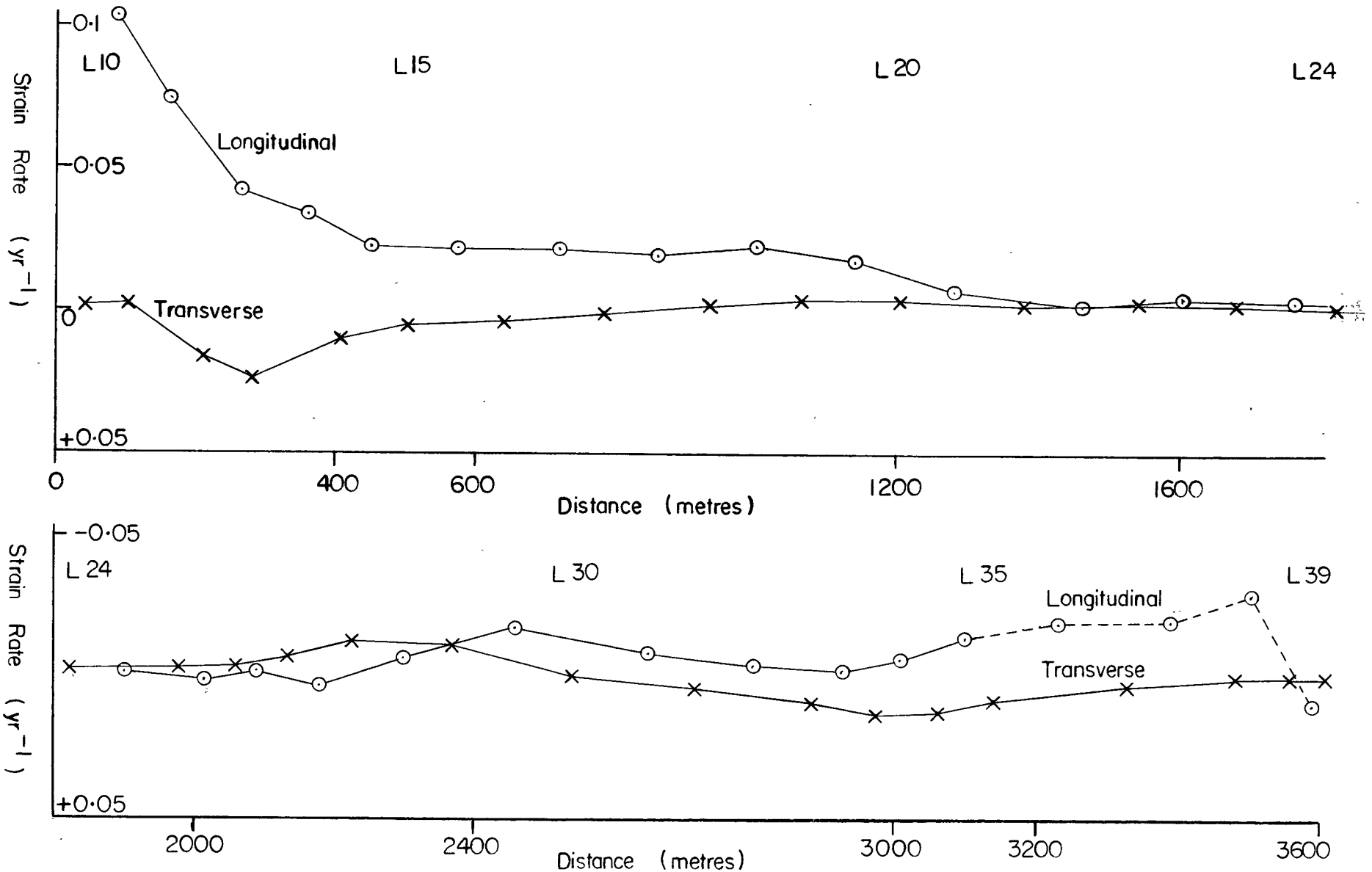

FIGURE 17 LONGITUDINAL AND TRANSVERSE STRAIN RATES ON LONGITUDINAL LINE

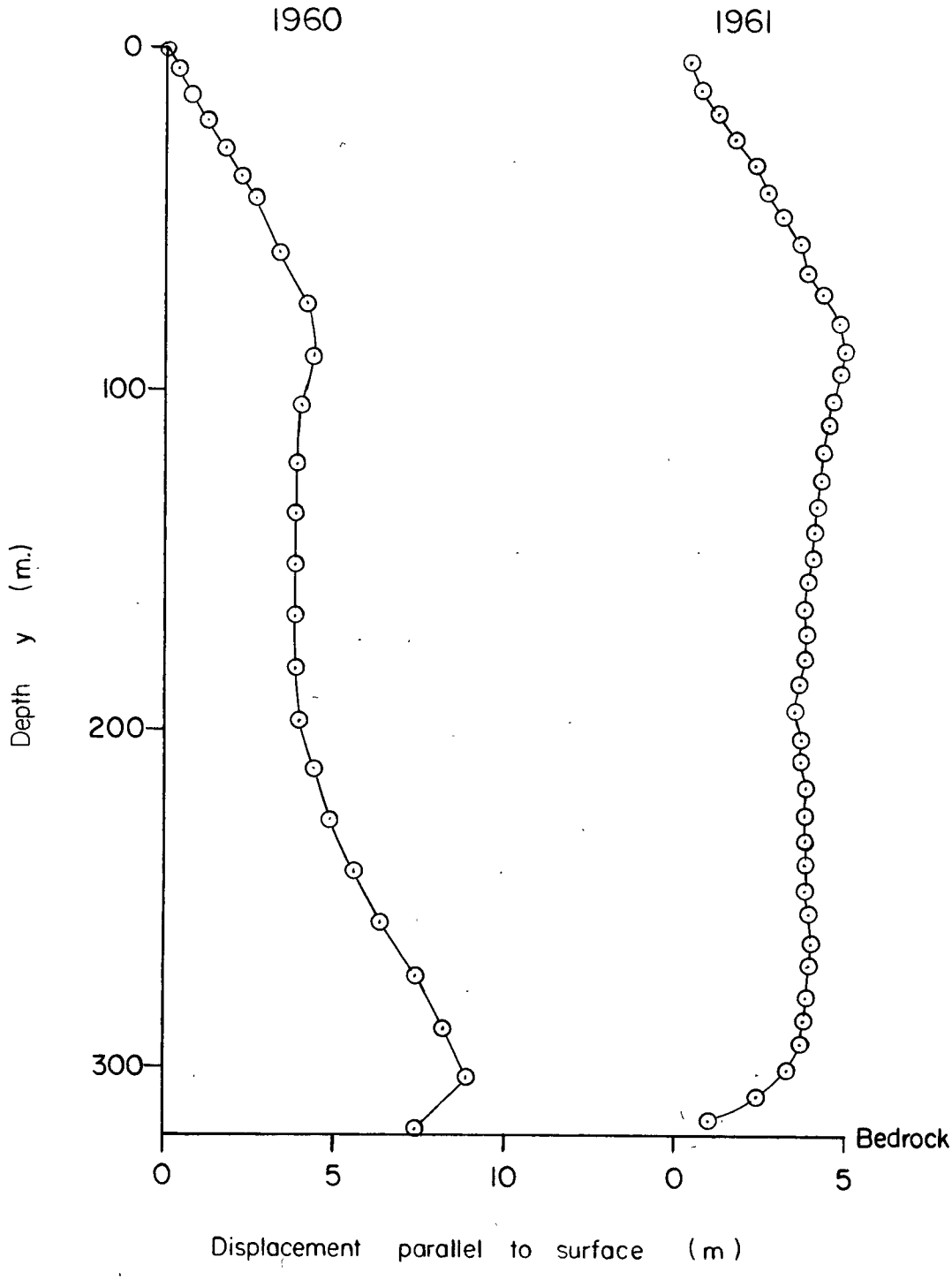

FIGURE 18 CHANGE IN CONFIGURATION – HOLE 322

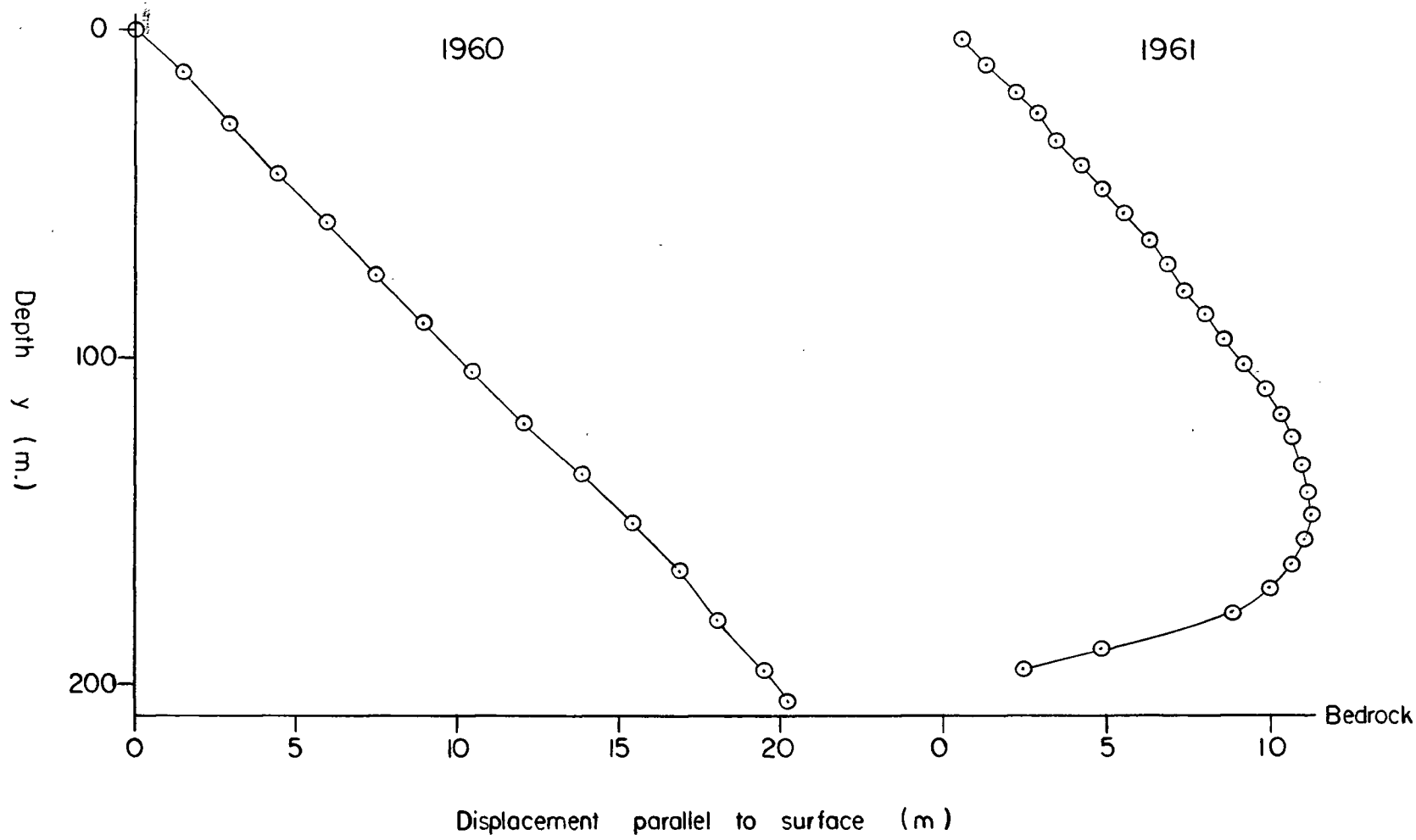

FIGURE 19 CHANGE IN CONFIGURATION – HOLE 209

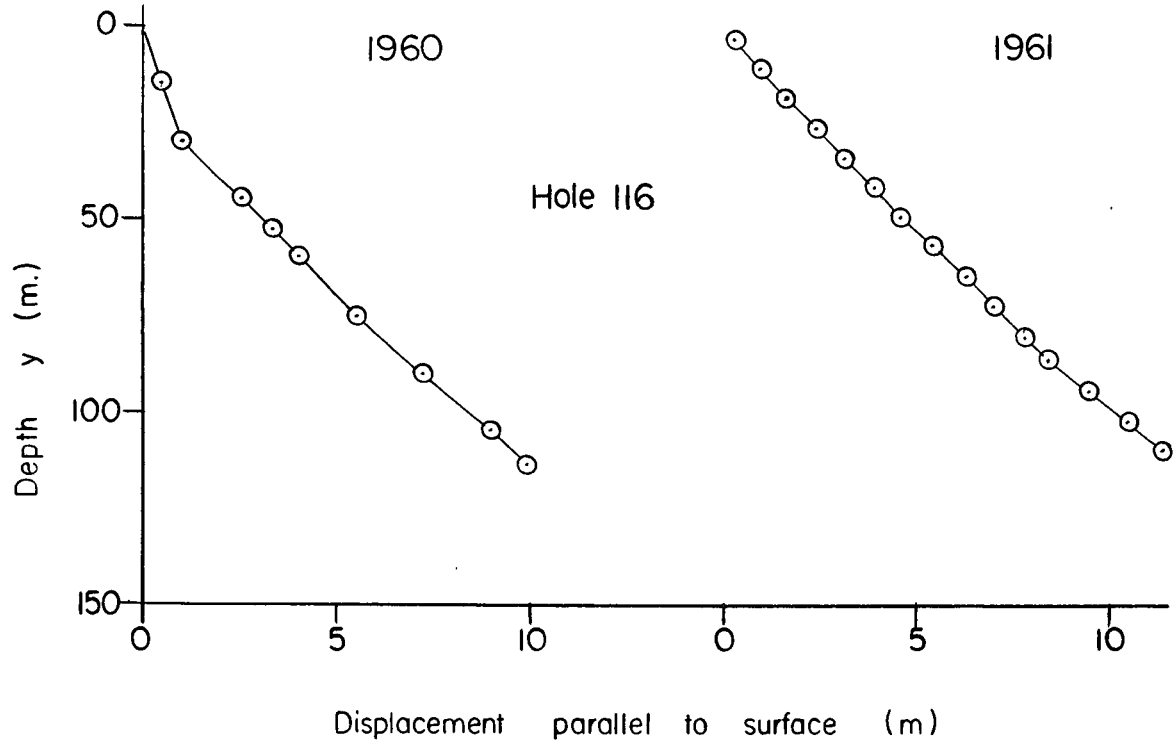

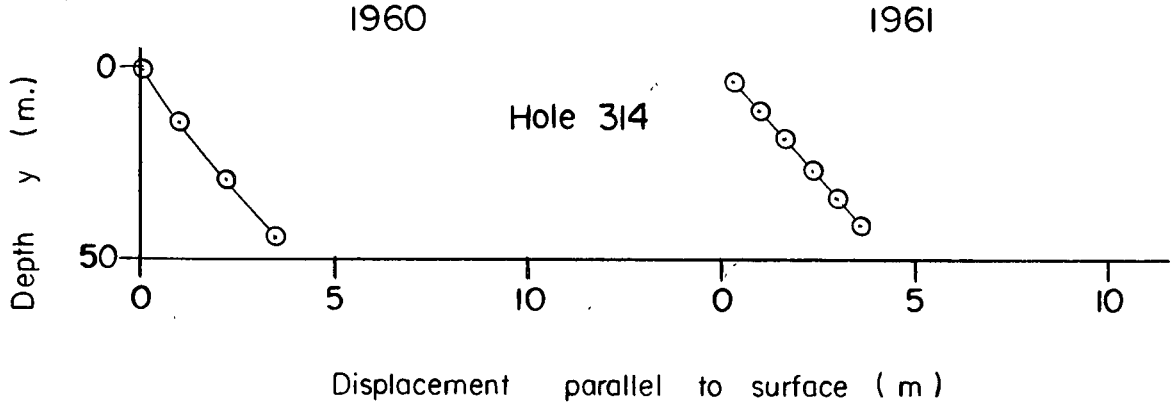

FIGURE 20 CHANGE IN CONFIGURATION - HOLES 116 & 314

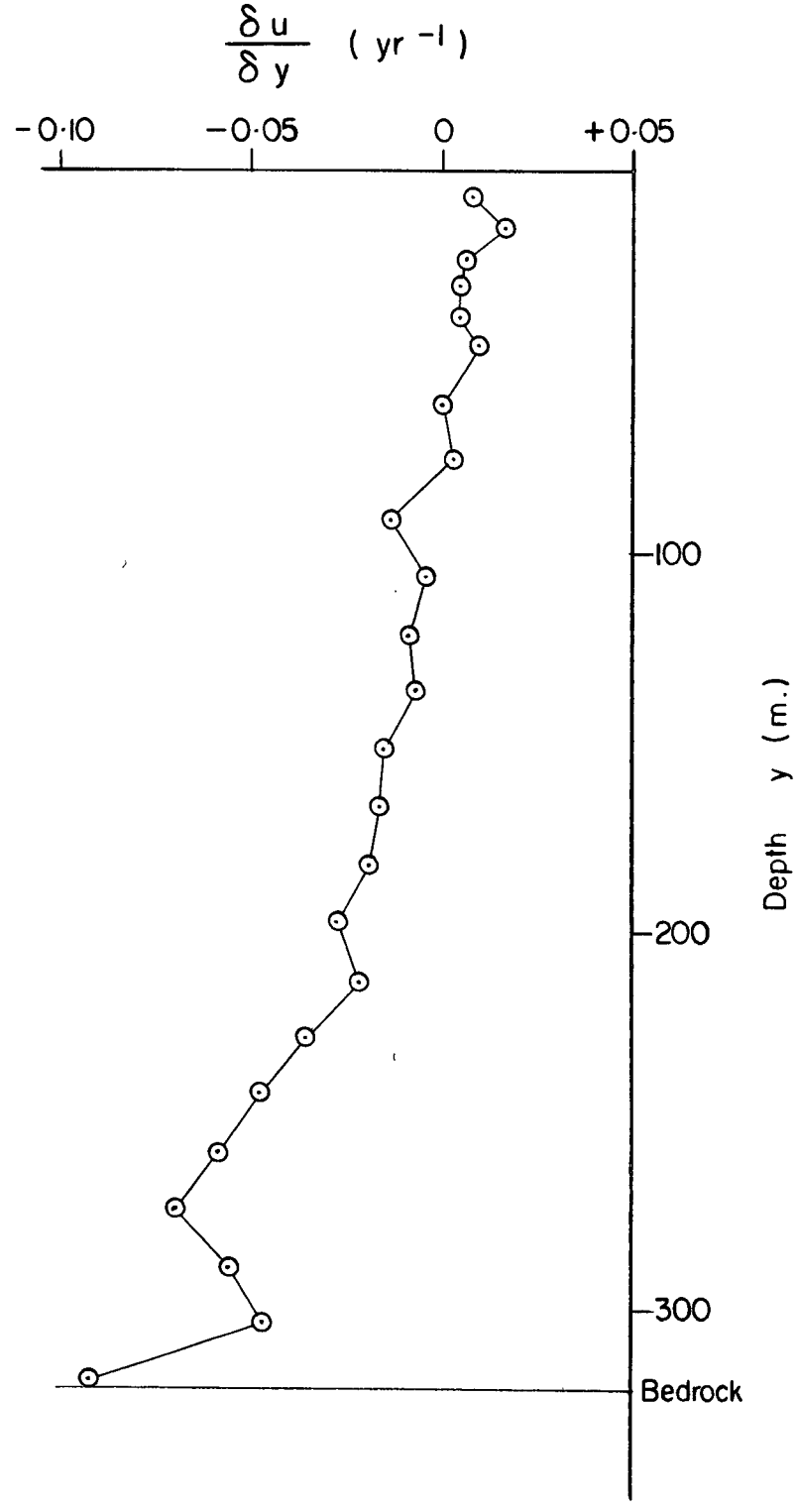

HOLE 322

FIGURE 21 VARIATION OF $\frac{\delta u}{\delta y}$ WITH DEPTH

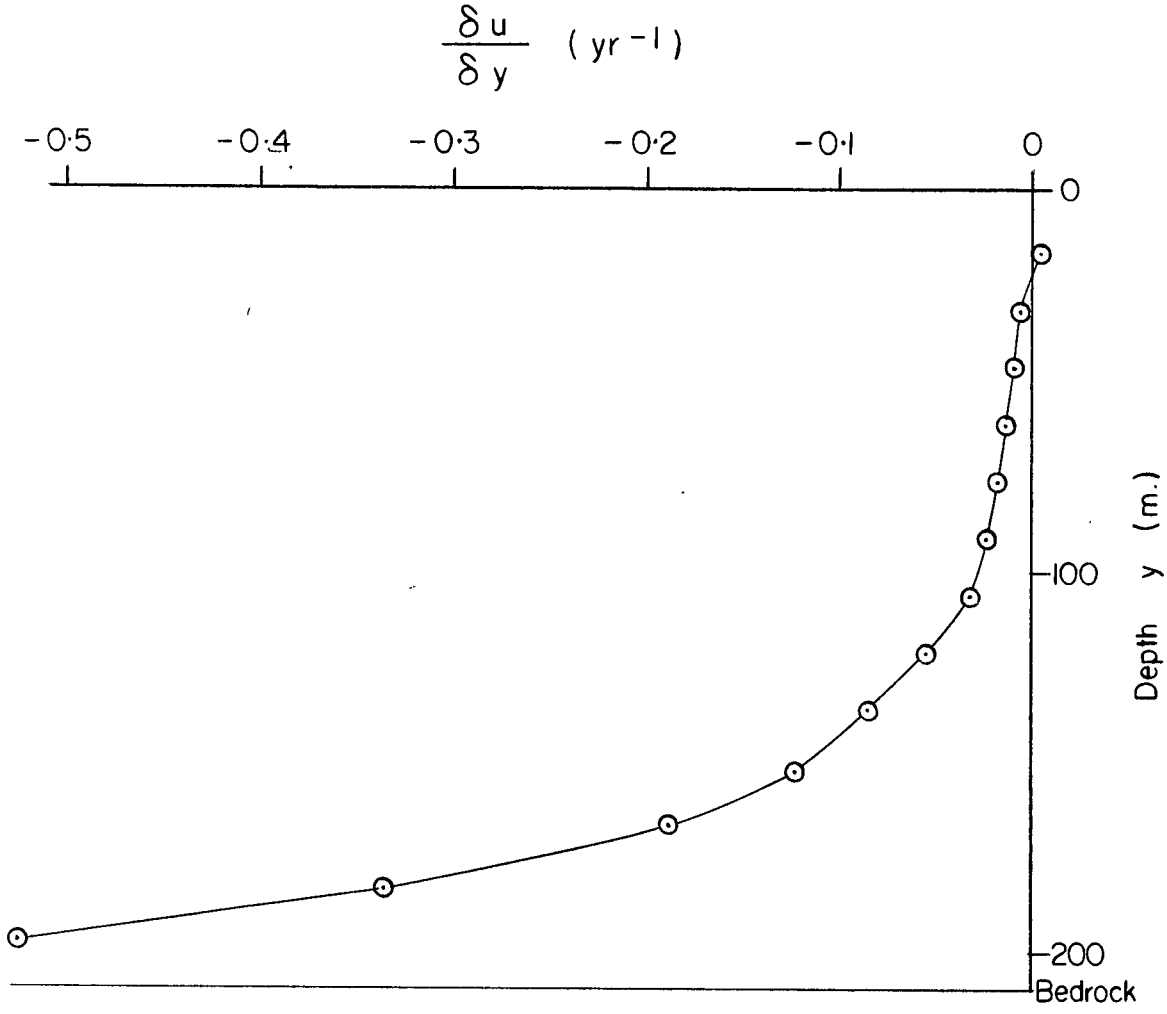

HOLE 209

FIGURE 22 VARIATION OF $\frac{\delta u}{\delta y}$ WITH DEPTH

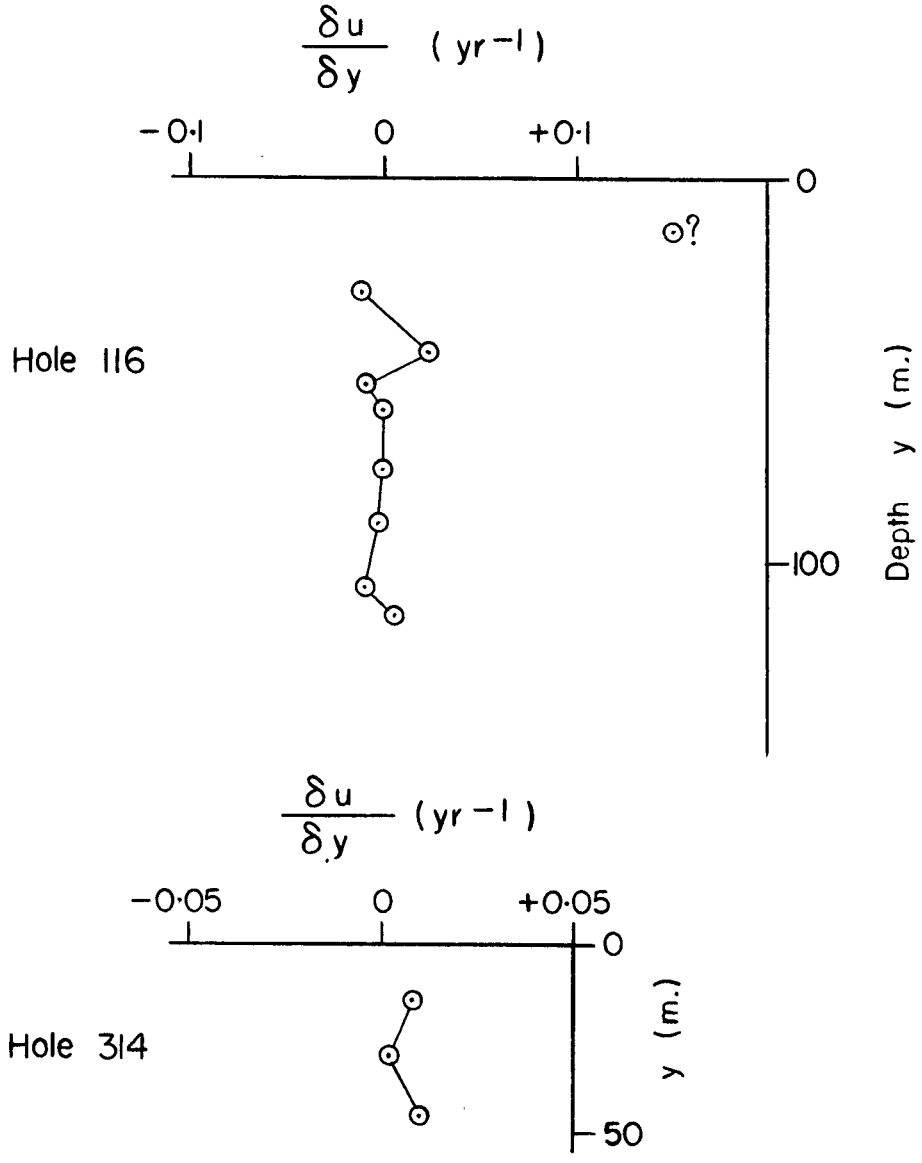

HOLES 116 & 314

FIGURE 23 VARIATION OF $\frac{\delta u}{\delta y}$ WITH DEPTH

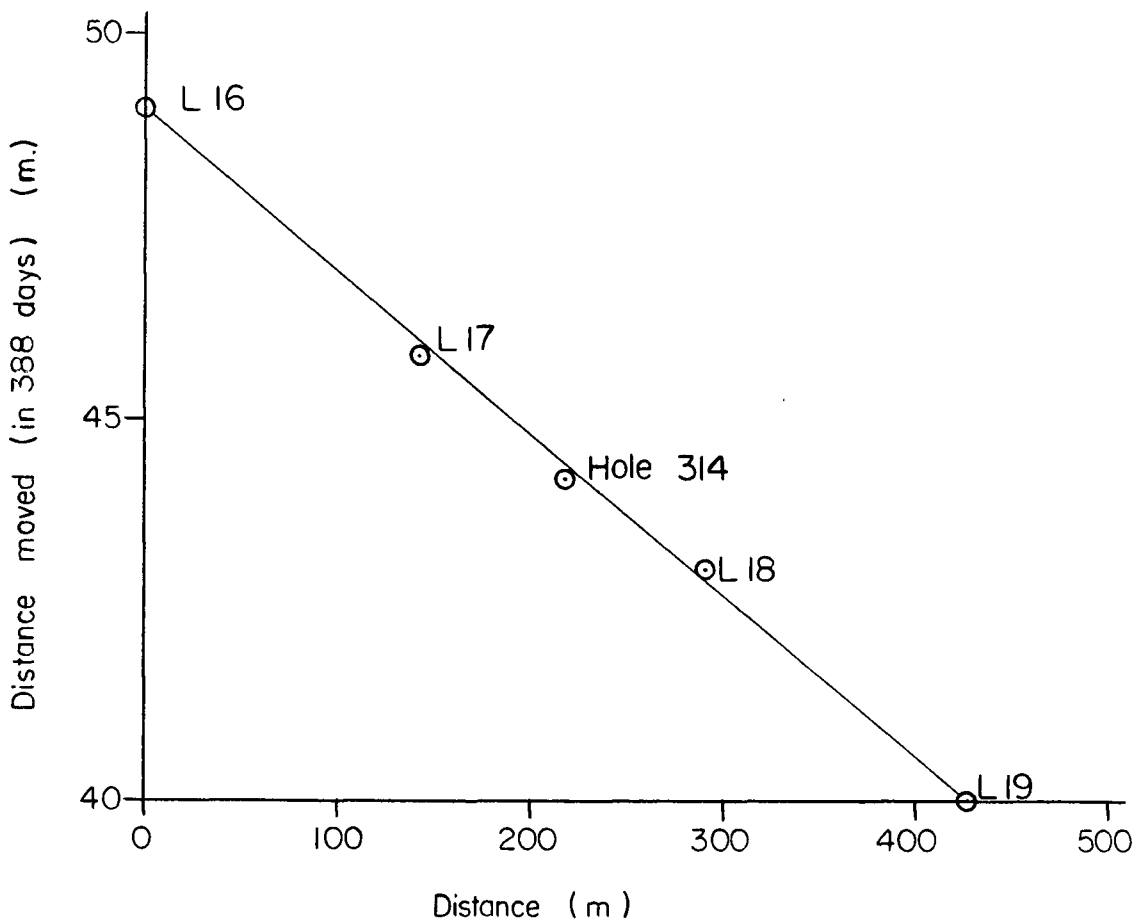

FIGURE 24 COMPARISON OF VELOCITIES OF PIPE AND MARKERS

FIGURE 25 EFFECT OF "SHAPE FACTOR"

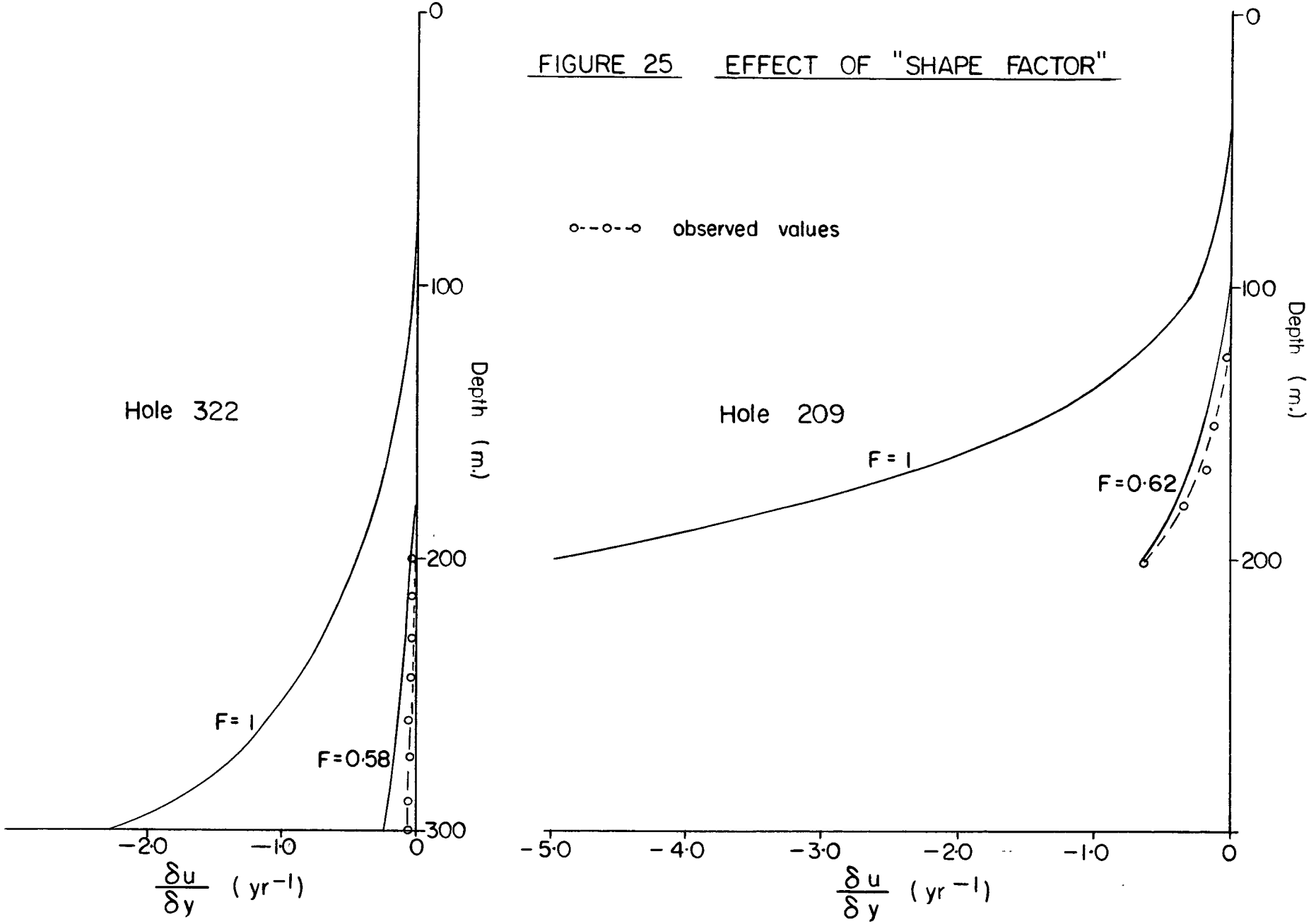

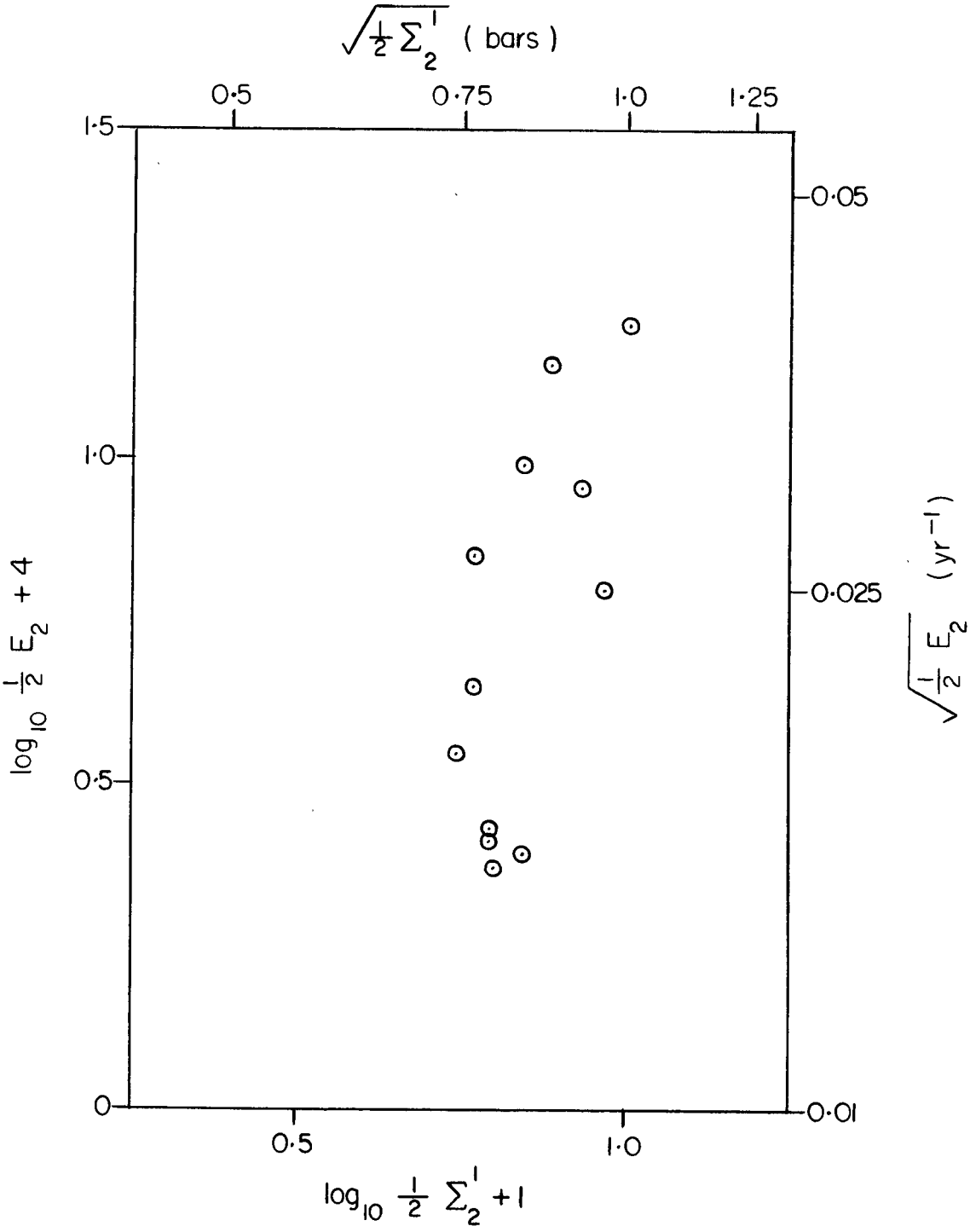

HOLE 322

FIGURE 26 STRAIN RATE AND STRESS

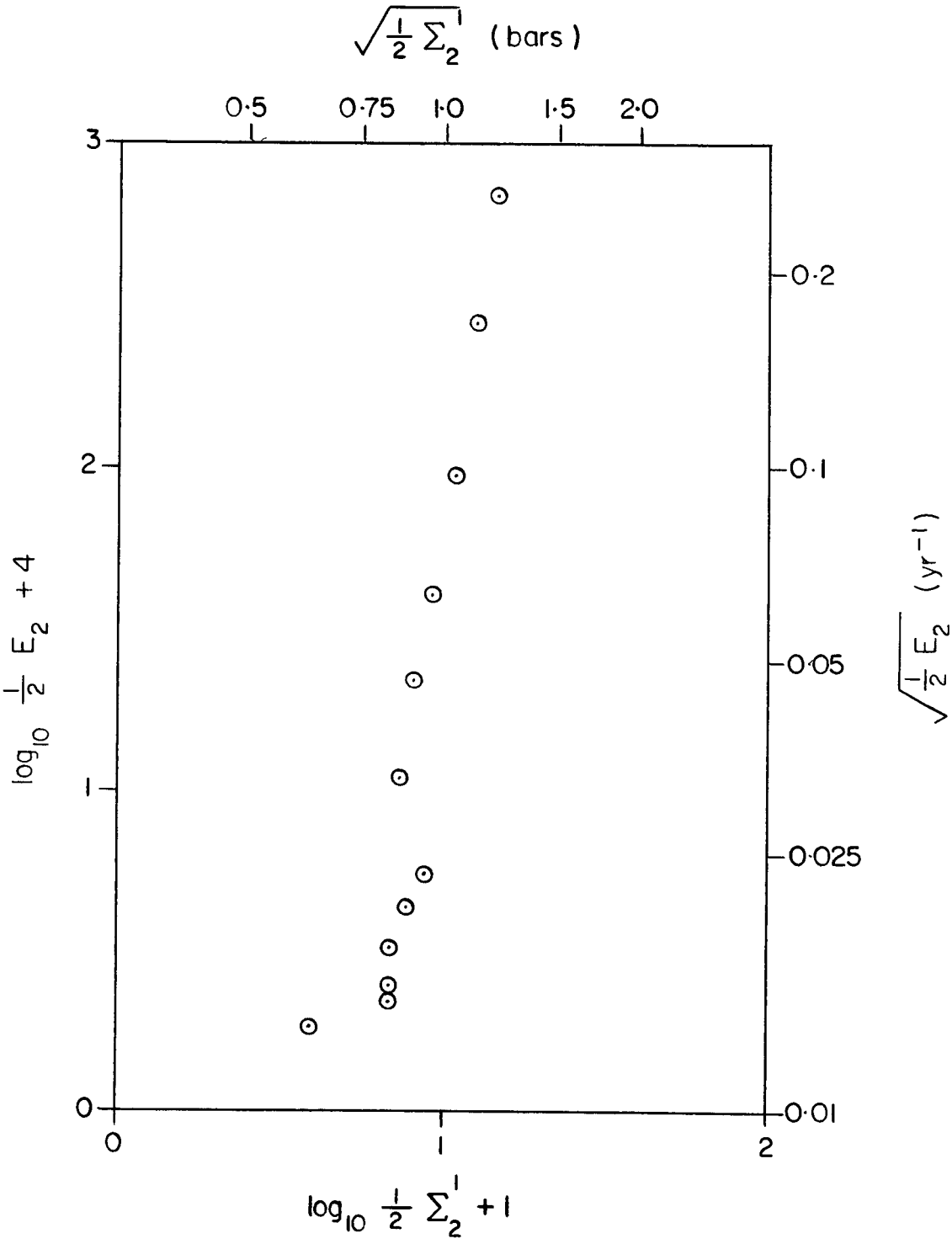

HOLE 209

FIGURE 27 STRAIN RATE AND STRESS

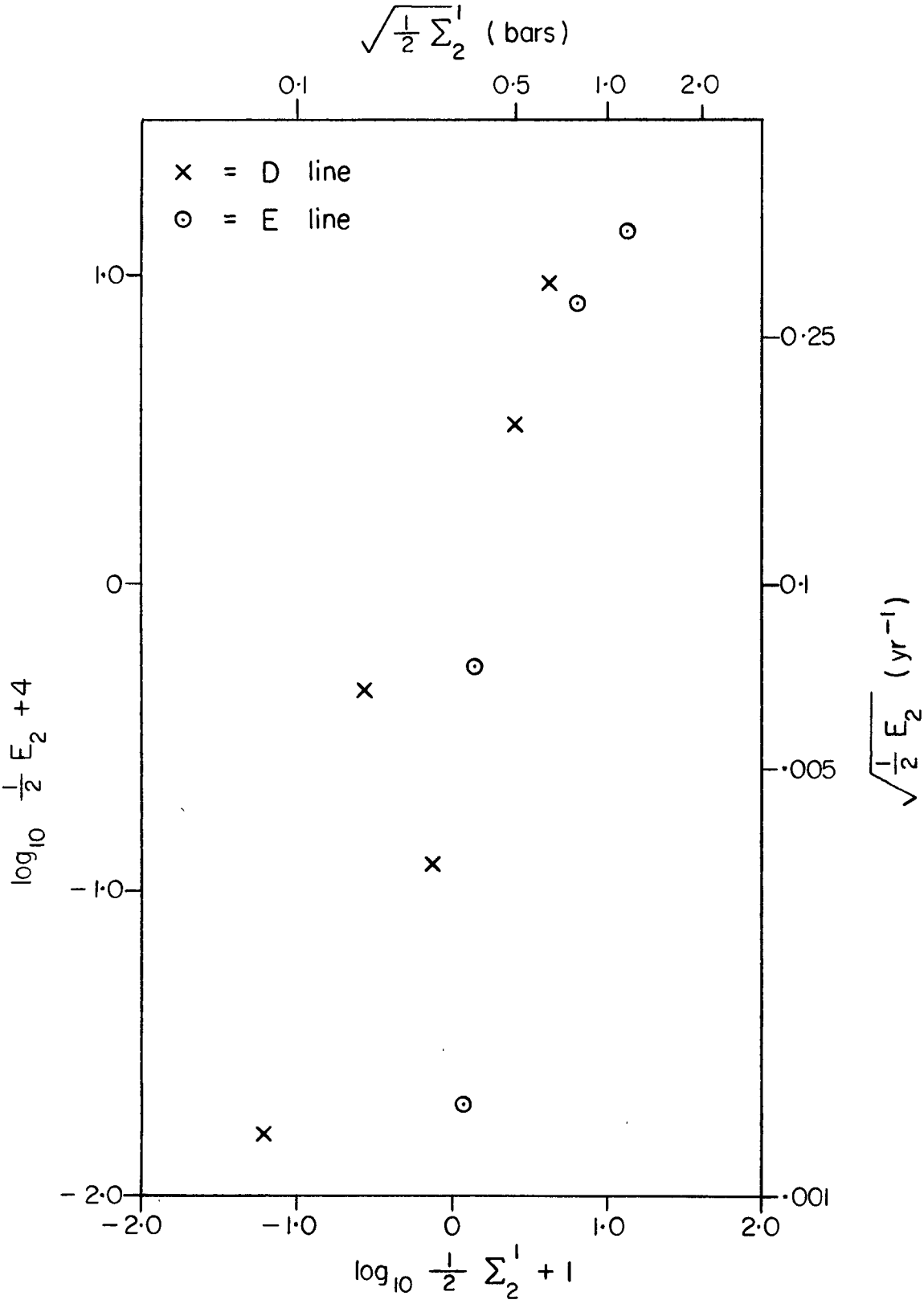

FIGURE 28 STRAIN RATE AND STRESS

TRANSVERSE LINES

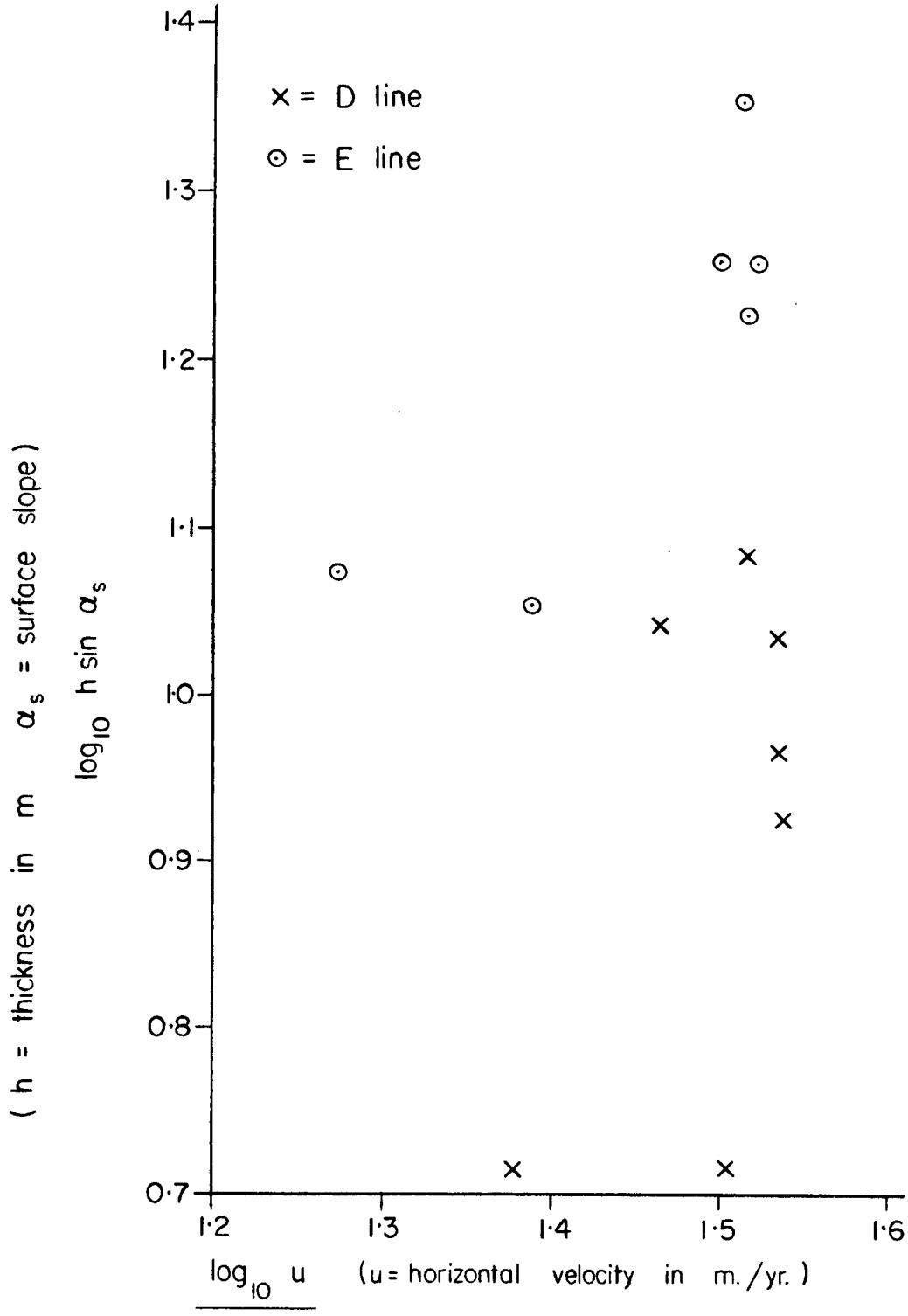

FIGURE 29 CORRELATION BETWEEN SURFACE VELOCITY AND ICE THICKNESS

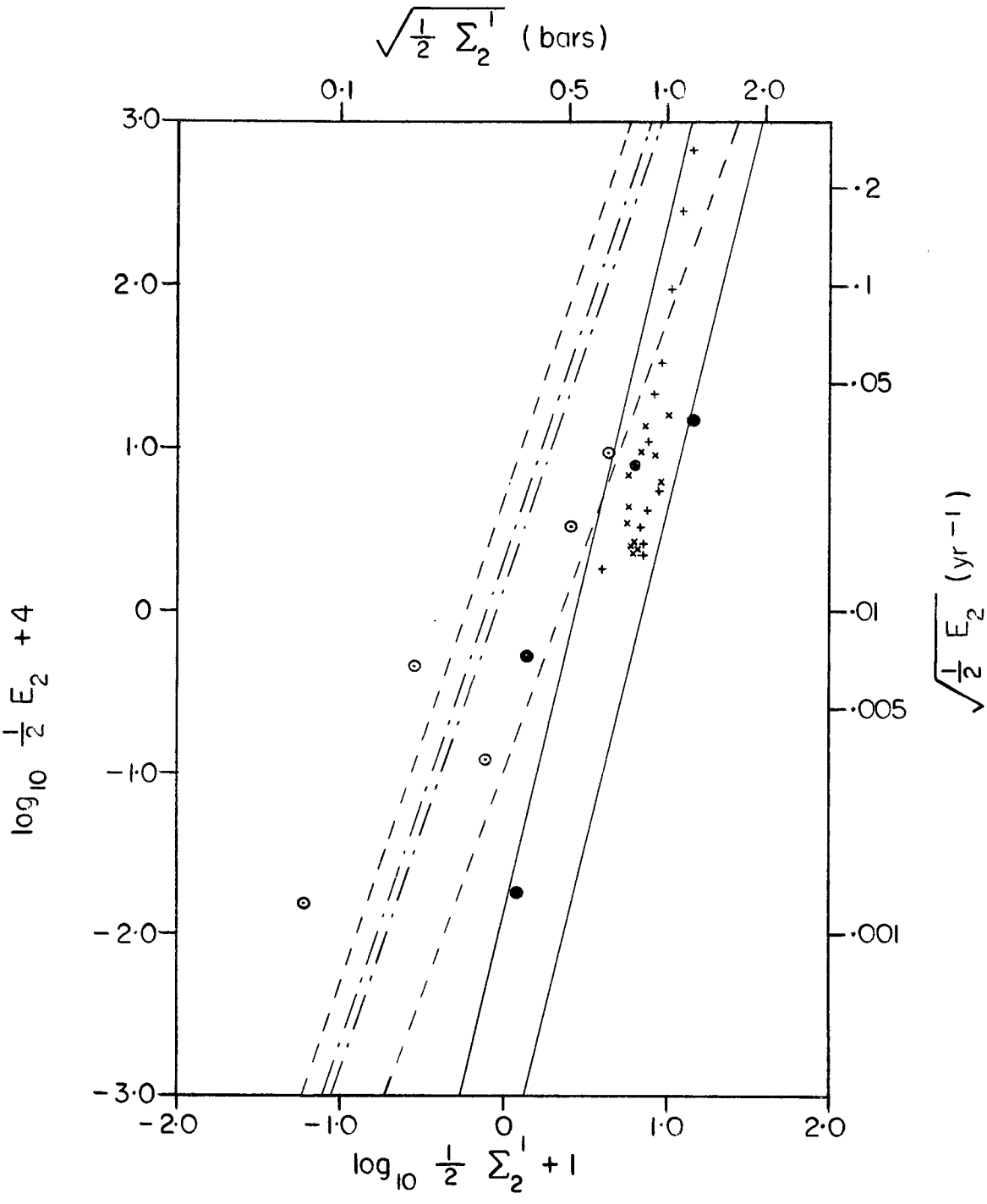

+ Hole 209 ——————— n = 4·2 (Glen)

× Hole 322 — — — — — — — n = 3·2 (Glen)

⊙ D line — · — · — · — n = 2·96 (Butkovich & Landauer)

● E line The lines of each pair refer to $0°C \propto -1·5°C$

FIGURE 30 COMPARISON OF DATA WITH FLOW LAWS

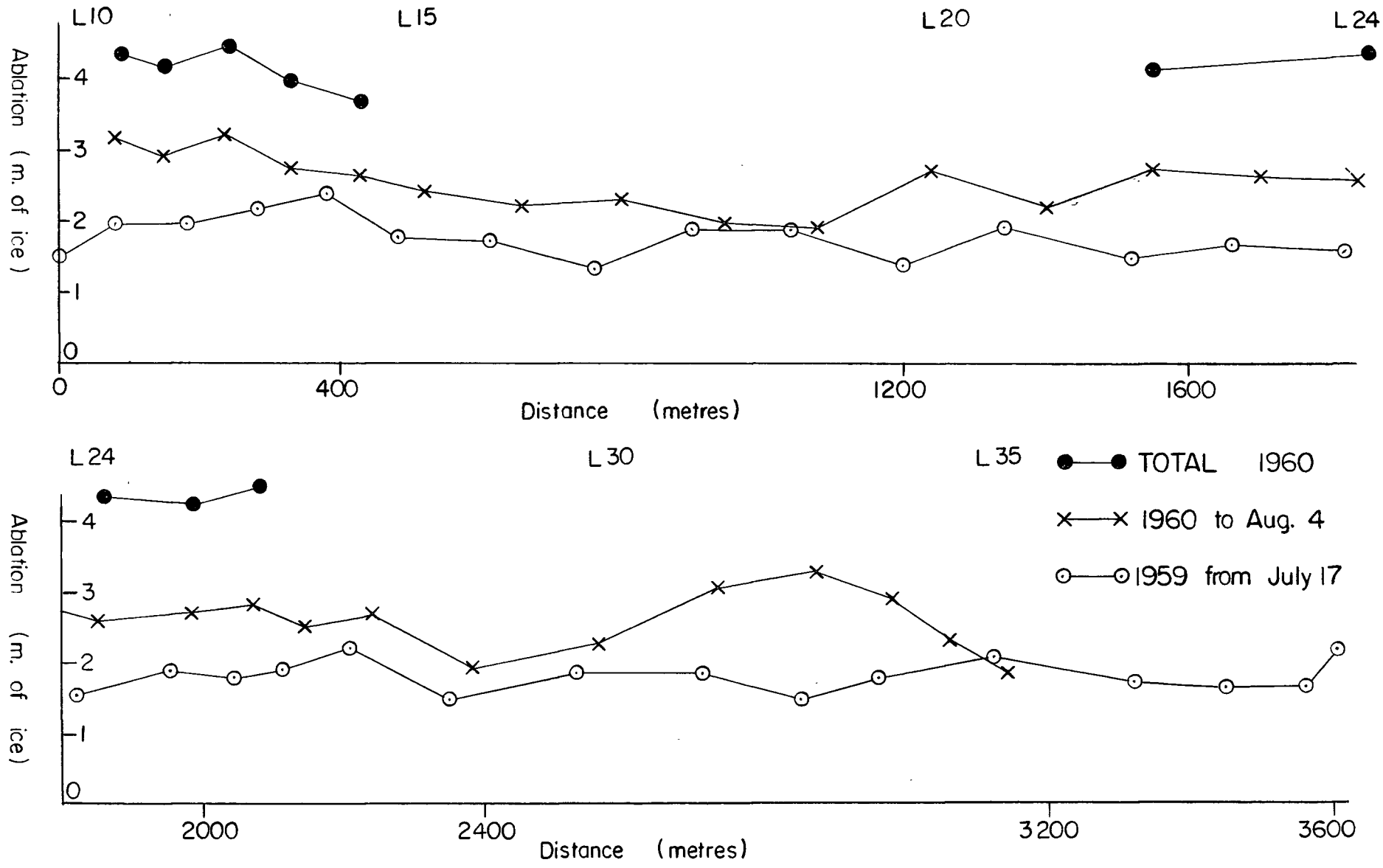

FIGURE 31 ABLATION ON LONGITUDINAL LINE